January 2019

Wind-Powered Water Injection in Offshore Oil Fields

Mohamed Mahmoud Hanafy Abdaltawab

Faculty of Aerospace Engineering

Faculty of Civil Engineering and Geosciences

TUDelft

Wind-Powered Water Injection in Offshore Oil Fields

By

Mohamed Mahmoud Hanafy

Wind Energy Research Group, Faculty of Aerospace Engineering

For obtaining the degree of

Master of Science
in Sustainable Energy Technology

at Delft University of Technology,
to be defended publicly on

Student number: 4626672

Thesis committee:
Dr. ir. M.B. Zaaijer (supervisor)   TU Delft - Wind Energy
Dr. Olwijn Leeuwenburgh (supervisor)   TU Deft - Civil Engineering
Prof.dr. Simon Watson TU D   TU Delft - Wind Energy

Acknowledgements

Abstract

The developments in offshore wind offer new opportunities for the powering offshore oilfields in general, and offshore water injection processes in specific. On the other hand, building on the strength of the oil industry could enable a faster development of offshore floating wind turbine technologies (for use in deep and ultra-deep water oilfields), access to capital, political connections, global reach, and state of the art technical capabilities. Both the use of water injection to enhance oil recovery in suitable reservoirs and use of offshore wind technology to harness power are proven to be commercially and technically viable, each on its own. However, the integration of both systems has not been adequately investigated.

This thesis investigates the potential of autonomous stand-alone wind-powered intermittent (fully wind powered, **Scenario A**) and cyclic water injection (wind and gas powered, **Scenario B**) schemes in offshore oilfields, specifically in heterogeneous layered oil reservoirs. The results obtained from analytical evaluations and numerical simulations of a 3D synthetic model demonstrates strong oil recovery performance, economic, and environmental feasibility, under modelled reservoir and economic conditions. Improved oil recovery is achieved by improved sweep of low permeable layers and previously poor swept areas. It is evident that reservoir performance favors the more intensive schemes (higher ratio off-injection period per cycle to the on-injection period per cycle and longer off-injection duration) with higher injection rates. Furthermore, a sensitivity analysis for offshore oil field characteristics (distance separating injectors and host platform, reservoir heterogeneity, reservoir symmetry, vertical transmissibility, rock wettability, reservoir pressure, capillary pressure, and intermittent injection initiation time) is conducted.

Wind-powered intermittent and cyclic injection schemes are economically feasible mainly in heterogeneous layered reservoirs. Offshore sites with superb wind power provides the highest internal rate of return (IRR) for the fully-wind powered scenario. Offshore Locations with relatively lower wind resource (down to good level of wind power potential) and favourable wind variability patterns can still achieve a higher net present value (NPV), yet at a lower IRR. As larger and more costly wind power systems is required to enhance the oil recovery. The economic and environmental benefits of wind-powered injection schemes is attributed to a higher energy efficiency (in terms of the number of crude oil barrels recovered per MWh), as well as a significant reduction in greenhouse gas emissions, fuel costs, and power transmission costs. Both fully and partially wind-powered schemes are considered more economically favourable under higher oil price environment, lower weighted average cost of capital, longer distances separating host platform and injection wells, higher carbon tax and more stringent environmental conditions.

Contents

List of Figures

List of Tables

List of Abbreviations

BTT: Water breakthrough time

CWI: Cyclic water injection

DC: Distance to coast

EWS: Extreme wind speed

EWSO: Effective wind speed occurrence

FOPT: Total oil field production

FOPR: Field oil production rate

FWPT: Total field water production

FWPR: Field water production rate

IRR: Internal rate of return

MW: Mixed wet

NPV: Net present value

OW: Oil wet

PDF: Probability distribution function

RLO: Effective wind speed occurrence

VT: Vertical transmissibility

WD: Water depth

WPD: Wind power density

WS: Wind speed

WW: Water wet

WF: Continuous waterflooding

1. Introduction

This thesis describes the potential use of autonomous stand-alone wind turbines for exclusively powering subsea raw seawater main injection pumps, and discusses these systems technical and economic feasibility compared to the conventional continuous gas-powered waterflooding. This introduction will briefly outline status quo, the motivation for this specific research topic, the objectives of the project and the structure of the report.

1.1. Research Motivation

Around one third of the global oil and gas production stems from offshore fields (Feller, 2017). Crude oil separation, gas compression and purification, wastewater treatment, seawater injection and petroleum export systems are among offshore oil production activities that consume the bulk of supplied energy and result in considerable emissions. Nearly all offshore installations generate their own electrical power by running open-cycle gas turbines to drive compressors and pumps. Approximately 80% of the CO_2 and NO_x emissions from offshore oil and gas installations originate from these turbines (Nord et al., 2016). With continuously increasing regulatory emissions standards for offshore operations, the oil and gas industry is under pressure to investigate means of enhancing its own environmental sustainability performance. The industry is increasingly investing in new energies to cope with the ongoing energy transition, promote a greener image, and potentially gain access to untapped resources in deep waters and environmentally sensitive areas as in the Norwegian Barents Sea (Arctic).

Water injection is a frequently used and highly effective means of increasing oil recovery from offshore reservoirs. Water is injected to maintain the reservoir pressure, and also to sweep or displace oil from the reservoir towards producer wells. Waterflooding is the standard recovery technique for most oilfields in the North Sea, for example, which are possible targets of offshore wind-powered injection strategies. It can increase reservoir recovery rates by up to 50% (Wei, 2013). It requires technically complex systems, high power consumption, and costly space consuming infrastructure.

Now, the developments in offshore wind offer new opportunities for the oil industry and offshore water injection in specific. Offshore wind turbines are capable of harnessing 6MW rated power, attaining load factors upwards of 50% (Wind Europe, 2017). Building on the strength of two industries, oil & gas with wind, could enable a faster development of offshore floating wind turbine technologies to be used for powering water injection in deep and ultra-deep water oilfields (wind-powered water injection is more likely to be a cost competitive option in such cases, as wind speeds increase further form shore). The offshore wind industry can definitely benefit from the petroleum industry's access to capital, political connections, global reach, and state of the art technical capabilities to navigate the way forward.

Offshore wind powered water injection could provide a commercial and environmentally friendly alternative means of enhancing oil recovery in deep water offshore oil fields across the globe, given that the reservoir characteristics and system design allow for intermittent raw

seawater injection (Feller, 2017). The potential advantages of the proposed autonomous subsea water injection system powered by an offshore wind turbine include:

1. Potentially adding oil recovery in the range of 2-20% using a renewable energy source to provide alternating injection rates (cyclic water injection) at lower costs over field life compared to a conventional continuous waterflood (Langdalen, 2013).

2. Reduction of greenhouse gas emissions and fuel costs in the offshore oil and gas industry. Since the traditional offshore water injection techniques rely on power to be supplied to platforms by gas turbines, decreasing power demand from these turbines by running water injection with wind power will lower fuel costs and emissions considerably, and consequently reduce CO_2 taxes related to the incremental emissions associated with gas turbines power production.

3. Reduction of power transmission costs and losses compared to traditional gas-powered water injection technique, especially when the host platform capacity is limited or injection wells are located far away. For the traditional solution for a subsea injection manifold, the costs of connecting a subsea power cable to the far host oil production platform, that supplies the required electric power to the subsea injection pump, can be substantial. These costs can be lowered significantly by powering the subsea pump with 1-2 offshore wind turbines that are placed within 100m of the subsea manifold. Since, there would be no need for either a long power cable and installation downtime required for the host platform (Slatte, 2014).

4. Allowing for a faster development of offshore wind turbines technology via increased investments and research from the oil majors in floating wind turbines for applying this thesis concept in deep and ultra-deep waters (if proven technically feasible from an oil recovery perspective), as well as access to their political connections and global reach. The concept creates a platform of collaboration, experience sharing and transfer, and creates a niche market for wind turbines which is not dependent on subsidies.

Both the use of water injection to enhance oil recovery in suitable reservoirs and use of offshore wind technology to harness power are proven to be commercially and technically viable, each on its own. However, the integration of both systems has not been adequately investigated. The literature main identified concerns were related to system availability, the effect of intermittency of the wind turbine power generation on oil recovery, power production at low wind speeds and other system control operational challenges (Feller, 2017).

1.2. Research Objectives

The main objectives of the paper are to investigate the conditions under which a wind-powered water injection process in an offshore oil reservoir is technically (from an oil recovery and wind resource perspectives) and economically attractive compared to a scenario of conventional water flooding powered by gas turbines. This will be concluded based on sensitivity analysis for reservoir characteristics, wind climate sensitivity, and main identified project economic drivers. The thesis will primarily focus on answering the main and sub-main research questions below throughout the text and in the conclusion (*Chapter 8*), among others.

- **Can the reservoir performance (from an oil recovery perspective) tolerate the intermittency of offshore wind power and hence, water injection?**
- **If yes, under which reservoir conditions can the offshore wind-powered water injection process be technically and economically feasible?**

- *For the modelled base case reservoir conditions (heterogeneous and layered structure), what is the best injection scheme among the simulated scenarios? What is the effect of increasing the injection rate for various schemes?*
- *What are the key reservoir performance indicators? What is the extent of the role of each indicator?*
- *How does different ranges of reservoir properties affect the total oil recovery achieved different water injection schemes, and the incremental recovery benefits achieved by wind-powered injection scheme over continuous flooding? And why?*
- *What is the optimum initiation time for wind-powered intermittent and cyclic injection schemes?*

- **Under which offshore wind resource conditions can the wind-powered water injection process be technically and economically feasible?**

- *What are the levels of wind potential, wind climate types, and wind variability patterns under which the project is technically and economically attractive?*
- *What are the suggested/common ways to characterize the wind resource and select potential candidate offshore locations for this thesis concept?*

- **Under which economic conditions can the offshore wind-powered water injection process be feasible?**

- *What are the key economic drivers of fully and partially wind-powered (in combination with storage or gas cogeneration) water injection schemes?*
- *For the modelled base case, how does various scenarios rank in terms of Capex, Opex, NPV and IRR? And why?*
- *How are the feasibilities of all scenarios affected under different economic conditions in terms of NPV and IRR?*
- *How do different levels of wind power potential affect the economics of the project?*

- **What are the environmental benefits resulting from applying fully and partially offshore wind-powered water injection in terms of energy efficiency and emissions reduction, approximately? What are the resultant fuel and carbon tax cost savings?**

1.3. Research Approach

This section paints the general approach that will be taken in this research, identifies the specific aspects that will be focused on, and states the assumptions and simplifications that will be made.

1.3.1. Technical Feasibility Investigation

Three locations will be selected for the study based on wind data availability, belonging to different wind class regions of wind resource based on Zheng (2018) map (Figure 8), belonging to different wind climate systems, and being locations of known major offshore oilfield accumulations. This will allow for investigating the feasibility of the thesis concept in a diversified range of wind conditions. Only offshore locations are of interest for the scope of this

study. This is to utilise the higher capacity factors, higher wind power potential, as well as enable investigation of potential reduction of power transmission costs and losses compared to traditional gas powered water injection technique (mainly for cases when the host offshore oil platform capacity is limited or injection wells are located far away).

Hourly offshore wind data over the course of the 10 years for the selected locations will be extracted. Other data related to assessment of candidate offshore wind installations locations including current conditions, wind direction, wave conditions, sea depth, soil type, distance to ports, distance to grid connection, and in their implications on the wind system design will not be considered in the analysis for being out of scope for this study. The collected hourly wind data will be processed into 3 hourly minimums, that is to ensure that the reservoir simulation limitation of studying 3-hourly variations of water injection rate is met. Four of 3-bladed wind turbine models will be examined for one of the selected locations. The optimum wind turbine will be chosen mainly based on capacity factor, LCOE, AEP, and power curves (known cut-in and cut-out wind speeds of the turbines) in **Location A** (base case location). Following that, the water injection schemes for the 3 locations will be estimated solely based on 3-hour generated power output of the selected turbine in respective locations. The water-injection pumps should ideally inject a specific total volume of water over the lifetime of the project to maximize oil recovery. The process is based on injecting at a target rate, that the reservoir injectivity allows, during time intervals when the wind turbine is producing the power required to run the injection pumps at full capacity, and then zero injection otherwise. This proposed injection scheme has the advantages of avoiding the need for pumps that can tolerate varying power input, and increasing the off injection period per cycle (which should provide more contact time between injected water and formation for capillary imbibition to become more dominant). The electrical system components and their suitability for 3-hourly on and off switching of pumps will not be addressed in this study. The purpose is to assess whether water injection could tolerate 3-hourly variations of wind speed and power generation from an oil recovery perspective. The effect of various wind systems and profiles on the efficiency of the concept of intermittent water injection will be examined via simulations using a simple synthetic Eclipse 3D reservoir model over a 10 year period. The injection scheme at **Location A** will form the basis of **Scenario A: Fully wind-powered.**

One concept in petroleum engineering literature that bears a resemblance to this intermittent form of flooding is cyclic water injection (CWI). CWI is a recovery technique which increases the oil production mainly in heterogeneous and stratified reservoirs. The process constitutes varying injection rates from high values to low or no injections in symmetric or asymmetric fixed cyclic periods ranging from days to months per period (**Scenario A** is expected to constitute of varying cyclic periods depending on wind availability). The main reasons for the improved oil recovery were found to be that cyclic injection schemes increase the sweep efficiency through oil migration on the high saturation gradient around swept zones, reducing water channeling and fingering by means of stabilization of the displacement front. The physical mechanism of oil recovery increase by cyclic water injection is a well-established phenomenon, although the theory does not define the amplitudes of injection variation, duration of cycles, nor the location of wells with periodical injection. One of the most important factors

related to a cyclic waterflood, considering both wind speed variation and oil recovery enhancement, will be the ratio of injection to no-injection (cyclic injection scheme). An infinite amount of different cycle schemes can potentially be used. In this thesis, two schemes (injection/no injection ratios 1:2, 1:3) will be tested with different cycle periods each (15 and 30 days), *Appendix B*. The optimum injection scheme will form the basis of **Scenario B: Wind + Storage/Gas cogeneration,** regardless of the wind variability pattern in the base case location. Due to the variable nature of the wind, this scenario will require a storage solution or gas cogeneration for firm power supply. In the performed study, gas cogeneration is used for simplicity. The designed control system should ensure that the pump's power demand is provided based on the optimum injection scheme, with priority of supply given to the wind system. Given that at the time either the supply or load changes, the system must reliably seek to restore balance. The option of dealing with intermittency of wind power generation with and without storage solutions or gas cogeneration via an intermittent water injection process will be investigated.

Scenarios A and B will be compared to **the conventional gas-powered continuous water flooding** (**Scenario C**) via simulations using a simple synthetic Eclipse 3D reservoir model (with 2 injectors and two producers) over a 10 year period, for execution time and better control of the physical mechanisms. The injection rate will be optimised for all scenarios, to showcase the effect of injection rate on the efficiency of each injection scheme, *Appendix B*. For the base case used for scenarios comparison, the total injection volume target is set at 87.5 MMbbls (MM = million). Furthermore, a sensitivity analysis for offshore oil field characteristics (reservoir heterogeneity, reservoir symmetry, vertical transmissibility, rock wettability, reservoir pressure, capillary pressure, and intermittent injection initiation time) will be conducted. As a conclusion to the offshore wind and reservoir characteristics technical sensitivity analysis, technical screening criteria for candidate offshore projects and the optimum wind-powered water injection scheme among **Scenarios A and B** (from an oil recovery perspective) will be presented.

1.3.2. Economic and Environmental Feasibility Investigation

In order to study the economic feasibility of the project, a financial model for the integrated system design is developed to estimate the Capex, Opex, NPV over field life, and IRR for all scenarios. For **Scenarios A and B**, total Capex for the wind structure and marine operations and logistics are the two main Capex drivers. The pump system and development costs are also significant in the overall investment and are expected to have higher costs for the intermittent and cyclic injection scenarios (due to higher requirements of injection rates and power capacity). The resulting annual average operation and maintenance include mainly parts, and vessel costs. The O&M cost and performance is highly dependent on detailed wind and wave data in the selected location. However, the O&M estimate in this study will be merely based on the general reference. Furthermore, wind and gas powered processes will be compared as a function of step out distance from the production platform. A sensitivity analysis for several key parameters including carbon tax, discount factor, wind system design, and distance separating host platform and injector wells. It is important to note, that Capex and Opex, will not include the costs of injector drills, power umbilical, nor development and maintenance of the offshore oil field etc. that are relevant to actual projects, but are equivalent for all simulated
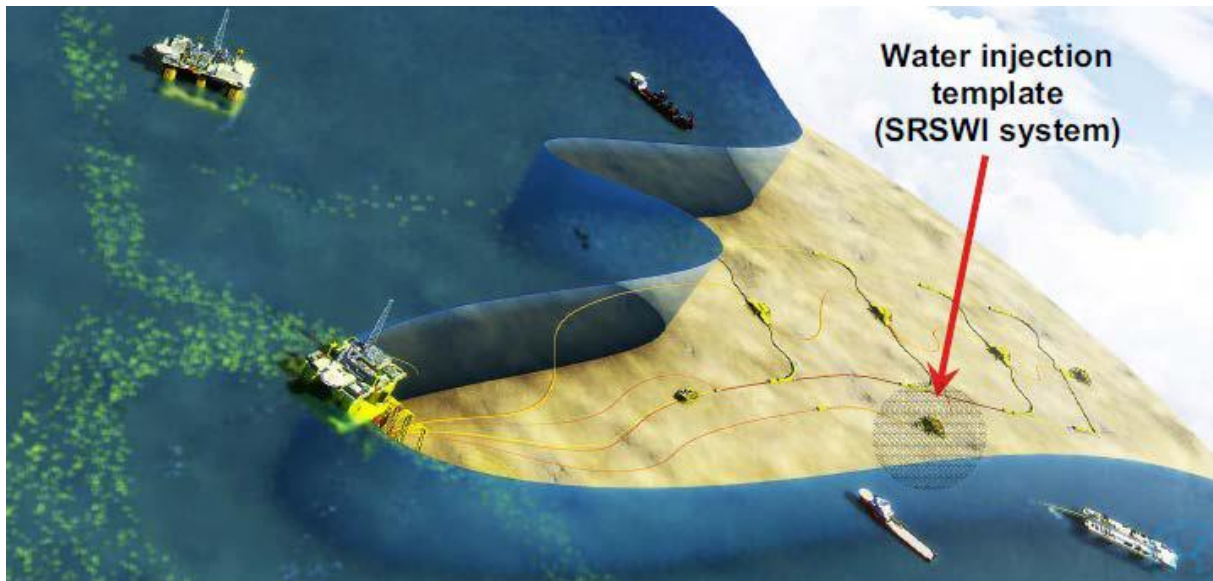
Figure 1: Conceptual graphic of a Subsea Raw Seawater Injection System, (Slatte, 2014)

scenarios. Thus, the results should be utilized for comparison rather than appraisal purposes. For all scenarios, a subsea raw seawater injection system is used, Figure 1. This, assuming suitable reservoir properties, minimizes the required water injection flowline. As injection water will be sourced straight from the sea by a seawater injection subsea unit rather than the host platform. For **Scenario C**, the subsea unit is expected to be powered from the host platform. As for **Scenarios A and B**, the wind turbine will be in proximity to the subsea water injection template, and no power connection with the host platform will be required. This condition is expected to showcase the potential economic benefits of applying **Scenarios A and B** over **Scenario C** in cases of long distance separating the host platform and injection wells. Finally, the long-term operation environmental benefits of wind power integration in terms of fuel savings, energy efficiency and CO_2 emissions reduction will be estimated.

1.4. Structure of the report

The report is structured in the following manner. *Chapter 2* describes global wind energy geographical classifications and local wind energy characterization by Weibull distribution parameters. *Chapter 3* presents an overview of cyclic waterflooding. *Chapter 4* describes the 3D reservoir model, the water injection schemes under study (**Scenarios A, B, and C**), locations selected for studying the effect of wind resource on the technical feasibility of the thesis project concept (**Locations A and B**), and wind data processing and characterisation at the selected locations. *Chapter 5* gives the simulation results and the comparison of all investigated scenarios, in addition to studying the effects of varying wind system and reservoir characteristics on oil recovery. The economic and environmental analyses are presented in *Chapter 6 and 7*, respectively. *Chapter 8* provides the conclusions, mainly regarding effect of various candidate offshore projects key controlling parameters and the optimum wind-powered water injection process design among **Scenarios A and B**. This will be based on the oil recovery, economic, and environmental performance of the compared scenarios, under similar reservoir and economic conditions to those modelled. The thesis limitations, as well as recommendations for future work will be the subject of *Chapter 9*.

2. Wind Resource Assessment/Location Sensitivity

This section discusses an essential step for the development of offshore wind powered water injection, being the knowledge of the offshore wind potential. Basically, determining different wind parameters that reflect different wind regimes and power extraction feasibility for a given application. Only offshore locations are of interest for the scope of this study. This is to utilise the higher capacity factors, higher wind power potential, as well as enable investigation of potential reduction of power transmission costs and losses compared to traditional gas powered water injection technique (mainly for cases when the host offshore oil platform capacity is limited or injection wells are located far away). The main wind potential elements that are relevant to the thesis concept includes wind system, average wind speed, variability of wind power, and power density.

2.1. Global Wind Energy Classifications

This section represents an attempt to do a preliminary zoning of the global offshore locations that can be considered for the application of the thesis concept.

2.1.1. Zoning of Global Wind Energy Resources

Based on a single consideration of wind power density (WPD), NREL (2005) presented a classification map of wind power potential across the global oceans (Figure 2). The results presented by NREL capture the general features of the distribution of global offshore wind energy potential. Figure 2 places almost the entire zone covered by the Northern and Southern Hemisphere westerlies in the highest class of wind energy potential (class 7). Since this does not reflect the regional differences highlighted by the Zheng et al. (2018) new wind energy classification, the latter classification will be used as a reference for the selection of candidate locations for this thesis.
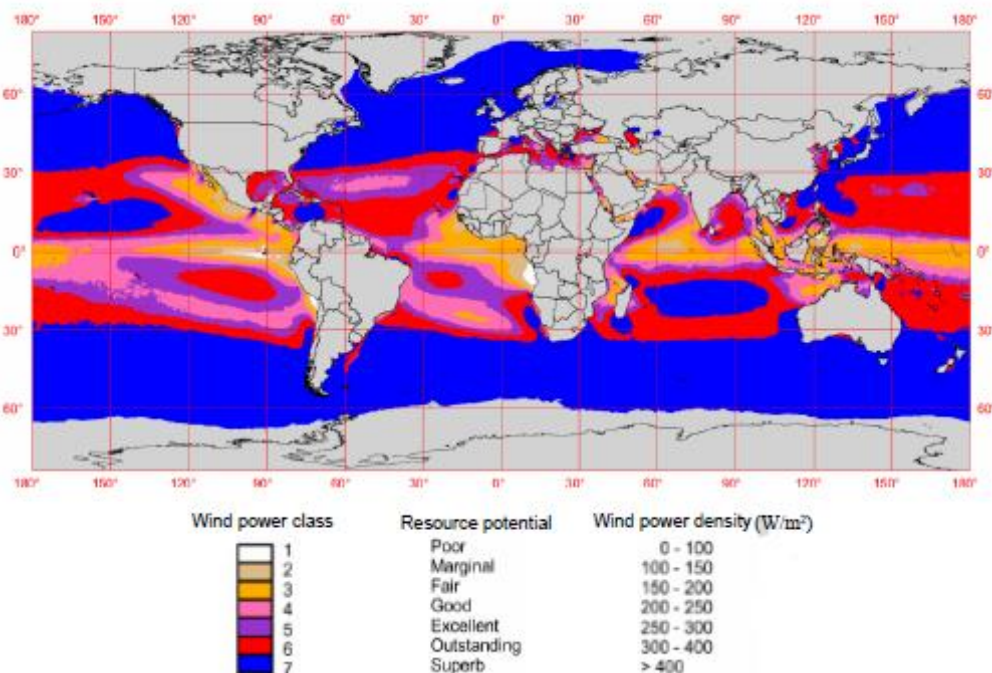
Figure 2: NREL global map of wind power potential classification (NREL, 2005)

Zheng et al. (2018) developed a new detailed wind energy classification scheme that clearly identified the potentially rich offshore wind regions around the globe though a number of

weighed factors. The comprehensive geographical classification provided a cartographic database and complex statistics on wind resource distribution and intensity from global to local levels. However, the data can not commonly be applied in the final phase of the location selection process for wind installations at local level, as supplementary data from on-site meteorological measurements is essential. This practice can be also considered useful to the purpose of a preliminary evaluation of the feasibility of application of the wind-powered water injection in offshore oilfields.

The considered factors include the wind power density (WPD), effective wind speed occurrence (EWSO), rich level occurrence (RLO), water depth (WD), distance to coast (DC), extreme wind speed (EWS), coefficient of variation (Cv), and monthly variability index (Mv). The suitable weighting coefficients for the eight factors above were evaluated by a number of experts and engineers in the field of wind energy development. All the normalized values were between 0 and 1, and both the positive and negative indicators were all converted to positive indicators. The optimal value is 1, and the most unfavorable value is 0. Using 6-hourly global wind data for the period 1979-2016 as well as obtained weighting coefficients, the expectation values of global offshore wind energy were used to zone global offshore wind energy resources.

It should be noted that all of the considered factors in the Zheng et al. (2018) classification are also deemed critical for the presented wind-powered water injection concept in a similar manner to power plants applications except for the DC index. Without normalization, the DC index is regarded a negative indicator for power plants applications, as a higher DC will result in increased connection to the grid costs and added complexity to the marine engineering aspects. As for the stand-alone wind powered water injection concept, the higher the DC, it is expected that this concept will become more feasible. However, the marine engineering complexities will remain. Thus, the weighing factor or scoring for this index could be refined to better suit preliminary evaluation of this thesis project feasibility from a wind/environmental assessment perspective. Yet, this is out of scope for this study. After standardization, the greater the value of the normalized DC and normalized WD, the more favorable the situation for wind energy development. The normalized DC and normalized WD values are presented in Figure 3 (a and b) respectively.
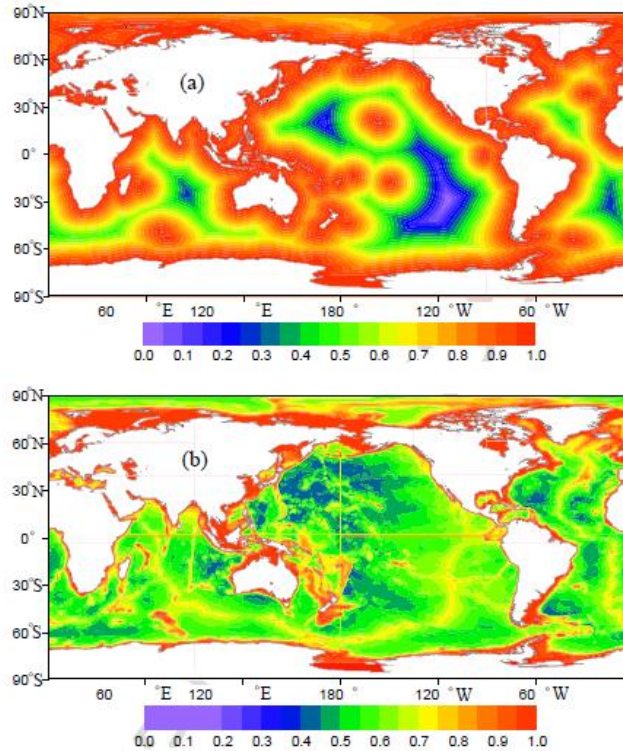
Figure 3: (a) Normalized DC map, (b) Normalized WD map (Zheng et al., 2018)

Generally, in wind energy developments, the normalized WPD value is the most critical measure of the potential of wind energy at a given site. The same trend is expected for the wind-powered water injection concept. High WPD areas are mostly spread in an east-west belt across the zones dominated by the Southern Hemisphere westerlies (greater than 800 W/m2) and the Northern Hemisphere westerlies (less than 600 W/m2). Areas with WPD greater than 100 W/m2 all combined are small, and are located generally in low-latitude waters.

The effective wind speed refers to the suitability of wind speed for wind energy development, and is defined within the range of 5-25 m/s (Miao and Wang, 2012). Obviously, the EWSO is directly connected to the wind energy utilization rate. As shown in Figure 4, the normalized EWSO throughout more than half of the global oceans exceeds 0.5, 0.7, and 0.9 in the zone dominated by the Northern and Southern Hemisphere westerlies. Low EWSO values merely exists in certain small regions in equatorial waters. There is a good agreement between the spatial distribution characteristics of the normalized WPD and normalized EWSO around the Southern and Northern Hemisphere westerlies. However, a noticeable difference is evident in the low-latitude waters. There are also some areas where the normalized EWSO values are high in low-latitude waters (for example, the lower latitudes of the North Atlantic, South Atlantic, and 20°S in the Indian Ocean). This suggests the potential for wind energy development in these low-latitude waters. The regions of typically high WPD and EWSO are expected to be a more viable fit for this thesis project. Wind energy with a WPD higher than 200 W/m2 are regarded as 'abundant', and the occurrence of WPD higher than 200 W/m2 (rich level occurrence; RLO) exhibits the richness of wind energy. It can be clearly seen Figures 4 and 5 that the similar spatial distributions of the normalized EWSO and normalized RLO values, respectively.
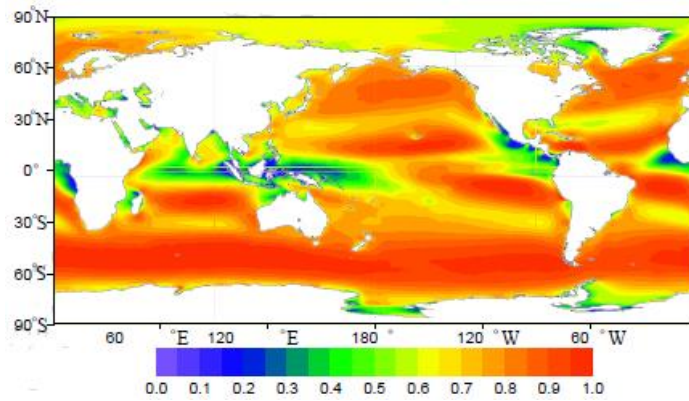
Figure 4: Normalized EWSO map (Zheng, 2018)
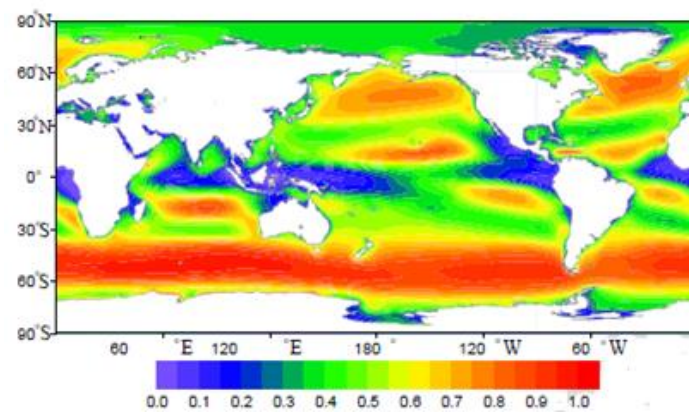
Figure 5: Normalized RLO map (Zheng et al., 2018)

During the development of wind energy, specifically for **Scenario A** application, it is necessary to consider the energy stability. This is beneficial for wind powered water injection, so as to ensure the intermittent injection scheme can be potentially optimized or controlled, as per reservoir characteristics. On the other hand, unstable energy can potentially compromise the intermittent injection scheme, and energy conversion efficiency. The Cv and Mv are generally used to demonstrate the stability and monthly variation of wind energy. After standardization treatment, the higher the magnitude of the normalized Cv and normalized Mv, the higher the stability of the wind energy. The monthly stability (Cv) at low latitudes is considerably better than that at higher latitudes. Also, it is better in the Southern Hemisphere than that in the Northern Hemisphere (Figure 6a). As shown in Figure 6b, low values of normalized Mv are mainly located in the mid-latitude waters of the North Pacific, the mid-latitude waters of the North Atlantic, the South China Sea, the North Indian Ocean, and especially the Arabian Sea. This indicates poorer stability of wind energy at the monthly scale. It is also worth noting that the spatial distribution characteristics of Cv and Mv show clear differences in some regions, such as the Arabian Sea.
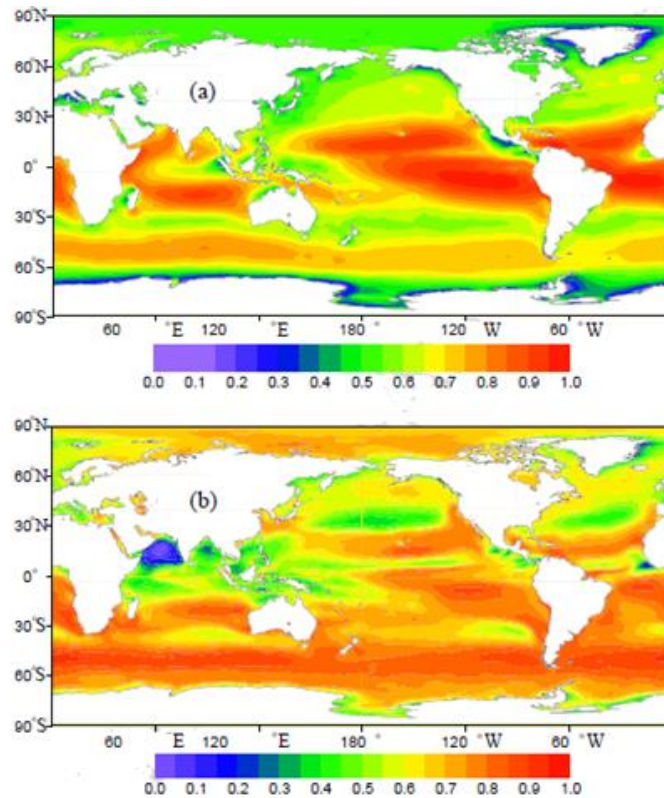
Figure 6: (a) Normalized Cv map, (b) Normalized Mv map (Zheng et al., 2018)

The EWS has a significant impact on the safety of marine engineering aspects of the project. The EWS with a return period of 50 years (U50) is calculated. Following that, the normalized EWS is obtained by applying the min–max normalization method (Figure 7). After standardization, the higher the value of the normalized EWS, the more favorable the ocean environment for this thesis project. The large values of normalized EWS are mostly present in the low-latitude water sites. The normalized EWS in the low-latitude waters is higher than that in the mid and high latitudes. Also, it is higher around the Southern Hemisphere westerlies than that around the Northern Hemisphere westerlies. The EWS values are higher in the Arctic than those in the Antarctic. The Northwest Pacific Ocean, the area of North Pacific westerlies, and the area of North Atlantic westerlies are situated in the low-EWS areas, which signifies a relatively unfavorable ocean environment.
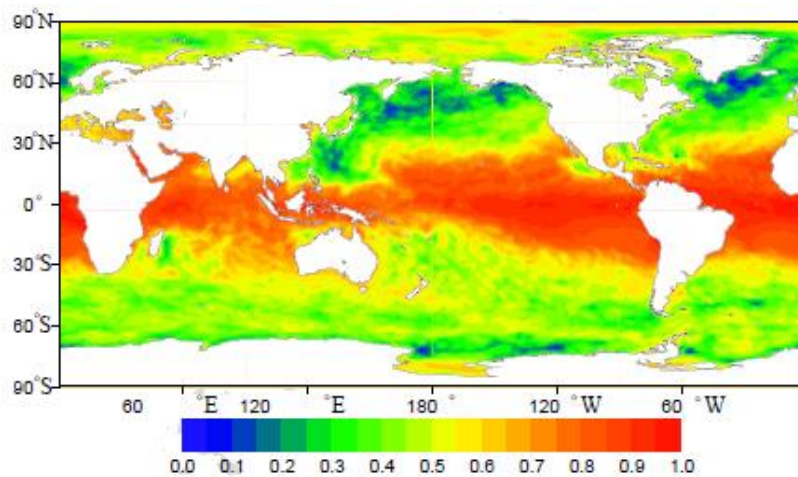
Figure 7: Normalized EWS map (Zheng et al., 2018)

According to the Zheng et al (2018) method, the expectation values of global offshore wind energy resources are obtained, as shown in Figure 8. These expectation values are then divided into seven classes being Poor (Class 1: indigent area), Marginal (Class 2: available area), Fair (Class 3: subrich area), Good (Class 4), Excellent (Class 5), Outstanding (Class 6), and Superb (Class 7: the last four are rich areas). Obviously, the rich areas are mainly distributed around the Southern Hemisphere westerlies, the North Atlantic westerlies, and the Alaska Peninsula. The waters around 30°S and 30°N belonged to the rich area in previous schemes, but are classified as available and subrich areas, respectively. It is worth noting that some low-latitude waters are also located in rich areas, as in the Caribbean Sea, an elliptical area to the south of the Hawaiian Islands, and waters to the west of Peru. The North Pacific westerlies mostly lies in the subrich area. Poor areas are largely located in the mid and low latitude waters (the east–central equatorial Indian Ocean, the western equatorial Pacific Ocean, offshore from the west of Mexico, 15°N in the Pacific Ocean, and 15°N in the Atlantic Ocean), while most of the Arctic belongs to the Marginal area.
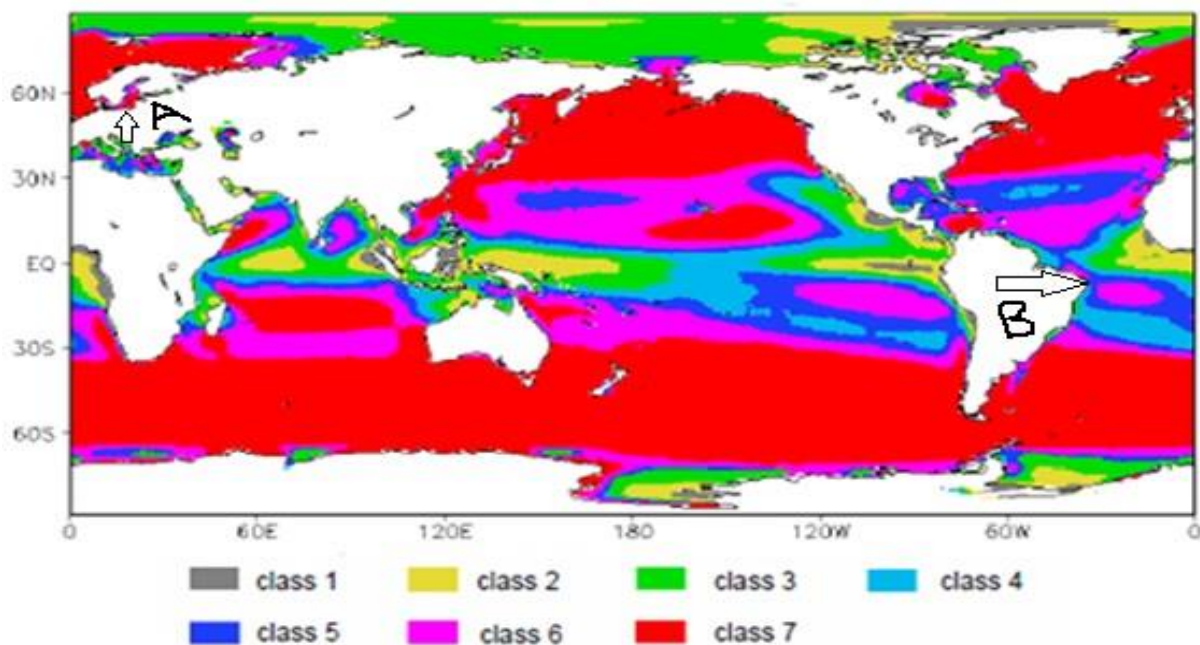
Figure 8: Final map of zoning global offshore wind energy resources (Zheng, 2018)

In conclusion, the Zheng et al (2018) final classification showed five major wind resource hotspots including the central-northern region of North America, southern South America, northern/northwestern Europe, northern Asia and the central-southeastern region of the Asian continent. This was identified based on the large-scale presence and homogeneity of EOS classes. Further researches on the wind climate could consider defining sub-regions. This classification can be used for preliminary investigation of candidate sites feasibility (on regional or sub-regional basis) from a wind resource perspective. However, more thorough analysis for local conditions will be required on case by case basis for the design of a wind-powered water injection system. For instance, complicated orography conditions near a specific site under study could affect the wind speed and direction. This paper will investigate the suitability of various classes to the application of wind-powered water injection from oil recovery and economic perspectives.

2.1.2. Zoning of Global Wind Energy Climates

This section elaborates on another mean of global geographical wind energy zoning/classification is based on type of wind climate (as shown in Figure 9). Main types of wind climates that have different signature annual and monthly wind variability, as well as Weibull distributions, will be briefly defined. Identification of wind climate type can potentially offer a preliminary regional characterisation of wind seasonal variability, wind strength and steadiness, and prevailing wind direction. A link could be established as to which wind climates are capable of providing monthly and seasonal variability patterns that are favourable intermittent water injection schemes for **Scenarios A and B** (Section 5.9). Also, the seasonal wind and monthly wind variability based on the type of climate is expected to affect the cyclic injection starting time, required energy balance by storage or gas cogeneration, and consequently the economic performance of **Scenario B** (Section 6.1.2).
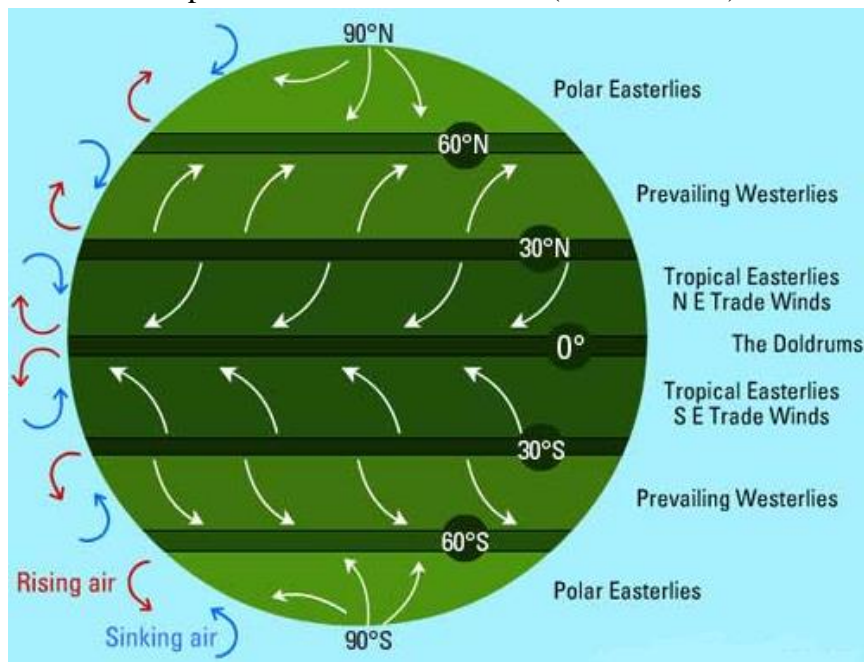
Figure 9: Global map of types of wind climate (National Geographic, 2012)

Wind climates are named after types of dominant winds. Prevailing winds are winds that blow predominantly from a distinct direction over a certain point on the Earth's surface. The dominant winds are the trends in direction of wind with the highest speed over a specific point on the Earth's surface. A region's prevailing and dominant winds are enacted by global patterns of movement in the Earth's atmosphere. In general, easterly flow occurs at low and medium latitudes globally. On the other hand, westerly winds are the rule and their strength is largely determined by the polar cyclone in the medium and high latitudes (Ritter, 2008). The sea and land breeze cycle is significant to the prevailing wind in areas where winds are mostly light. While, mountain and valley breezes are the most important to the wind pattern in areas with a variable terrain (Ackerman, 2005). It should be stated that local winds are those that are created as a result of scenery such as mountains, vegetation, and water bodies. These winds are known to blow for very short distances, and have high variability. As for global winds, they are very large air masses that are created mainly as a result of the earth's rotation, the shape of the earth and the sun's heating power. According to Ritter (2008), the wind systems present on the earth's surfaces may be categorized as following:

Doldrums:

There is a general rise of air in the low pressure equatorial trough as a result of the strong solar heating, leading to the break of moist air into great convection columns. The equatorial belt of calms and variable winds (the doldrums) refers to this region, roughly situated between 5 degrees North and 5 degrees South latitudes. The region has no prevailing winds, however there is a fair distribution of directions. Calms are prevailing for around one third of the time. However, it should be noted that fierce thunderstorms are common in this area. Since this zone is located on a belt of low pressure, it has no strong pressure gradients to induce persistent flow of wind.

Trade wind belts:

The trade wind belts are located to the North and South of the equatorial belt of calms and variable winds. This is roughly situated in the northern and southern zones between latitudes 5 degrees and 30 degrees. These winds are the result of a pressure gradient from the subtropical belt of high pressure to the equatorial trough of low pressure. In both hemispheres, therefore, these winds tend to blow from the east to the west and towards the equator. Sometimes the trade winds are just called "easterlies" to avoid having to specify the hemisphere. The trade winds are characterized by great directional and speed steadiness. It should be noted that the trade wind belts tend to shift towards the North around summer and South in winter, which is attributed to the northern hemisphere large land. The trades are best developed over Atlantic and Pacific oceans.

Winds of horse latitudes:

Winds of horse latitudes are roughly located between 30 and 40 degrees in both northern and southern hemispheres. Horse latitudes winds are focused into distinctive centers over the oceans, rather than continuous belts. The apparent outward spiraling movement of air is directed equatorward into the easterly trade wind system; poleward into the westerly trade wind system. These winds are most commonly developed in the summer in both Northern and Southern hemispheres. It should be noted that horse latitudes tend to shift by roughly less than 5 degrees in Southern hemisphere, and around 8 degrees in the North Eastern Pacific. Furthermore, horse latitudes are known to have low directional steadiness.

Westerlies:

Westerlies winds belt are roughly located between the latitudes 35 and 60 degrees in both Northern and Southern hemispheres. Westerlies winds blow from a southwesterly quarter in the Northern hemisphere and from a northwesterly quarter in Southern hemisphere towards the subpolar lows. However, winds flowing from polar direction in that area are still strong and frequent. This does not negate the fact that the westerly constituents are certainly predominant. The westerlies belts commonly have storm winds and winds are known highly changeable. Westerlies are known to be strongest when the pressure is lower over the poles in winter, and vice versa in summer. The Southern hemisphere westerlies are stronger and more persistent, as the large land in the Northern hemisphere disrupts the Northern westerlies belt.

Polar easterlies:

The prevailing winds blowing from Northern and Southern Poles high pressure areas towards the westerlies areas of high latitudes and low pressure is referred to as Polar easterlies. Polar easterlies have an outward spiraling movement in the Antarctic. It should be noted that Polar

easterlies tend to shift left in Southern hemisphere producing a system of southeasterly winds. These are known to flow the east to the west, and are mostly unsteady and weak.

2.2. Local Wind Energy Characterization

This section elaborates on Weibull distribution (named after the Swedish physicist W. Weibull, who applied it when studying material strength in tension and fatigue in the 1930s) as a tool for wind power prediction, variation of wind speeds, and subsequently, wind energy and wind-powered water injection potential assessment depending on the shape and scale parameters. Weibull distribution is often used as a good approximation of wind speed distribution. The statistical distribution of wind speeds (both in its shape, and in its mean value) varies from place to place around the globe, depending upon local climate conditions, the landscape, and its surface. Thus, it offers another preliminary local/global characterisation of wind profiles and wind resource assessment. A link will be established in section 5.7 as to which wind parameters values are capable of providing favourable intermittent water injection schemes for **Scenarios A and B**. The following sections discuss how the values of the shape and scale factors affect the wind speeds Weibull distribution (Wais, 2017).

2.2.1. Scale factor

'a' is the Weibull scale factor in m/s; a measure for the characteristic wind speed of the distribution. It is proportional to the mean wind speed. As the scale factor increases, the Weibull curve is more stretched, proportionally. Thus, it indicates the potentiality of the wind power of that site, whereas the greater the value of a means higher wind speeds and higher potential of wind sites.

2.2.2. Shape factor

'k' is the Weibull shape parameter. It specifies the shape of a Weibull distribution and takes on a value of between 1 and 4 according to the nature of wind wave. A small value for k (below 2) signifies very variable winds, while constant winds are characterized by a larger k (fairly consistent wind speed around the median will have a k of 3). Also, the higher the k, the higher the median wind speed, the more peaked the curve, and the higher the probability the wind speed will be in a very narrow range. If the shape parameter is exactly 2, the distribution is known as a Rayleigh distribution.

3. Overview of Cyclic Water Injection

This chapter provides an overview of literature on cyclic water injection. This topic is relevant to this thesis study, as from a petroleum engineering and injection scheme's perspectives it matches **Scenario B**. The literature on cyclic water injection could provide the basis for analysis and understanding of the reservoir's response (in terms of oil and water production) upon applying **Scenario A**.

Cyclic water injection (CWI) is a recovery method which enhances the oil production mainly in heterogeneous and stratified reservoirs. The process constitutes varying injection rates from high values to low or injections in symmetric or asymmetric cyclic periods, ranging from days to months per period. This period of injection is referred to as the pressurizing half cycle (on-injection interval). After a certain period of injection, the injector is stopped or reduced for a given time period, which is referred to as the de-pressurizing half cycle (off-injection interval). According to Zhongrong et al. (1995), the CWI process have been confirmed to be technically and commercially viable in a number of Russian and Chinese fields. Early publications related its application to dual-porosity systems, specifically fractured reservoirs (Yanosik et al., 1988). It has been proposed as a zero cost EOR process, wherever facilities for water injection are already available. According to Elkens et al. (1968), the enhanced recovery is achieved by improved sweep of previously bypassed oil in lower permeability layers. The process makes use of the pressure transient response in regions of different permeability, leading to forced imbibition of the lesser permeable layers, in the case of stratified reservoirs.

3.1. Potential of Cyclic Water Injection

Surguchev et al. (2008) stated that CWI has been proven to have the highest potential in cases of layered heterogeneous reservoirs, low communication between reservoir zones of low and high permeability, large pressure differentials between reservoir units, fractured reservoirs, and pressure-dependent permeability in fractured zones. The potential of cyclic injection was globally confirmed in a number of fields, laboratory and numerical investigations (Pooladi-Darvish and Firoozabadi, 2000). However, there has not been a clear consensus on the theoretical explanation of the process and its basic mechanisms (Qingfeng et al., 1995). All the simulated cases produced additional oil in the range of 2-20%, as well as reduced water production, compared to a conventional waterflood (Langdalen, 2013).

The results of field tests show that the recovery factor can be enhanced from 3 to 10% compared to traditional waterflooding, while maintaining lower watercut and for minimal additional costs (Zhonggrong, 1995). Perez et al. (2014) mentioned that mainly thin fluvial sands saturated with viscous heavy oil, high area-thickness ratio, long history of secondary flooding, high water cut, and low recovery factor reservoirs were the selected candidates for CWI. In West Siberia, cyclic waterflooding was successfully applied at several major oil fields like Trekhozernoye, and Ust-Balyk among others. The total cumulative additional oil production in the three main oil producing regions of Russia amounted to 23.2 million tons in 1984 (Surguchev et al., 2002). CWI was also applied to the Spraberry field in Texas, and showed an improvement in cumulative oil production and lower water cut level (Elkins et al., 1968). The increment in recovery is claimed to be better when CWI is combined with pattern rearrangement. Such effect

was shown by plugging high water producing intervals for a 4-year simulation study (Surguchev et al., 1999).

The uncertainty in the mechanism is demonstrated in the fact that a number of field trials have shown inconsistent results, whether as lower increments of cumulative production compared to simulations or no actual production change compared to conventional water flooding. For example, when a field test was performed on an oilfield in Germany, there was no confirmed increase in oil production (Groenenboom et al., 2003). This uncertainty provides a basis for investigating potential yield patterns on a case-by-case basis, specifically by using numerical simulations.

The main risk associated with using cyclic injection, apart from loss of production, is damage to the formation and infrastructure (wellbore integrity and surface facilities). Casing deformation is the major concern for a compacting reservoir (Fjær et al., 2004). Furthermore, fracture pressure (horizontal stress) could be lowered significantly in high permeable layers of depleted reservoirs without a change in collapse pressure (pore pressure) in very tight and low permeable shale layers (Fjær et al., 2004). This in-situ state could perhaps result in stability difficulties for infill drilling. Thus, changes in reservoir pressure by alternating injection pressure must be equalized by increased injection in an offset injector.

3.2.   Mechanism of Increase in Oil Recovery by Cyclic Water Injection

This section explains the mechanisms associated with the additional oil production resulting from CWI. During the pressurizing half cycle water is injected and the reservoir pressure increases. Water is expected to imbibe into the low permeable layers from the high permeable zones. The magnitude of the imbibed water is depending on wettability, injection rates and pressure gradient between the layers. With a longer injection period, more of the low permeability rock surface area will be affected by the injected water. When the injection is reduced or shut-in the reservoir pressure will drop and countercurrent flow of both oil and water, from the low permeability rock into the high permeable zones, will take place. As the injection is restored initiating a new cycle, the newly mobilized oil in the high permeable layers can easily be swept towards a producer (Yaozhong et al., 2006).

Surguchev et al. (2008) carried out a number of CWI simulations below bubble point pressure, designed to ensure gas saturation not exceeding the critical level, which yielded additional recovery of 5.9% of OOIP. This effect was credited to the energy of released gas, expelling the matrix oil into the fracture.

Perez et al., (2014) offered an alternative theoretical interpretation of the process. It was argued that the high oil incremental from CWI can still be achieved even in total absence of capillary forces or heterogeneity. Oil saturation gradients on the displacement front (after the on-injection period) were explained to be the main cause for the oil migration towards the higher permeability layers, which takes place during the off-injection interval. During the off-injection period, the incremental oil saturation in the higher permeability layers forms increased mobility

paths to the producers. As the oil saturation is increased in the high permeability layers, water mobility is also diminished.

The oil recovery efficiency has been shown to improve by an increase in fluid and volumetric displacement efficiency. Surguchev et al. (2002) proposed two types of mechanisms that affect oil recovery by CWI based on a number of simulation investigations:

1. Improved microscopic sweep efficiency, due to hysteresis of the capillary and relative permeability curves at the micro-level. In a water-wet rock, the relative permeability of water will increase with increased water saturation, while that of oil will decrease. As a result of the low relative permeability of water at low water saturations and the capillary pressure in a water-wet rock, water has a low flow capacity in the low permeable layers (Surguchev et al., 2002). During pulsing, oil, water and gas flow switches between imbibition and drainage, and vice versa, as pressure differences increase or decrease. Halted water injection permits capillary pressure to become the dominated force. This could lead to a more effective recovery, because of possible increased water saturation in lower permeability regions by means of water retention. Rock and fluids will expand because of lower pressure, and improve expulsion of oil from matrix into fractures through compressibility (Elkins and Skov, 1963). Furthermore, sweep efficiency is enhanced through oil migration on the high saturation gradient around swept zones, reducing water channeling and fingering by means of stabilization of the displacement front. In addition, by keeping injected water in the reservoir, its energy is raised, oil production is increased and water cut is reduced.

2. Improved vertical sweep efficiency, due to better sweep of the least permeable layers in contact with most permeable ones, caused by forced imbibition or improved cross-flow between layers. The cross flow occurs naturally by means of gravity or capillary forces, but the pressure transient should accelerate this process (forced imbibition). From pressure response analysis, it should be expected that in layered reservoirs pressure should be restored at different rates. Pressure differences between zones will control the compressibility, and be the main provider of cross flow. Compressibility is a function of pressure; hence the pressure will change faster in water saturated layers than in an oil saturated layers (Schipanov et al., 2008). Therefore, in the high permeable layers mostly saturated with water, pressure drops faster compared to the low permeable layer with more oil, and the vertical pressure difference between low and high permeable layers is increased (Qingfeng et al., 1995). The cross flow magnitude of each phase is controlled by the phase's relative permeability at a specified point in the reservoir. Therefore, the mobility of a fluid is strongly controlling the success of CWI.

The hysteresis effects will not be considered for the analysis of this paper results, due to time limitation and the added complexity of having different capillary pressure and relative permeability curves for drainage and imbibition. The capillary pressure curve applied for all three wetting- cases is fitted for a water-wet rock. Thus, the base case will be tested under water-wet conditions to obtain higher accuracy of the results. Different wettability profiles will be created, mainly by different residual oil saturations in the reservoir which is a major controlling factor for a waterflood. In conclusion, analysis of the simulation results will be done on basis

of capillary imbibition, reservoir compressibility, pressure and saturation gradients, and relative permeability effects in the cases under study.

3.3.   Parameters Affecting the Performance of Cyclic Injection

This section explains the detrimental effect that some key reservoir parameters can have on the success of CWI. These parameters include injection rate, vertical transmissibility (VT), reservoir pressure with respect to the bubble point, wettability, initiation time, injection scheme, well spacing, fractures, fluid and rock compressibility, oil saturation profile, and reservoir heterogeneity among others.

3.3.1.   Injection Rate Effect

Babadagli (1994) stated that after a certain value an increase of injection rate will worsen the effect of capillary imbibition. Putra et al. (1999) showed that as the injection rate is increased beyond a critical value, the contact time between injected fluid and matrix is reduced, and the capillary imbibition efficiency is limited. The critical water injection rate is defined as the maximum injection rate where the benefit of the capillary imbibition is absent, and the optimum injection rate is achieved where the capillary imbibition and capillary forces are balanced (Putra et al., 1999). A critical water injection rate is best evaluated experimentally, whilst an optimum injection rate must be attained by simulation studies.

3.3.2.   Vertical Transmissibility Effect

Vertical communication between the high and low permeable layers is considered as a crucial parameter for the amount of increase in oil production by the CWI approach. An increase in VT should lead to higher effect of gravitational force and enhance the vertical sweep. Thus, higher VTs increase the incremental recovery by CWI via cross flow, but there is a level beyond which the benefit from cycling is negligible (Qinfeng et al, 2018). A VT above the critical level reduces the benefit of CWI compared to continuous waterflooding (WF). This can be explained by the fact that the increase in transmissibility enables gravitational segregation, improves the communication between the layers allowing a better vertical sweep, and outweighs the advantage of the pressure differential as (pseudo-) full communication between layers exists. Langdalen (2014) concluded via simulations that the increase in VT is discouraging for the cyclic injection effect. The results showed an incremental increase in cumulative oil production by 1.17% and 3.16% for the higher (VT = 0.5) and lower transmissibility (VT = 0.1) models respectively.

3.3.3.   Reservoir Pressure Effect and critical gas saturation

Qingfeng et al. (2018) showed that CWI is beneficial at any level of reservoir pressure, but this incremental recovery over waterflooding diminishes as the pressure is lowered below the bubble point pressure. This effect can be attributed to the energy of released gas phase at saturation below critical gas saturation increasing compressibility of the fluid system. However, the incremental gain from CWI, compared to WF, when applied at a reservoir pressure below the saturation pressure. It was pointed out that CWI should not be effective below the bubble point. Putra et al. (1999) argued that three-phase flow effects may or may not be beneficial for the process, as added compressibility from the released solution gas could also make CWI more effective.

3.3.4. Wettability Effect

Some authors claim that the process is more favorable in water-wet reservoirs, while others indicate that the process is more efficient in oil-wet systems. Prabhakar (2013) stated that the oil-wet rock is more suitable for cyclic injection. For the oil-wet case, the remaining oil volume in the reservoir is considerably higher than for the water-wet case, due to high water relative permeability. High oil saturations present in the reservoir provides greater benefit of CWI, in terms of the fluid magnitude exchanged by capillary imbibition during the pressurizing half cycle and compaction during the de-pressurizing half cycle. As injection is reduced with cyclic injection, the contact time between water and formation is enhanced and more imbibition of water into the low permeable layers takes place.

Langdalen (2014) confirmed Prabhakar (2013) findings, and mentioned that the cumulative water and oil production for CWI were, as expected, between the respective values for the water and oil-wet case. The results also showed in all three wettability cases, the optimum injection scheme was similar.

3.3.5. Initiation Time Effect

Langdalen (2014) explained that at lower water cuts pressure alternation could enhance oil recovery only due to the effect of increased oil distribution gradient between the high and low permeable layers. The water saturation difference between different permeability layers is increasing as the waterflood matures. In a mature flood, the oil saturation in the low permeable layers is greater compared to in the high permeable layers, where water has displaced more of the oil.

Yaozhang et al. (2006) explained that under a relative low water cut the exchange rate of oil by water will be low and RF will see less enhancement. CWI was concluded to be best applied at water cuts of 95% or higher. As the capillary and gravitational forces will better enhance oil production with higher water saturations in the high permeable zones. In this case, the difference in fluid mobility and phase pressure between the high and low permeable layers is increased. This creates excellent conditions for water to displace oil from the low permeable zones.

Prabhakar (2013) observed that highest incremental benefits achieved by CWI compared to WF took place when initiated at medium-high water cuts. CWI (with 30 days base period) applied at a water cut of 75%, produced 14.1% additional oil over the conventional WF. Initiating the CWI at higher water cuts had a negative effect on oil recovery, where an unexpected decrease in incremental oil production occurred as CWI was started at 85% water cut. Moreover, the incremental reduction in water production was decreasing with higher water cuts.

Shchipanov et al. (2008) conducted a number of fractured systems core experiments showing that the benefit from CWI when initiated from the start. It was also found that below a critical oil saturation, no benefit from cycling was seen. Thus, it was concluded that the cyclic initiation time in ongoing waterflooding projects is a critical parameter to be considered for the process design.

Shchipanov et al. (2008) showed that the duration of the cycle length is controlling the influence of compressibility, gravity and capillary forces on cross flows and the process efficiency. Sheng (2013) stated that the effectiveness of CWI increases for larger shut-in periods. Nevertheless, for too long shut-in periods, reservoir pressure drops too much and the pressure limit in the producer well restricts the oil production.

Stirpe and Guzman (2004) numerically investigated the effect of cycle symmetry and base period length of CWI efficiency. Various symmetric cycles using base period of 15 days, 1, 3 and 6 months were investigated. The cumulative oil production did not show significant differences versus continuous WF. Only a modest increment in recovery factor for a period of 4 years was found, going from 28.8 for WF up to 29.5 for CWI in the best case.

Rublev (2012) also simulated a number of symmetric and asymmetric injection schemes, within a total duration of 6 months and using a constant injection rate, including 1:1 with 7 days as a base period (7 days injection followed by 7 days injection shut in), 1:1 with 5 days as a base period, 1:2 with 5 days base period, 2:1 with 5 days bas period, and 1. The best variant was concluded to be the asymmetric injection scheme of 1:2 with 5 days base period. Putra and Schechter (1999) similarly concluded that a 1:2- cyclic scheme, yet with a base period of 30 days, is optimum.

Langdalen (2014) analyzed three types of cycles, ratios of 1:2, 1:3 and 2:1 injection to shut-in periods, with base periods of 15 and 30 days. The 1:3 injection scheme was shown to be the best scenario for the 2 base period cases, however the incremental benefit of CWI compared to WF was higher for the 30 days base period case. Thus, it seems that longer asymmetric cycles (3-month case) yield better oil recovery.

Prabhakar (2013) discussed the possibility of varying the cycling period as the flooding progresses. A few cases were run to test this idea, but no significant improvement was evident. It was observed that compressibility-induced cross flow is dominating if the cycle lengths are short, and during a long-time cycle period the capillary and gravity forces are the dominant forces.

Prabhakar (2013) stated that increasing injection pressure is beneficial to increase oil recovery. The high pressure can lead to generation of fractures in the reservoir, thus the extended stimulated volume contributed to additional oil recovery.

Sheng (2013) carried out a series of CWI core experiments that showed that RF increased with the injection pressure, which can be identified since the first cycle. For extremely low injection pressures, the total water injected by CWI becomes too low to be compared to the continuous injection case. This also lowers the increment in oil production and the water production. The incremental RF achieved by CWI was attributed to the greater pressure gradient between the high and low permeable zones during production. As injection pressures in excess of 5,000 psi were applied, fractures were generated in the core plug after 6 cycles. Furthermore, injecting above reservoir initial pressure lowered the incremental recovery achieved by CWI compared to conventional WF.

3.3.8. Well Spacing Effect

Langdalen (2014) investigated the effect of well spacing on the efficiency of CWI. Two well spacing cases were simulated using a 2D model, a shorter well spacing case of 1640ft and a longer well spacing case of 3280ft. For the case with shorter distance, the water injection and liquid production rates were adjusted to the new reservoir volume; 700STB/day of injection and 640STB/day of liquid production for the longer well spacing case. The short spacing case resulted in an over 1% higher incremental production increase compared to long spacing. The short spacing resulted in a larger increase in oil production regardless of the cyclic setup nor the base period. As the distance separating the wells is reduced, the relative size of formation directly influenced by the CWI is enhanced as the reservoir is being produced over the same period. Thus, injected water in a reservoir with short well spacing will faster reach the producer. In other words, the effective contact time between formation and water for a short spacing system will be longer compared to a long-spaced system over the same time period. Both the short and long spacing case achieved higher RFs via CWI.

3.3.8. Fluid and rock compressibility:

Fluid and rock compressibility affect the reservoir pressure response and hence the choice of cycle parameters, including injection scheme and base periods. During off-injection intervals, the reservoir pressure will be lowered and stress changes can lead to the mobilization of new oil. Decrease in reservoir pressure will compress the rock and lower porosity. As compaction leads to a decrease in porosity, the residual oil volume in the reservoir will be less than the initial condition without compaction. Thus, zeroing of the injection rate should be expected to mobilize new oil.

3.3.9. Oil Viscosity:

Yaozhong et al. (2006) reported that as the oil viscosity increases, the oil cumulative recovery decreases, yet the CWI shows better efficiency compared to continuous WF (up to 20% incremental oil in 12 years). It has been reported that the efficiency of the CWI should increment at higher oil viscosity, implying increased control over viscous fingering by means of pulsing, but not further details were provided in the paper. Furthermore, it was stated that for oil viscosity bigger than 100cp, the simulation model showed injectivity issues because of the limit on injection pressure.

4. Simulations

4.3. Black Oil Simulator 3D Model

In this section the 3D reservoir simulation models are elaborated, and the base case reservoir properties are described. For a better understanding of the physical benefits at micro-level (changes in reservoir pressure cause capillary and viscous forces, gravity and compressibility to behave different than under a conventional, steady-state waterflooding), a black oil model is applied with Eclipse100. Eclipse100 is a fully implicit, 3-phase and 3-dimensional black oil simulator. Black oil simulation and streamline models are effective tools working with CWI. The results obtained with Eclipse100 are expected to provide a low numerical error as Newton's method of solving the non-linear equations is used (Langdalen, 2014). The purpose of the study is to analyze critical variables and physical mechanisms therefore, an idealized model was built and simulated.

The 3D model input parameters and simulation grid are based primarily on literature values (Langdalen, 2014). The reservoir model was developed by choosing a consistent set of fluid and flow properties. A 3D-model was created for more realistic results, and to be able to detect potential alternation of flow patterns in the reservoir that is expected to be associated with intermittent or cyclic injection. The model size is $1000x1000x10 m^3$, and consists of 9000 active grid cells distributed in a 30x30x10 grid system along the x, y and z direction for a corner point grid. Parameters have been set in a way to ensure that the numerical dispersion is limited to an acceptable error.

Rock data, fluid data and initial conditions are given in Tables 2 and 3. The majority of the data in *Appendix B* were sourced from the second SPE comparative solution project (Weinstein et al., 1986) to build up a functional model. The base case model has a symmetric permeability and layer thickness as shown in Figure 10 and Table 1. The vertical permeability was set by kv/kh ratio of 0.1 (meaning that the vertical permeability is equal to 10% of the horizontal permeability). If more than one fluid is present in the system, the effective permeability measures the ability to flow a particular fluid through the reservoir rock (Ezekwe, 2011). The ratio of effective permeability to absolute permeability is defined as the relative permeability (Ezekwe, 2011). Water relative permeability and oil relative permeability are referred to as K_{rw} and K_{ro}, respectively. Water-wet relative permeability curves (Figure 11 and *Appendix B*) were calculated from the Corey equations and are considered to be reasonable. The Corey coefficients were set to be within the range of those proposed by Behrenbruch and Goda (2006). A water-wet reservoir has often a lower residual oil saturation and higher relative oil permeability, and is expected to have a higher ultimate recovery than the mixed and oil-wet cases.
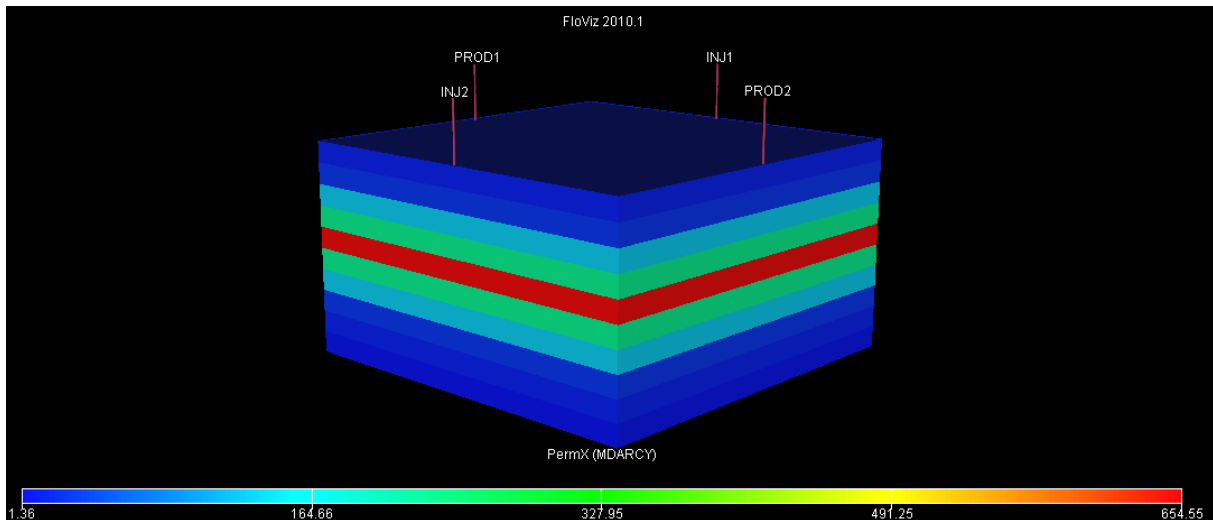
Figure 10: 3D model and the horizontal permeability distribution
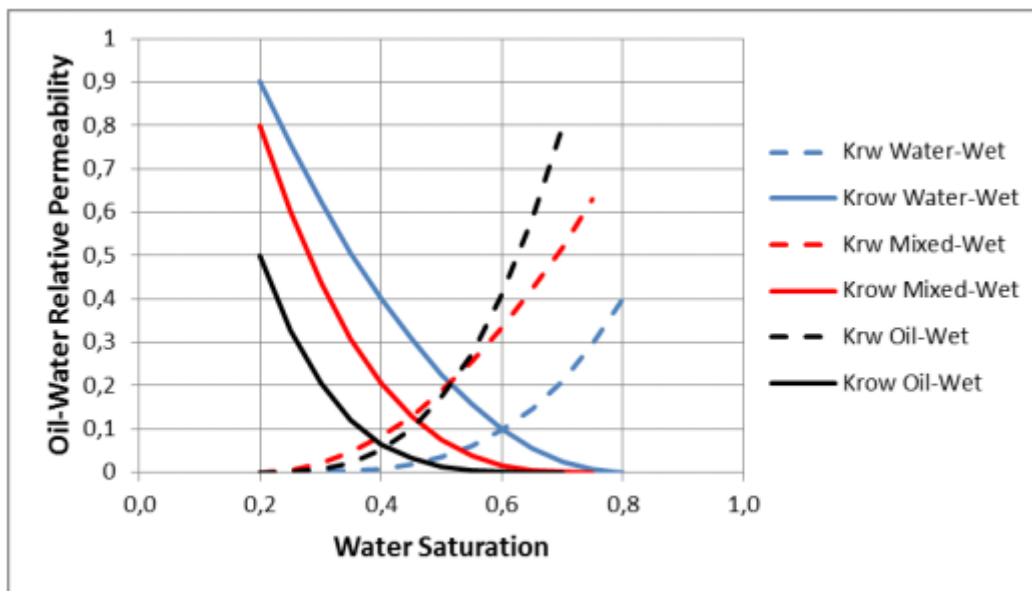
Figure 11: Oil-water relative permeability for all wettability cases (Langdalen, 2014)

Two pairs of wells were created in the model. The two injectors (INJ1 and INJ2) are located at the grid blocks (15,1) and (15,30), respectively, as illustrated in Figure 10. The production wells (PROD1 and PROD2) are located at the center of the y axis, in grid blocks (1,15) and (30,15), respectively. This well placement is not optimum, as a significant amount of oil is expected to be left in the center and in the reservoir corners (waterflood pattern alteration induced by CWI can potentially extract that bypassed oil). All wells are completed throughout the reservoir (from z=1 to z=10). The producers are controlled by a BHP limit of 5500 psi (38MPa). By maintaining the producer BHP and total injection volume for each scenario, potential benefits or limitations are merely related to the parameters studied and can be compared with certainty.

Numerical results accuracy is strongly dependent on the simulation model time step length. In this study, the injection schedule was designed with the potential to vary to either zero or maximal value every 3 hours, depending on wind resource availability. Even though Eclipse100

24

applies a fully implicit approach to maintain stability during long time steps, the simulation time step size was set at 3 hours for higher accuracy. Obviously, the simulation error is limited with shorter time steps, yet another aspect is to be able to model the pressure variations within each cycle to accurately simulate the cyclic process. PermX is permeability in the X-axis direction, and DZ is layer thickness.

Table 1: Layer thickness and permeability distribution for the symmetric base case

Layer	PermX (md)	DZ (ft)
Layer 1	13.64	32.8
Layer 2	27.27	32.8
Layer 3	136.36	32.8
Layer 4	231.82	32.8
Layer 5	654.55	32.8
Layer 6	231.82	32.8
Layer 7	136.36	32.8
Layer 8	27.27	32.8
Layer 9	13.64	32.8
Layer 10	1.36	32.8

Table 2: Rock and fluid data and initial conditions, (Langdalen, 2014)

Rock compressibility	4E-06 psi
Water compressibility	3E-06 psi
Stock tank oil density	45 lb/ft
Stock tank water density	63.02 lb/ft
Standard condition gas density	0.0702 lb/ft
Saturation pressure	5600 psi
Porosity	0.3
Oil pressure at GOC	6600 psi
Depth of GOC	8990 ft
Depth of OWC	9500 ft
Payzone thickness	328 ft

Table 3: Endpoint fluid saturations and Corey coefficients for the Base Case (water wet), (Langdalen, 2014)

S_{wi}	0.2
S_{orw}	0.2
S_{org}	0.2
S_{gc}	0.05
$K_{ro@Swi}$	0.9
$K_{ro@Sgi}$	0.9
$K_{rw@Sorw}$	0.4
$K_{rg@Sorg}$	1
n_o	3.5
n_w	2
n_g	1.5

4.4. Selection of Study Locations

General considerations taken into account for the selected locations included the following: wind data availability, belonging to different wind class regions of relatively high wind resource based on Zheng (2018) map (Figure 8), belonging to different wind climate systems, and being locations of known major offshore oilfield accumulations. Based on the pre-mentioned criteria and using the classifications shown in Figures 8 and 9 (sections 2.1.1 and 2.1.2), **Locations A, B and C** (presented in Table 4 and shown in Figure 7) were selected. The aim of this study is to gain an insight into the effect of various wind classes and wind climates on the outcome of the wind-powered water injection process, rather than ranking locations among one another from a wind installation feasibility perspective. Thus, locations were selected randomly from different regions around the globe and no scoring or weighting of the selection criteria indicators will be made.

Table 4: Selected locations

Site	Sea	Country	Distance to shore (km)	Water depth (m)	Coordinates
Location A	North Sea	Netherlands	28	25	52.250 N & 3.592 E
Location B	South Atlantic Ocean	Brazil	20	50	8.150 S & 34.567 W
Location C	Gulf of Mexico	United States	127	85	26.968 S & 96.963 W

Location A (North Sea, Dutch Economic Zone NL7, 52.25 N & 3.59 E) is around 28km from shore of the Netherlands at 25m depth. It is situated within the Dutch Exclusive Economic Zone (EEZ). Governmental regulation describes which regions are reserved for wind farm installation. It belongs to the prevailing westerlies wind climate. According to Figure 8, the majority of the North Sea, including the selected location, lies within wind class 7 (highest class). From a wind energy perspective, other advantages included ease of access from both Rotterdam and Ijmuiden harbours. Given that this site is not too far offshore, the relatively shallow water depth will allow for lower cost support structure designs. From an oil industry perspective, after over 50 years of development the North Sea remains an important part of the global offshore oil landscape. Exact Figures are difficult to ascertain, however there is a general consensus amongst analysts that around 24bn barrels of recoverable reserves exists in the North Sea (Forbes, 2018).

Location B (South Atlantic Ocean, Offshore Brazil, Brazilian Navy Hydrographic Center Buoy 8.150 S & 34.567 W) is 20 km from shore of Brazil at 50m water depth. It belongs to the southern tropical easterlies wind climate. As a result of having billions of crude oil barrels trapped under a thick layer of salt offshore, world class geology, and reduction of reserves elsewhere, Brazil has become Latin America's top oil producer (Reuters, 2018). According to Figure 8, the majority of the South Atlantic Offshore Brazil region, including the selected location, lies within wind classes 4 and 5. There are no regulations in Brazil concerning the distance to install offshore wind turbines, in order to avoid causing a visual impact. Kim et al.

consider that the areas that are located at more than 10km from the coast cause no visual impact. Thus, offshore oil fields in proximity of the site under study can be considered for the application of the wind powered water injection project.

As for **Location C** (Gulf of Mexico, Offshore United States, American National Data Buoy Center 26.968 S & 96.963 W) is 127 km from shore of the United States at 85m water depth. It belongs to the northern tropical easterlies wind climate. According to the Energy Information Administration, Gulf of Mexico federal offshore oil production accounts for 17% of total U.S. crude oil production. Oil production from US Gulf of Mexico reached an all-time annual high of 1.65 million barrels per day in 2017. Production of oil is anticipated to maintain the rising trend in 2018 and 2019, based on ten new oil fields which are planned for production in those years (EIA, 2018). According to Figure 8, the majority of the Gulf of Mexico region, including the selected location, lies within wind class 6. Thus, offshore oil fields in proximity of the site under study can be considered for the application of the wind powered water injection project.

The Argoss database have been used to obtain the environmental data for **Location A**, while the American National Oceanic and Atmospheric Administration (NOAA) was used for **Locations B and C**. The timeline series provided a data record every three hours of the past 10 years (January 1st 2008 till December 31st 2017). The output file provided a dataset where the rows hold the three-hour average value of the corresponding column variable (windspeed, direction, wave height, etc.).

Other factors related to assessment of candidate offshore wind installations locations including current conditions, wave conditions, sea depth, soil type, distance to ports, distance to grid connection, were not considered for being out of scope for this study. However, this section will touch upon the general relevancy of these factors to the concept under study. First, current conditions are of crucial importance for the support structure design and scour assessment. Second, distance to ports is significant for the logistics of offshore wind installations. Proximity to a port facilitates the installation process, mainly a result of shorter travel time over the water with all components. Additionally, being close to the shore during the operational life of the turbine guarantees to a higher extent that maintenance crews are able to reach the wind installation fast and secure. This vastly influences the O&M costs of the wind system. Since average wind speed increases farther from shore/port, hence a compromise should be made.

Third, distance to power grid connections dictates the needed cable length for connecting the wind installation to the onshore power grid. Given the high costs of electrical cables, distance to the power grid controls a considerable percentage of the total installation cost. Furthermore, a longer cable also results in higher loses between the wind farm and the onshore electrical station. This parameter should not be taken into account, if the designed wind system is assumed to be entirely autonomous as it is the case in this thesis. Fourth, wave conditions influence the support structure design. For instance, mild wave conditions requires lighter and less costly support structure designs. It should be mentioned that wave conditions also significant for choice of suitable installation methods, as not all installation techniques can be applied in high seas. Therefore, wave conditions are also influencing the installation time and costs.

Fifth, wind speed conditions play a major role in the power generation performance of a wind turbine. The higher the wind speeds, the higher the generated power can be. However, higher wind speeds also imply higher loads on the support structure and turbine. Sixth, sea depth largely dictates the type of the support structure. Generally, with deeper seas, the support structures become heavier and more costly. Sea depth also affects the choice of wind installation infrastructure and technique. Finally, soil type is a factor that bear crucial significance in the bottom foundation type and installation method. For instance, the harder the soil is, the more complicated the installation process become. However, the bearing capacity for harder soils is greater than that of lower soils. Most commonly, the associated with the cheapest foundation structure is considered more favourable.

The typical associated offshore fields characteristics, and environmental conditions at the selected location also will not be addressed at this stage, yet the effect of key performance parameters will be discussed in *Chapter 5*. It should be mentioned that all of the pre-mentioned out of scope factors, should be considered on case by case basis for the application of the concept of wind-powered water injection in offshore oilfields. Commonly, to be able to assess different candidate sites on the relevant parameters, multi criteria analysis is performed. In this analysis, few weighted criteria are compared to get an indication of the value of each location. Eventually the sites scoring higher compared to other sites should be considered more favourable for application of this thesis concept. It is important to note that no political or company influences were discussed in this section, which will certainly be the case for a real project.

4.5. Wind Data Processing and Characterization

The timeline series provided a data record every three hours of the past 10 years (January 1st 2008 till December 31st 2017). The output file provided a dataset where the rows hold the three-hour average value of the corresponding column variable (windspeed, direction, wave height, etc.). This section elaborates on how the data from the Argoss and NOAA databases was processed into useable wind data with the use of MATLAB.

The raw wind data from the Argoss and NOAA databases were recorded at 10 and 5 meters altitude, respectively. The three-hour average intervals and the respective wind direction are recorded into one array each. The objective is to determine the wind speed at the hub heights of the turbines at the selected sites. Initially, wind data is converted to the meso-height (60 meters) with the logarithmic profile, Equation 1. Then, the power law use used for the height above 60m with the meso altitude as a reference altitude (h_{ref}), Equation 2. Additionally, z_0 is the surface roughness length and α is a power coefficient which on open water are equal to 0.0002 and 0.143 respectively.

$$U(h) = U\left(h_{ref}\right) \cdot \left(\frac{ln\frac{h}{z_0}}{ln\frac{h_{ref}}{z_0}}\right) \quad (1)$$

$$U(h) = U\left(h_{ref}\right) \cdot \left(\frac{h}{h_{ref}}\right)^{\alpha} \quad (2)$$

The Weibull distributions (Figures 12-14) have been evaluated at an altitude of 100 meters, however the code has been written in such a way that the G136-4.5MW turbine hub height (120m) was used for the respective power calculations. Prior to using the Weibull function in MATLAB, the wind speed arrays were sorted by a sort command, and zero values were replaced by the lowest positive non zero value. Given that 0 m/s and 0.2 m/s fall in the same 1 m/s bin width, this should not alter the obtained Weibull distribution results. The estimated shape parameters k, scale parameters a, as well as the average wind speeds for **Locations A, B and C** are shown in Table 5. The Weibull distributions have been fitted to the empirical wind speed distributions. While the wind speed distribution for **Locations A** showed a good fit, it is graphically obvious that the Weibull distribution does not perfectly match the raw 3-hour interval wind speed data for **Locations B and C**. Therefore, the raw data will be used to estimate power output and water injection scheme instead of the Weibull distribution. By choosing the unique wind speeds U with the MATLAB `unique' function the probability density function can be evaluated as shown in equation 3:

$$f(U) = \frac{k}{a} \cdot \left(\frac{U}{a}\right)^{k-1} \cdot e^{-\left(\frac{U}{a}\right)^{k}} \qquad (3)$$

For **Location A**, half of the blue area is to the left of the vertical black line at 9m/s (Figure 12). The 9m/s is called the median of the distribution. This means that half the time it will be blowing less than 9m/s, the other half it will be blowing faster. The mean wind speed of 9.43m/s is actually the average of the wind speed observations at this site. At **Location A**, the highest percentage of occurrences belongs to WS of 8-9m/s (modal value of distribution) and then, 7-8m/s (Figure 12). High wind speeds of greater than 24m/s occurred occasionally.

In **Location B**, half of the blue area is to the left of the vertical black line at 5.1m/s (Figure 13). The 5.1m/s is the median of the distribution. This means that half the time it will be blowing less than 5.1m/s, the other half it will be blowing faster than 5.1m/s. The 5.65m/s is the average of the wind speed observations at this site. The distribution of wind speeds is skewed. High wind speeds are observed, but they are rare. So, this site has enough available power to drive a small wind turbine for electricity generation. The highest percentage of occurrences belongs to WS of 4-5m/s, and 5-7m/s, respectively. High wind speeds of greater than 16m/s occurred occasionally. As it is expected, higher wind speeds experience lower frequency of occurrences. For example, the frequency of wind speeds in range of 11-12m/s is half of 1-2m/s.

As for **Location C**, half of the blue area is to the left of the vertical black line at 5.8m/s (Figure 14). The 5.8m/s is the median of the distribution. This means that half the time it will be blowing less than 5.8m/s, the other half it will be blowing faster than 5.8m/s. The 5.59m/s is the average of the wind speed observations at this site. Highest wind speed observed at the site was 20.5m/s. The highest percentage of occurrences belongs to wind speeds of 3-5m/s, and 5-6m/s, respectively. High wind speeds of greater than 16m/s occurred occasionally. As it is expected, higher wind speeds experience lower frequency of occurrences. For example, the frequency of wind speeds in range of 9-10m/s is half of 2-3m/s.
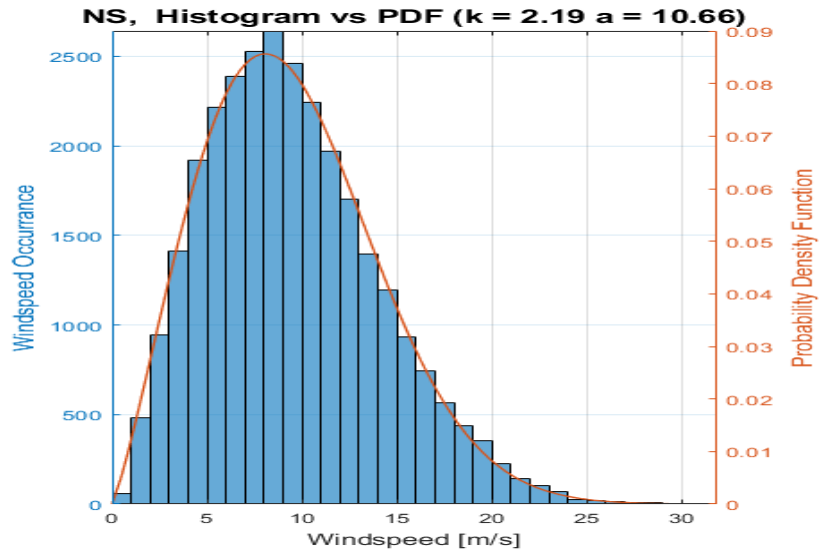
Figure 12: Weibull curve of Location A
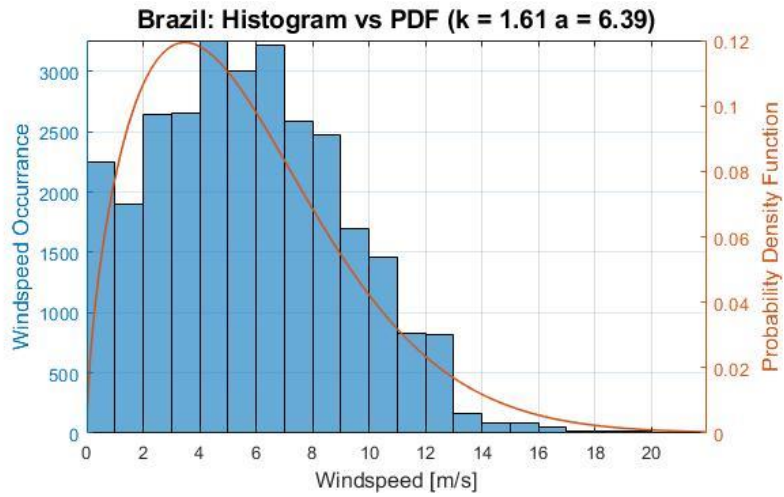
Figure 13: Weibull Curve of Location B
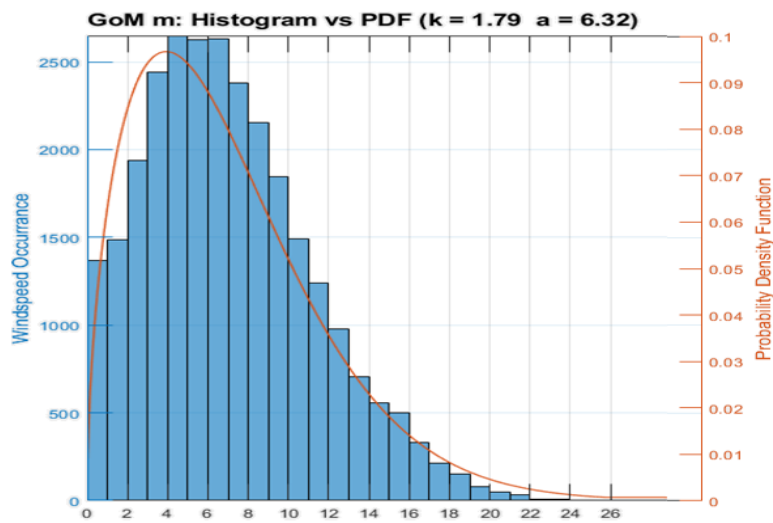
Figure 14: Weibull Curve of Location C

Table 5: Weibull parameters of selected locations at 100m

Location	k	a	Uavg
A: North Sea, Netherlands	2.19	10.66	9.43
B: South Atlantic, Brazil	1.61	6.39	5.65
C: Gulf of Mexico, USA	1.79	6.32	5.59

The variation of wind and wave parameters is evaluated in terms of monthly and seasonal distributions in the whole domain, and the quantitative assessments are carried out in the specific locations to represent the wind characteristics. Finally, different climates of the wind in the selected locations will be evaluated. This investigation will help better understanding of the potential of application of wind powered water injection in the study areas in order to be utilized for preliminary screening of candidate offshore sites and wind climates.

The wind speed data is statistically analyzed to find out different wind characteristics of the selected sites. The ten years annual mean wind speed data is shown in Table 6. For **Location A**, annual mean wind speeds at 100m height in the region varied between 9.1-10.3m/s. Monthly mean wind speeds were in range of 5.9-14m/s (*Appendix B*). In **Location B**, annual mean wind speeds at 100m height in the region varied between 5.2-7m/s. Monthly mean wind speeds were in range of 3.4-11.5m/s (*Appendix B*). As for **Location C**, annual mean wind speeds at 100m height in the region varied between 6.8-7.4m/s. Monthly mean wind speeds were in range of 4.6-10.5m/s (*Appendix B*).

Table 6: Annual mean wind speeds of selected locations

Annual Mean Wind speeds (m/s)			
Year	Location A	Location B	Location C
1	9.3	5.4	6.8
2	9.3	7.0	7.2
3	9.6	6.6	7.4
4	9.7	5.6	6.9
5	9.2	5.4	7.1
6	9.1	5.4	7.0
7	10.3	5.4	6.8
8	9.5	5.3	7.4
9	9.6	5.2	7.1
10	9.1	6.9	6.9
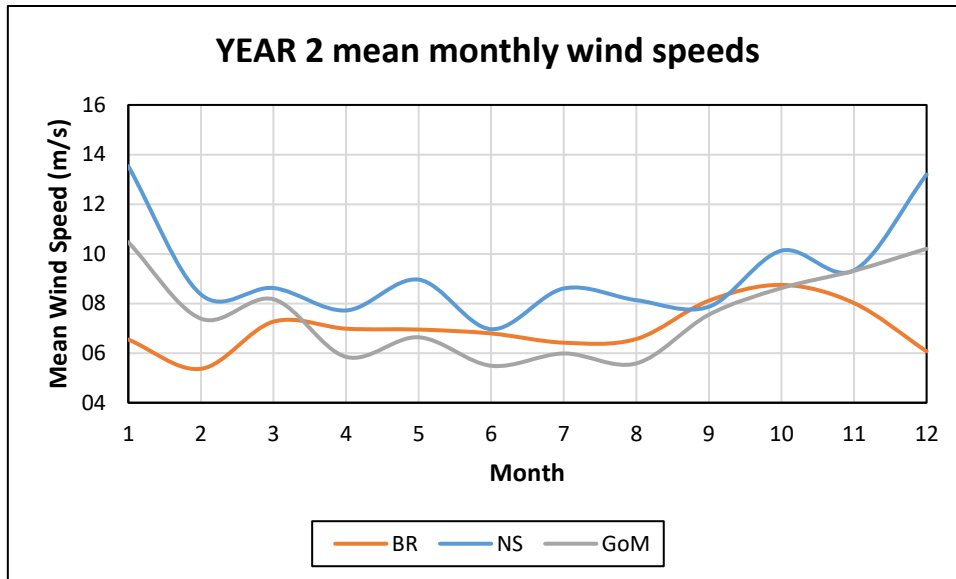
Figure 15: Year 2 mean monthly wind speeds for Locations A (NS), B (BR), and C (GoM)

Figure 15 shows the monthly variation in wind speeds at all sites under study in Year 2, which conforms to expectations based on their respective type of wind climate. In order to a clearer idea of wind characteristics at these two locations, monthly and hourly variation of wind speed distribution is presented in *Appendix B* showing the 3-hourly mean wind speed measured at **Locations A, B, and C** for the 10 years under study. Large seasonal variability was observed at **Location A**, where wind and wind power were relatively large in late Autumn and Winter, and were smaller in Spring and Summer (Appendix B). Monthly variability for **Location A** was relatively higher in Spring and Summer as well. At **Location B**, seasonal variations were relatively small with monthly wind speeds experiencing around 2 small peaks per annum around mid-Spring and late Summer. At **Location C**, seasonal variations were relatively large, where wind and wind power were relatively large in late Autumn and early Winter, and were smaller otherwise (*Appendix B*). Comparison of seasonal and monthly variability indices for both locations indicated that generally, the variability of is highest at **Location B** followed by **Locations C and A**, respectively. Highest monthly mean wind speeds observed at **Locations A, B and C** were 14m/s, 11.5m/s, 10.5m/s, while the lowest monthly wind speeds were 5.9m/s, 3.4m/s, and 4.6m/s for the respective locations (Appendix B). It is clear from Figure 15 that the mean wind speed at **Location A** is higher than **Locations B and C**, respectively.

4.6. Selection of Wind Turbine

A wind turbine is a mechanical structure that converts the kinetic energy of the wind into mechanical energy through the induced rotation of aerofoil-shaped rotors. The rotational force of the rotors is then used to drive a generator and produce electricity. There is a limitation to the percentage of kinetic energy that a wind turbine can extract from the wind, which is equal to 59.3% known as Betz limit. The proportion of energy extracted is generally referred to as the Power Coefficient. This limit was determined by assuming an ideal rotor extracting energy from a homogenous tube of air flowing through the rotor at a constant velocity. Obviously, if all kinetic energy is extracted from the air, zero energy can be removed as a result of static air mass prohibiting further the flow of air through the rotor.

In practice Betz' limit has not been reached in all commercially available turbines at any given wind speed. The power curve of a single wind turbine model determines its power output. A power curve is an experimentally measured relationship between wind speed and expected power output. This is constructed by means of averaging corresponding wind speeds and power outputs over 10-minute intervals, and then placing the results into 1m/s wide bins. The power outputs are then averaged again within each individual bin. Therefore, the power curve, along with the Weibull distribution, is one of the two main components required to estimate the AEP of a turbine at a particular site. This is the industry standard at the moment, but recent studies have suggested that a dynamic power curve will produce more accurate results (Milan et al., 2008). For the purpose of this study, the power curves provided by the manufacturer will be used (Figure 16).

For the wind-powered water injection, firstly the wind characteristics were taken into account. In **Location A**, the average wind speed has been 9.11 m/s (at a height of 100m) in the past 24 years according to data obtained and scaled by the Argoss database. In addition, it was observed that wind speeds of 25 m/s are hardly ever exceeded. Thus, turbines with rated power output slightly above 10 m/s and cut-out around 25 m/s were examined. The reliability of the manufacturer is another extremely significant aspect to be considered for offshore wind turbine selection. Since accessibility in remote offshore locations can be relatively expensive in case of failures or unplanned maintenance, and it also strongly depends on weather conditions. Therefore, choice was made for only reputable and trustworthy manufacturers with outstanding track records.

All the relevant data for the wind turbines under study were sourced from WindPro 3.1 software, in addition to turbines manufacturers' brochures, depending on availability. The combination of the WindPro 3.1 software and the manufactures brochures provided a very long database and comprehensive description of the available turbines in the market. The sourced turbine data included power curve as well as blade diameter, power and thrust coefficient, top mass, and RPM range, among others. The selected turbines for further evaluation and their main characteristics are shown in Table 7. The turbines provided below are all designed for offshore use. It should be stated that only turbines with complete datasets containing all the main characteristics required for the explained analysis were selected for further study, in order to reduce assumptions to a minimum.

This section aims at selection of the optimum wind turbine for **Location A**. As explained in the previous section, the Argoss database was used to collect and process the environmental data, so as to create a MATLAB model that shows the exhibited wind speeds and their probability of occurrence, estimating AEP and capacity factor. Using the MATLAB model, 4 commercially available wind turbine models in range of 4-5MW, which matches the power requirement of the water injection base case configuration, were tested: V117-4MW, SWT130-4.2MW, G136-4.5MW, and G136-5MW. The power output of each turbine in relation to the wind speed is illustrated in Figure 16. According to common investment decision making, the turbine which has the lowest LCOE is the best possible choice. Obviously, the favourable outcome for a wind turbine is to produce as the highest amount of electricity possible at the lowest attainable cost

for maximum profits. Energy infrastructure projects are commonly compared based on their Levelized Cost of Electricity (LCoE), which is defined by equation 4:

$$LCOE = \frac{C_{invest}}{aE_y} + \frac{C_{O\&M}}{E_y} + \frac{C_{decom}(1+r)^{-T}}{aE_y} \qquad (4)$$

Where E_y is the annual energy production. A simple cost estimate calculation was carried out, as the actual price of the turbines under study was not provided by the manufacturer. The initial investment costs (C_{invest}) and lifetime operational costs ($C_{O\&M}$) were estimated to be 1400 \$/Kw and 0.0375\$/kWh, respectively (Mone, 2016). A discount rate of 8% was chosen, the annuity factor (a) was also calculated through the discount rate (r), and a project lifetime (T) of 10 years. The resulting LCOE was calculated for each turbine, Table 8. It is important to mention that this economic analysis is not fully accurate but it can give a good estimation for this initial economic assessment. Given that the LCOE results were based on a number of assumptions and turned out to be quite very close for all turbines, additional analysis was carried out to reach a conclusion so as to the most reliable choice possible. Following the LCOE calculation, performance of each turbine was studied. The selected turbine should optimally have the highest AEP and capacity factor, as AEP is not sufficient as the sole basis of selection. Specifically for this project in which the power production isn't the ultimate goal nor the source of revenue. The wind capacity factor of a candidate location is one of the most significant criteria to be taken into account by the investor, since it will have the largest impact on the expected investment returns. Also, it is a useful indication of the suitability of the turbine to the location of interest. Therefore, the capacity factor was calculated to investigate the performance of all turbines under study, Equation 5. It is defined as the proportion of time a wind turbine is operating at its own rated capacity:

$$C_f = \frac{AEP}{P_{rated} \times 8760} \qquad (5)$$

Where P_{rated} is the rated power of the turbine (i.e. generator capacity) and 8760 is the number of hours in a year.

Table 7: Wind Turbine Models

Model	Rated Power (MW)	Rotor Diameter (m)	Default Hub Height (m)	Cut-in (m/s)	Rated Speed (m/s)	Cut-out (m/s)
V117-4MW	4	117	91,5	3	14	25
SWT130-4.2MW	4.2	130	85	3	15	28
G136-4.5MW	4.5	136	120	3	13	25
G128-5MW	5	128	120	3	15	30
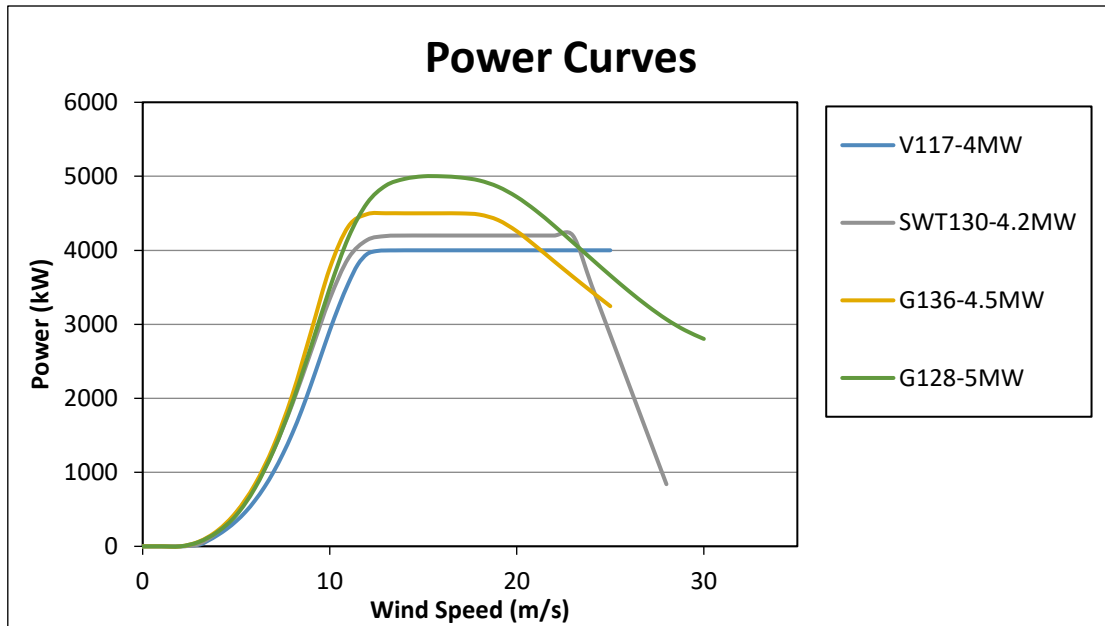
Figure 16: Wind turbines power curves

Knowing that the turbines under study had different default hub heights, wind speeds were converted to the default hub height of the respective turbines using the same procedure described above. Consequently, a different Weibull distributions was obtained for each model. Following that, the AEP for each turbine was calculated by means of combining the Weibull distributions the corresponding turbine power curves via MATLAB. According to Table 8, the two leading turbines are the Gamesa G136-4.5MW (highest capacity factor and second highest AEP), and the Gamesa G128-5MW (highest AEP and second highest capacity factor). As expected, the largest turbine Gamesa G128-5MW has the highest AEP. This could be explained by the fact that this model has a higher power output at lower wind speeds, and these lower wind speeds had a higher probability of occurrence relative to that of the higher wind speeds. However, the Gamesa G136-4.5MW showed a better performance, since it has the highest capacity factor and the second highest AEP. Furthermore, selecting the Gamesa G136-4.5MW, is considered more suitable to the application at hand in which the availability of rated power production to meet the target injection rate for longer periods has higher priority over the total energy production. Finally, G136-4.5MW is a turbine which already has an excellent track record in offshore wind farms. Considering all of the mentioned facts, a decision was made to proceed with the Gamesa G136-4.5MW wind turbine. Table 8 shows all the relevant data used for the final turbine selection.

In order to choose the best turbine for an offshore site a lot of factors need to be taken into account such as the type of the drive train (geared or direct) and the generator, resistance of the blades and other equipment to erosion caused by humidity and salt, power electronics configuration, etc. For this project all of the previous mentioned aspects were not taken into account, since it will greatly increase the complexity. As of this project, the main factors which were considered were the rated power and cut-in, rated and cut-out speed alongside the reliability of the manufacturer. The turbine selected for **Location A** will be used for **Location B and C** injection scheme designs for simplicity. Since the purpose is to study the reservoir response under various realistic wind variability patterns and consequent intermittent injection

schemes, this is considered acceptable. Ideally the same analysis applied for turbine selection in **Location A** should be repeated for **Locations B and C**.

Table 8 Wind turbine performance characteristics in Location A

Model	AEP (GWh/yr)	Cf	LCOE ($/kWh)
V117-4MW	11.9	0.34	0.107
SWT-4.2MW	12.9	0.35	0.105
G136-4.5MW	13.8	0.35	0.106
G128-5MW	14.5	0.33	0.109

4.7. Intermittent Water Injection Schemes

This section elaborates on the intermittent and cyclic water injection schemes designed for this these, which are summarised in Table 9.

4.7.8. Scenario A: 100% Wind

MATLAB was used to create an injection schedule that varies every 3 hours based on the wind power output in **Location A** (North Sea, Dutch Economic Zone NL7) throughout the day. In order to represent daily, monthly, and annual variability, 3-hourly average wind data over the period of 10 years were sourced from Argoss database. This was adapted to the water injection rate. The injection schedule includes injecting at 44,000b/d per injector during time periods when the wind turbine is producing the power required to run the injection pumps at full capacity (4MW), and then zero injection otherwise. This power configuration and injection rates were broadly based on Slatte (2014) DNV GL's WINWIN pilot study. This power configuration is only valid assuming the candidate reservoir has sufficient injectivity, and thus could potentially be scaled up or down on case-by-case basis. This was simulated as on and off injection cycles using the keyword WCYCLE in Eclipse 100. The purpose is to assess whether water injection could tolerate 3-hourly variations of wind speed and power generation from an oil recovery perspective, through comparison of the results with **Scenarios B and C**. Figure 17 shows the FWIR for all scenarios over 3650 days. This scenario resulted in a total of around 994 days of water injection, amounting to 87.5MMbbls of water, over the course of 10 years. This corresponds to a water injection capacity factor of around 27%, and injection to no injection ratio of 1:2.8. The longest period of continuous injection was 6 days and 15 hours, while the longest period of no injection was 23 days and 18 hours. The most occurring on-injection period was 3 hours, on the other hand the most occurring off-injection period was 12 hours.

4.7.9. Scenario B: Wind + Storage, Cyclic Water Injection

Scenario B aims at maintaining control over the intermittent injection schedule via using a storage solution in addition to the wind turbine or a hybrid. The aim is to fix the duration of the on and off injection intervals per cycle, and consequently the injection scheme, throughout the simulation period. Taking the cyclic scenario that had the most consensus in the literature, the 1:3-scheme with a base period of 30 days was simulated to be the basis of **Scenario B**. The injection schedule includes a constant repeated cycle of 30 days of injection, followed by 90 days of no injection, which amounts to a total of around 931 days of water injection over the course of 10 years. Figure 17 shows the FWIR for **Scenario B** over 3650 days. This was simulated as on and off injection cycles using the keyword WCYCLE in Eclipse 100. For the

base case of this scenario, the total injection volume target is set at 87.5 MMbbls, matching that of the base cases of **Scenarios A and C**. Thus, the injection rate was designed to be 47,000bbl/d per well. The power system design of this scenario, including the wind turbine, storage solution, water pumps configuration, were not considered at this stage and will be later presented in *Chapter 4*. This scenario will be compared with **Scenarios A and C** in order to investigate its technical feasibility from an oil recovery perspective, as well as its economic feasibility (*Chapter 6*).

Table 9: Injection schemes with their respective injection rates

Scenario	Description	Injection Rate (bbl/d)	Injection Volume (bbl)	Injection Scheme	Base Period
Scenario A	Intermittent (fully wind powered)	44,000	~87.5	Variable (based on wind resource)	Variable
Scenario B	Cyclic (wind and gas powered)	47,000	~87.5	1:3	30 days
Scenario C	Continuous (fully gas powered)	12,000	~87.5	Continuous	NA
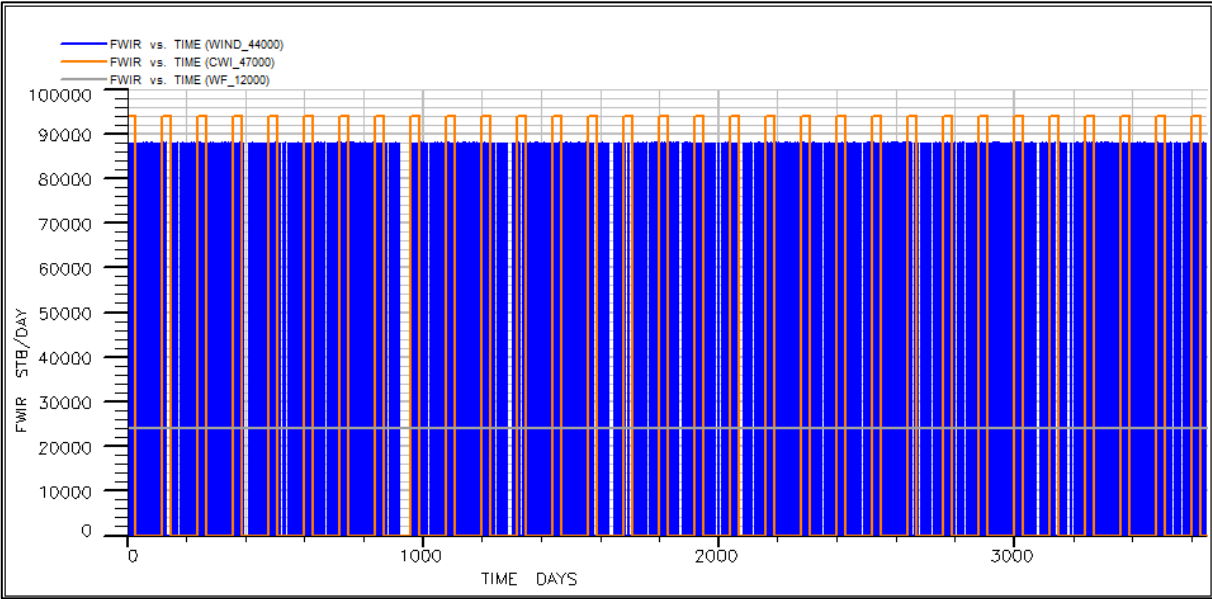
Figure 17: FWIR of all main scenarios over 10 years, Scenario A (Blue), Scenario B (Orange), Scenario C (Grey)

Scenarios A and B will be analyzed in comparison with **Scenario C** (which represents the conventional gas-powered continuous water flooding) for a fixed volume of water injected, with respect to a number of critical wind and reservoir variables including wind climate (effect of average wind speed and wind variability pattern at a given site, optimum process design (injection rate, ratio of on/off periods, base period of on and off cycles), wettability conditions, vertical transmissibility, symmetry of permeability distribution, water injection initiation time and reservoir heterogeneity.

5. Results and Discussion

The simulation results presented in this chapter are related to the case, system design and scenarios described in chapter 4 (Table 9) with an average reservoir pressure above the saturation pressure – no gas present in the reservoir and a constant gas-oil ratio.

5.1. Effect of Injection Scheme Design

Using the base case 3D reservoir model and **Location A** wind data, all cycles are initiated at the beginning of the production period, at day 1. Therefore, the dominant recovery mechanism is water drive. Total water injection for **Scenarios A and B** deviated with -0.2% over **Scenario C.** It was clear that **Scenario B**, being the more intensive injection scheme that provided the highest injection rate (provided that the reservoir has sufficient injectivity) and longest injectors shut-in period per cycle as well as overall, resulted in the greatest increase in cumulative oil production, Figure 18. An incremental cumulative oil production increase of 2.3% was seen for the **Scenario B** injection scheme, with one month of injection and three months of injector shut-in, compared to **Scenario C** (continuous water injection). Table 10 shows that **Scenario A** injection scheme resulted in the second highest oil recovery with an incremental increase of 0.7% over **Scenario C**. Figures 18-20 also show how the injection scheme is affected by the length and overall duration off-injection periods. As the length of the off-injection period is reduced from **Scenario B** (90 days per cycle and overall duration of 2719 days) to **Scenario A** (12 hours was the most occurring duration per cycle, maximum of 23 days and 18 hours per interval, and overall duration of 2656 days), the additional oil recovery over **Scenario C** decreased. This can be attributed to the decrease in contact time between the injected water and formation, especially with the low permeable zones, under shorter off-injection periods per cycle in **Scenario A**. Thus, improved water imbibition towards the lower permeability layers was more evident for **Scenario B**.
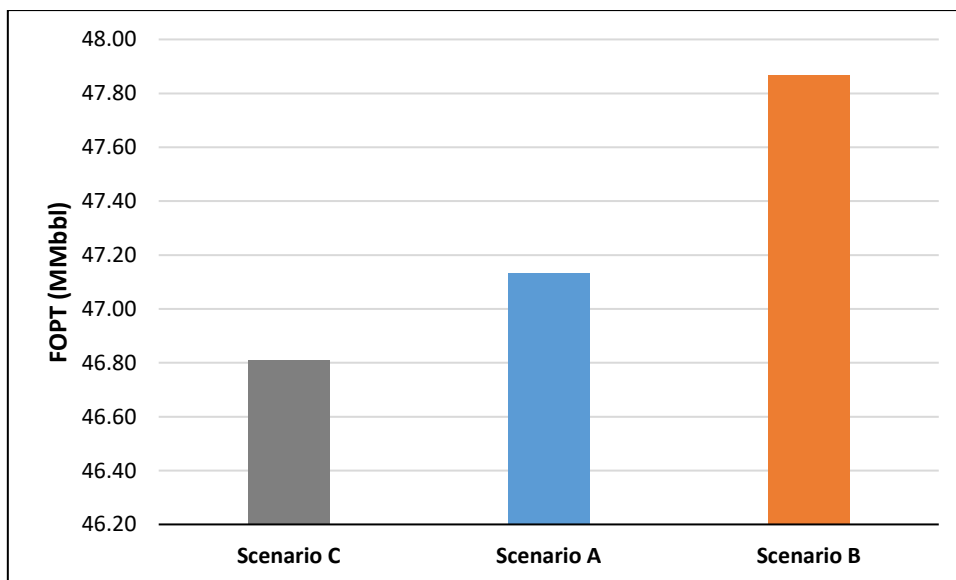
Figure 18: FOPT (total oil field production) of all main Scenarios under the base case

Table 10: Intermittent water injection scenarios with their respective incremental change in FOPT and FWPT (total field water production), BTT (breakthrough timing)

Scenario	Incremental Increase in Oil Recovery	FWPT (bbl)	BTT (days)
Scenario A	0.7%	30,193	1,500
Scenario B	2.3%	29,146	1,470

A large amount of the additional oil produced during the **Scenario B** can be directly related to the greater pressure amplitude observed during the pressurizing (on-injection) and de-pressurizing periods (off-injection), Figure 19. The pressure was fluctuating above and below the pressure observed under **Scenarios A and C**, Figure 19. The water injection rates were modified for the intermittent and cyclic water injection schemes to yield approximately the same volume of injected water as **Scenario C**. This resulted in **Scenario B**, with the longest overall shut-in duration, having the highest injection rate and greatest pressure amplitude. As the intensity of the injection is reduced in **Scenarios A and C**, in respective order, the injection rates were reduced, and less additional oil production was observed. Hence, clearly a more intensive injection scheme should be applied for a water-wet reservoir. However, it should be noted that for a real field the injection pressure is limited with respect to capacity and formation damage, and could not be increased above any unreasonable value.
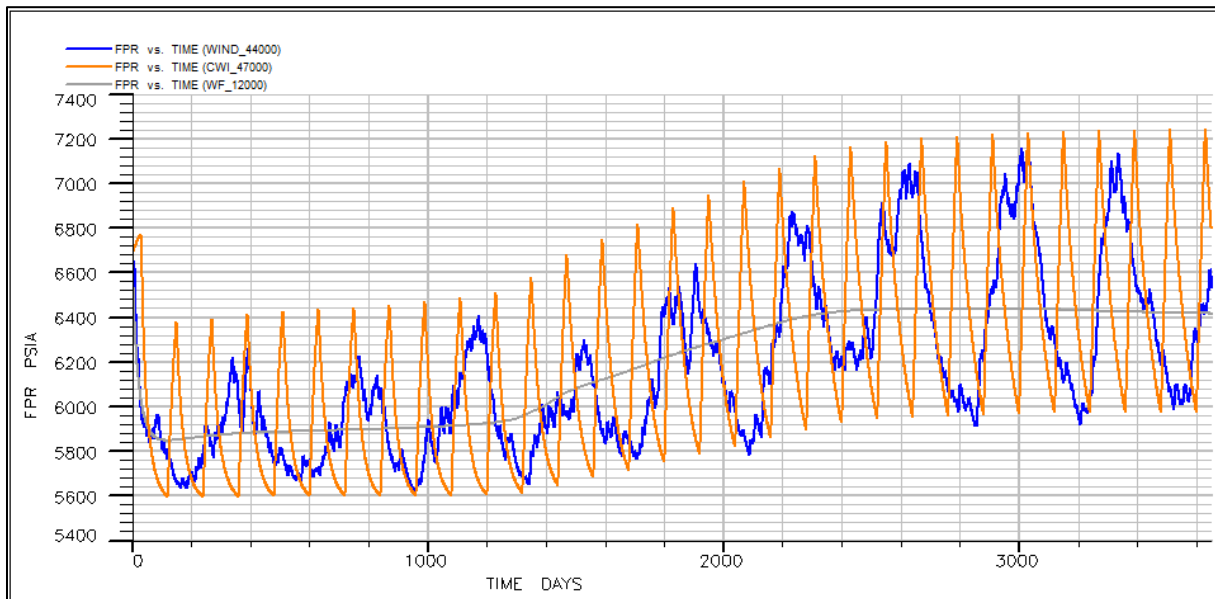
Figure 19: FPR (average field pressure) of all main Scenarios under the base case over 10 years
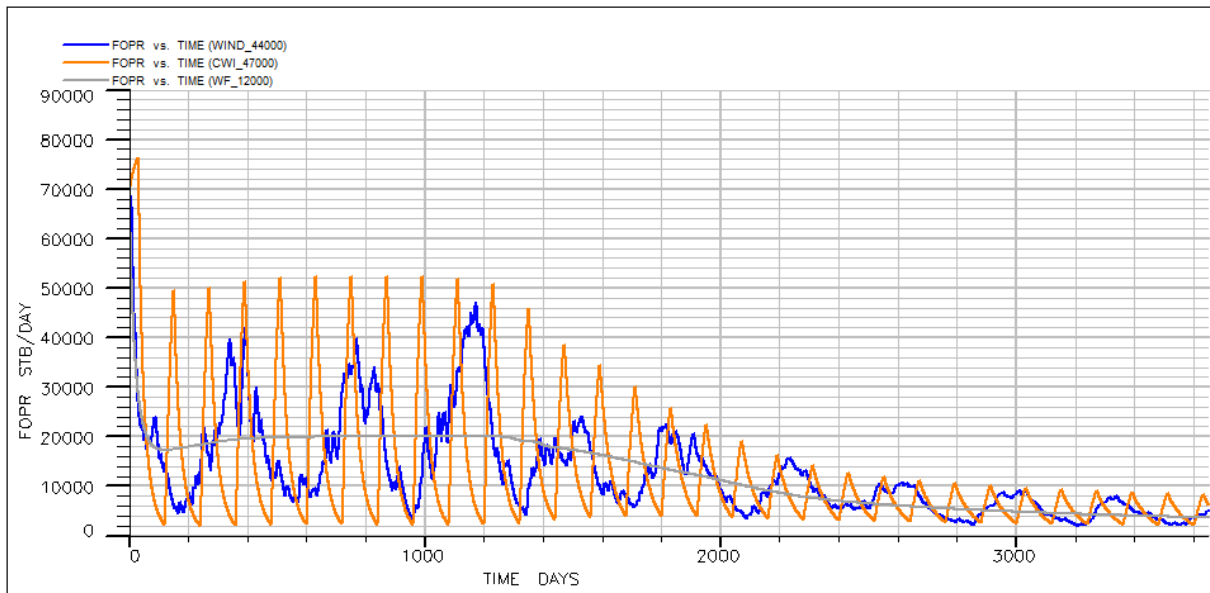
Figure 20: FOPR (field oil production rate) curves of all main scenarios under the base case over 10 years

Increasing the oil saturation in the high permeable layers by gravitational and capillary forces is of critical importance to the success of intermittent and cyclic injection schemes. Cyclic and intermittent injection appears to better sweep previous poor swept areas, and leave less oil behind. In all scenarios, high permeable layers have experienced approximately the same sweep, and early water breakthrough. Major difference in oil saturation was observed in the low permeable layers. This effect is clearly seen from Figures (21-23). The layers 2 and 8 which are among the lowest permeability zones, are better swept with the **Scenarios B and A**, respectively, compared to **Scenario C**. During the on-injection periods, pressure can reload energy in the reservoir and low pressure zones can be formed during production. The pressure transferring capacity in the high permeable layers are greater than in the low permeable layers. This means that the high permeable zones will become low pressure zones. In the off-injection periods, oil in the low permeable layers is swept vertically (cross flow) into the adjacent high permeability layers, and eventually towards the producers. In addition to the expected enhancement in vertical cross flow and compaction at pore level, the CWI can alternate the waterflood patterns laterally, and increase the areal sweep efficiency. The variation in total cumulative oil recovery among the simulated scenarios is quite notable, despite the total water injected in the reservoir being equal. It can be, then, concluded that the positive effect of cyclic and intermittent injection is clearly present.
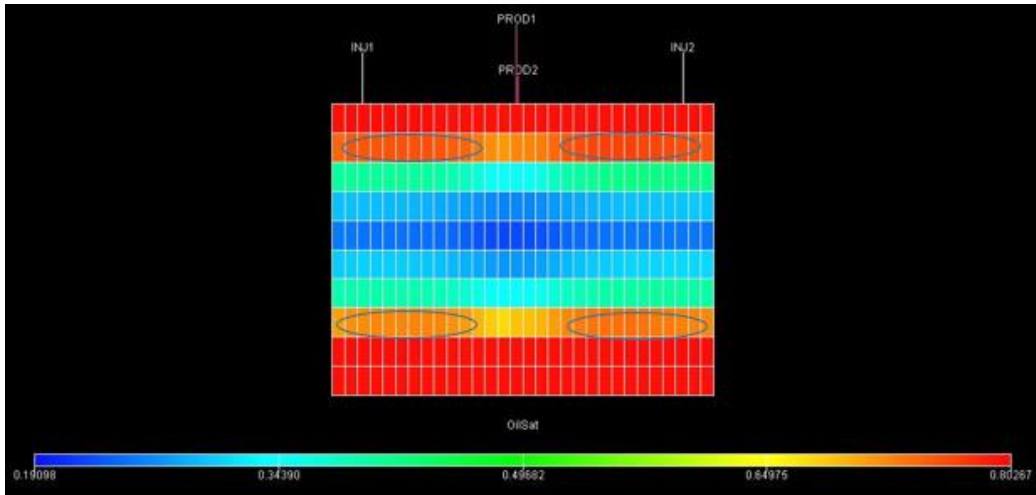
Figure 21: Scenario A oil saturation under the base case after 10 years
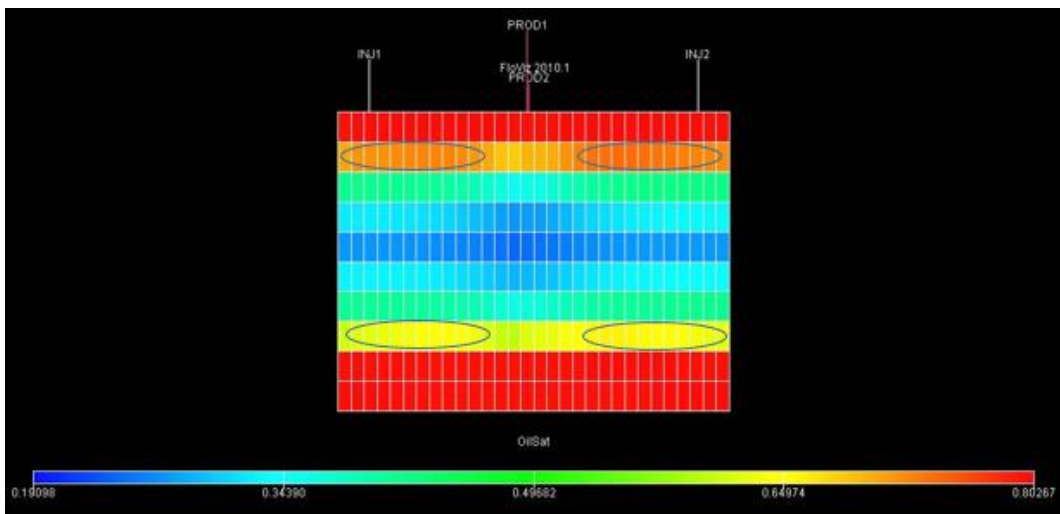
Figure 22: Scenario B oil saturation under the base case after 10 years
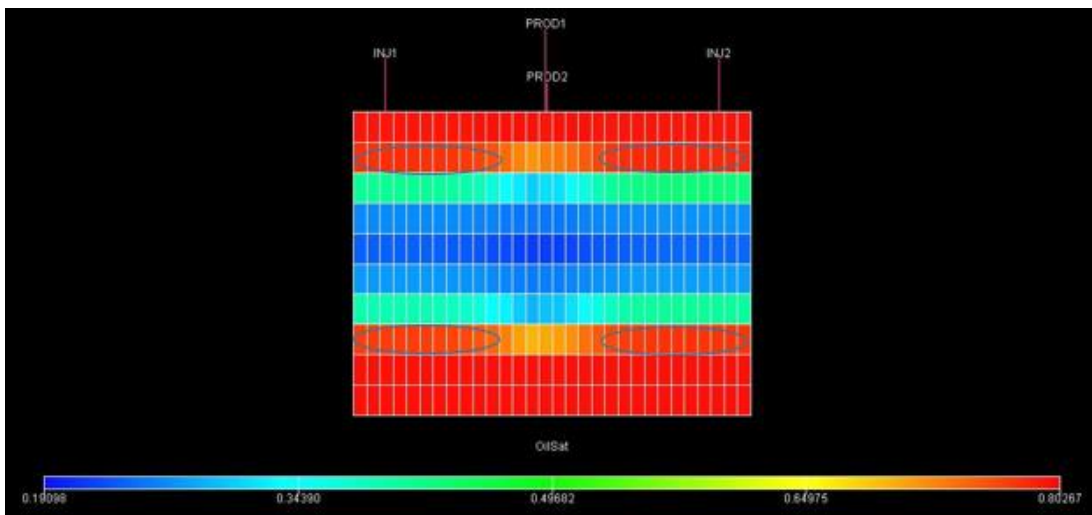
Figure 23: Scenario C oil saturation under the base case after 10 years

An additional aspect with the cyclic and intermittent injection schemes is the reduction in water production. Table 10 shows the decrease in total water production for **Scenarios A and B**. Similar to the improved oil production case, a more intensive injection scheme results in less water production and a greater amount of water is retained in the formation. **Scenario B** resulted

in a reduction of 7.2% in total water produced compared with the conventional waterflood. Water cut is changing between high and low percentages, following the pattern of the on and off injections periods (pressurizing and de-pressurizing). Figure 24 shows the Field water production rate (FWPR) of all scenarios. As the injector is online a rapid increase in water cut is observed, with a similarly quick reduction when the injection stops. Meaning, more water is retained in the formation and expels a larger amount of oil from the low permeable areas. Thus, increasing the recoverable oil volume. A greater increase in cumulative oil production has shown to result in a greater reduction in water production. The reduction in water production was proved to also favor the intermittent and cyclic schemes (**Scenarios A and B**). **Scenario B** had longer duration of on-injection intervals per cycle (30 days per cycle) and higher injection rate compared to **Scenario A** (3 hours was the most occurring on-injection interval duration per cycle, and the maximum was 6 days and 15 hours per cycle), and consequently had lower total water production.
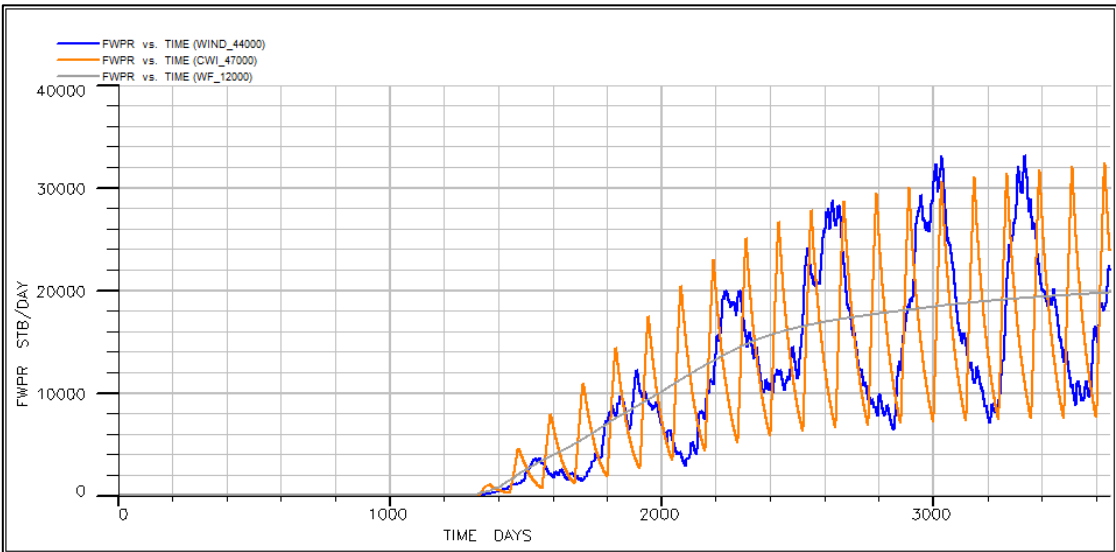
Figure 24: FWPR of all main scenarios under the base case over 10 years

The oil and water production profiles over time for the **Scenarios A and B** are given in Figures 20 and 24, respectively. The simulation results indicate that during the simulated period of 10 years, the daily-intermittent scheme of **Scenario A** is viable from an oil recovery performance perspective, having produced slightly more oil than the conventional waterflood. However, the reservoir simulations show that daily, monthly and annual variations in the wind-generated water injection is reflected as similar oscillations in oil rate, as shown in Figure 20. The designed liquid production and injection rates for all scenarios have not been optimized, and could have been modified for better performance (the effect of injection rate variation results are shown in *Appendix B*).

5.2. Effect of Wettability

The different wettability profiles were mainly created by different residual oil saturations in the reservoir which is a major controlling factor for a waterflood. For different wettability cases, the reservoir fluids are expected to behave differently for the given injection and production rates. The same injection schemes and rates were applied for all the simulated wettability cases, as shown in Table 9. For the oil and mixed wet cases (Tables 12 and 13, respectively), the relative permeability profiles presented in Figure 11 were applied in the model. The oil wet

case has high residual oil saturation and low relative oil permeability, while water wet model has a lower residual oil saturation and higher relative oil permeability. Consequently, ultimate recovery is expected to be more favorable for the water wet case. Taking that into account, the additional increments must be used for comparison in order to confidently gain insight on the intermittent and cyclic injection schemes under different wettability conditions. It should be mentioned that the capillary pressure as a function of fluid saturation is maintained the same for all three wetting conditions. This was done to facilitate studying the effect of wettability, as well as shortage of good capillary pressure data. It should be noted that this will not be the case in a real reservoir, and some numerical error in the results could take place that should be corrected for real oil field application. Moreover, the reservoir pressure for the three wetting conditions are not the same, and is highly likely to be influencing the results. However, given that the reservoir pressure is always above the saturation pressure for all the simulated cases, it is valid to compare the incremental changes in oil and water production.

Changes in wettability conditions are associated with changes in Oil and water relative permeability. For stronger oil wet conditions, the relative permeability of water is increasing and that of oil is decreasing. Oil and water mobility are mainly influenced by the relative permeability of the respective fluids. The mobility ratios for the water and mixed wet conventional waterflooding cases were favorable (less than 1), and unfavorable for the oil wet case, as calculated by Equation 6 and shown in Table 11. Oil and water viscosity used in these calculations were chosen to be the value at bubble point, due to the fact that the reservoir pressure was maintained above the saturation pressure.

$$M = \frac{k_{rw}}{k_{ro}} \cdot \frac{\mu_o}{\mu_w} \qquad (6)$$

M is mobility ratio, k_{rw} is relative permeability to water, k_{ro} is relative permeability to oil, μ_o is oil viscosity, and μ_w is water viscosity.

Table 11: Mobility ratios at different wettability cases, (Langdalen, 2014)

Wettability	Mobility Ratio
Oil wet	1.48
Mixed wet	0.73
Water wet	0.41

Table 12: Endpoint fluid saturations and Corey coefficients for the oil wet case, (Langdalen, 2014)

S_{wi}	0.2
S_{orw}	0.3
S_{org}	0.2
S_{gc}	0.05
$K_{ro@Swi}$	0.5
$K_{ro@Sgi}$	0.5
$K_{rw@Sorw}$	0.8
$K_{rg@Sorg}$	1
n_o	3
n_w	4
n_g	2

S_{wi}	0.2
S_{orw}	0.25
S_{org}	0.2
S_{gc}	0.05
$K_{ro@Swi}$	0.8
$K_{ro@Sgi}$	0.8
$K_{rw@Sorw}$	0.63
$K_{rg@Sorg}$	1
n_o	2
n_w	3
n_g	2

Scenario C under the oil-wet case recovered 35.2% less cumulative oil production in comparison with the water-wet reservoir. As a result of poor recovery, more oil is left behind and the effect of intermittent and cyclic injection could be advantageous. Figure 25 shows that **Scenarios A and B** have also shown lower cumulative oil production in the oil-wet case compared to the water-wet one (34.9% and 34.3%, respectively), as expected.

For the oil wet case, **Scenarios A and B** resulted in 1.2% and 3.6% more cumulative oil production, as well as 2.8% and 4.9% less water production compared to **Scenario C**, respectively (Table 14). Those trends are similar to that of the water-wet case, yet in a higher magnitude of incremental benefit. Oil and water production for all scenarios under the oil-wet case are presented in Figure 26.
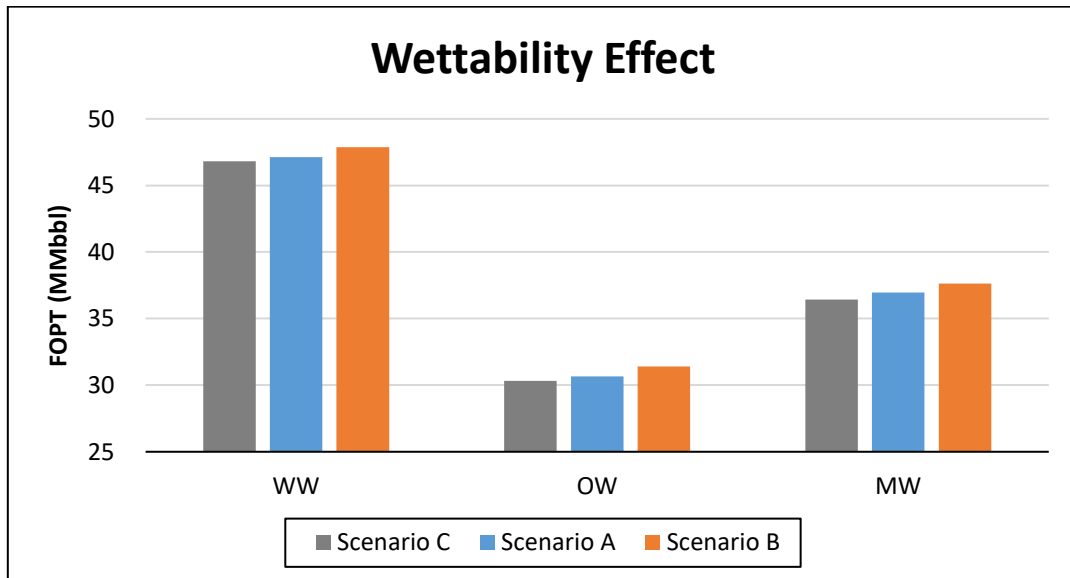
Figure 25: FOPT of all main scenario and different wettability cases
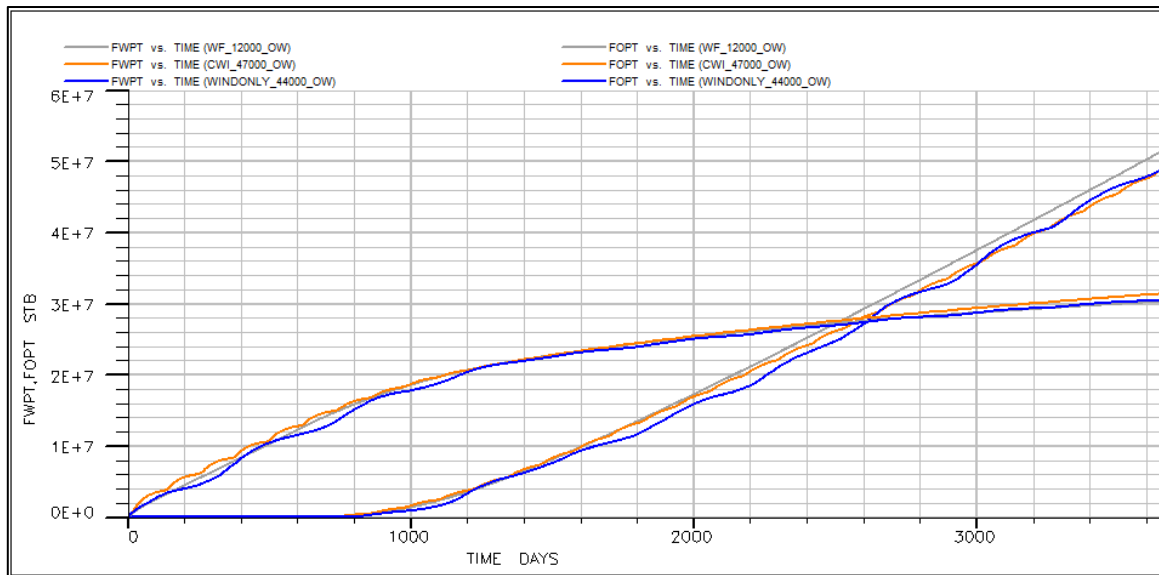
Figure 26: FOPT and FWPT curves of all main scenarios (WIND = Scenario A, CWI = Scenario B, WF = Scenario C) under the oil wet case over 10 years

For the mixed-wet reservoir, the cumulative water and oil production for all scenarios were, as expected, between the respective values for the water and oil-wet case. **Scenario C** under the mixed-wet case recovered 20.1% less cumulative oil production in comparison with the water-wet reservoir. Similar to the oil wet case, yet to a lesser extent, the effect of intermittent and cyclic injection could be advantageous as more oil is left behind. Figure 26 shows that **Scenarios A and B** have also shown lower cumulative oil production in the oil-wet case compared to the water-wet one (20.5% and 19.8%, respectively), as expected. **Scenarios A and B** for the mixed-wet reservoir resulted in 1.5% and 3.3% more cumulative oil production, as well as 3.1% and 2% less water production compared to **Scenario C**, respectively. Oil and water production for all scenarios under the mixed-wet case are presented in Figure 23.

Oil saturation distribution at the end of the simulation period for the three wettability conditions after applying **Scenario C** is given in Figure 22, 26 and 29. Figures (20-21), (24-25), and (27-28) illustrates an important factor for the success of intermittent and cyclic water injection, being the oil distribution in the reservoir. The fluid saturation in the reservoir is influencing the respective phase's relative permeability. For the oil-wet case, the remaining volume of oil in the reservoir is significantly greater than for the water-wet case. In the oil and mixed wet reservoirs, water breakthrough occurred approximately 706 and 566 days earlier than for the water-wet case, respectively, as shown in Table 12. Water channels will form and flow through the reservoir, leaving significant amounts of oil behind. This resulted in low recovery. Thus, applying intermittent and cyclic injection to this case is expected to yield greater incremental recovery due to the difference in mobility between the water and oil phase at different water saturations.

Table 14: FWPT and BTT for all main scenarios and different wettability cases (Mbbl = bbl10^3)*

Scenario	Water wet (WW)		Oil wet (OW)		Mixed wet (MW)	
	FWPT (Mbbl)	BTT (days)	FWPT (Mbbl)	BTT (days)	FWPT (Mbbl)	BTT (days)
Scenario A	30,193	1,500	49,933	800	42,846	938
Scenario B	29,146	1,470	48,833	730	41,990	876
Scenario C	31,412	1,466	51,356	760	44,195	900

Combining **Scenarios A and B** with oil-wet conditions, water channels are limited by allowing the fluids to redistribute during the off-injection interval, and thus restrict channeling of water flow. The saturation differences within the reservoir are greater between the **Scenarios A and B** over that **Scenario C** for the oil and mixed-wet compared to the water-wet case, as shown in Figures (27-28) and (30-31). High oil saturations present in the reservoir provides greater effect of intermittent and cyclic injection in terms of the fluid magnitude exchanged by capillary imbibition during the on and off-injection intervals. Another important aspect is the effect of phase relative permeability. Oil relative permeability is lowered more rapidly with increasing water saturation (associated with water injection) for the water-wet case faster than for the oil-wet case (as shown in Figure 11). This effect is more evident at high water saturations, which is the case in the high permeable layers after water breakthrough in conventional waterfloods or prolonged on-injection periods. This is explained to be the main factor for bypassing of oil for **Scenarios C**'s oil wet case. Thus, reducing the continuous on-injection intervals, as in **Scenarios A and B**, the contact time between water and formation is enhanced, and more imbibition of water into the low permeable layers occurs. This is shown in Figures 27 and 28, as the lower permeability layers (see blue circle) are better swept, due to the effect of cyclic and intermittent injection. High permeable layers in the center of the reservoir was shown to be less swept with the cyclic injection. This can be attributed to the fact that the more oil from the low permeability layers are swept towards the adjacent higher permeable zones. On the other hand, capillary imbibition lead to more water from the low permeable zones entering the high permeable layers.

Figure 27: Scenario A oil saturation under the oil-wet case over 10 years

Figure 28: Scenario B oil saturation under the oil-wet case over 10 years

Figure 29: Scenario C oil saturation under the oil-wet case over 10 years

Comparing the mixed wet case to the oil wet reservoir, **Scenario A** has shown to perform slightly better in terms of incremental benefit over **Scenario C**. As for **Scenario A**, being the less intensive or intermittent injection scheme with dominantly shorter off-injection intervals per cycle, injected water gets less contact time with the formation than **Scenario B**. Thus, less water is imbibed into the lower permeability layers. **Scenario A** simulation results have shown that have performed better when relatively less oil is left behind, and in case of higher oil relative permeability and lower water relative permeability compared to the oil-wet case. It can be concluded that **Scenario A** is best applied in mixed-wet or weak oil-wet reservoir conditions.
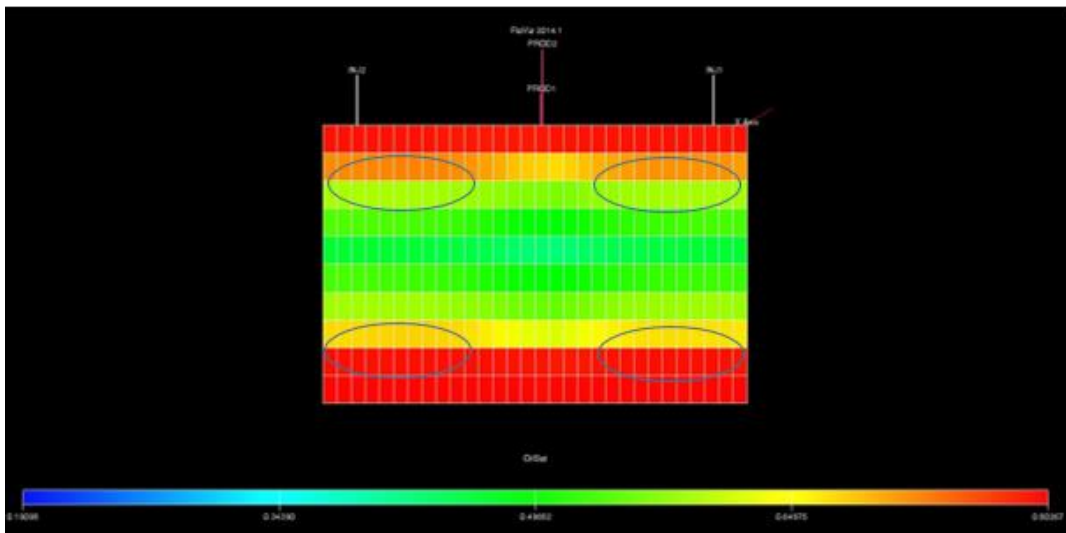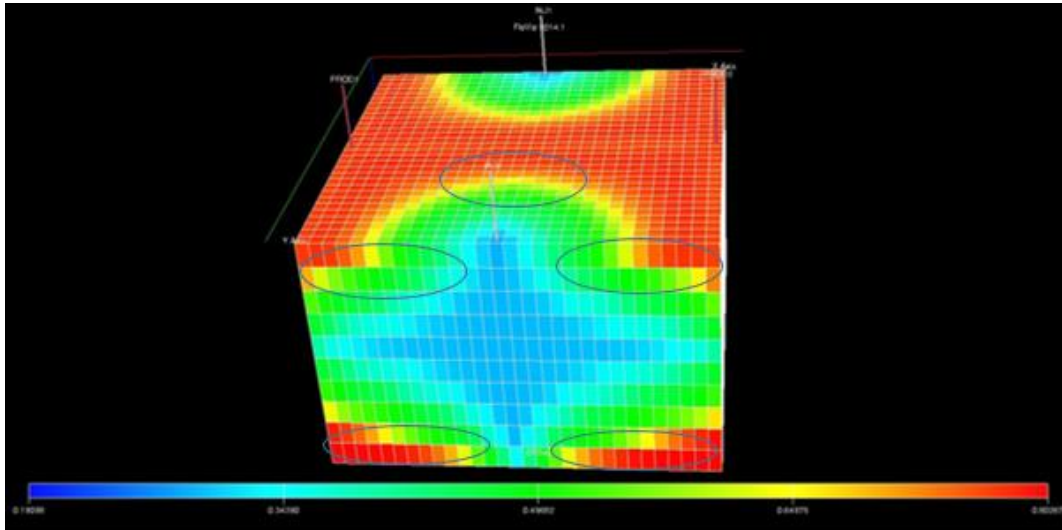
Figure 30: Scenario A oil saturation under the mixed-wet case over 10 years
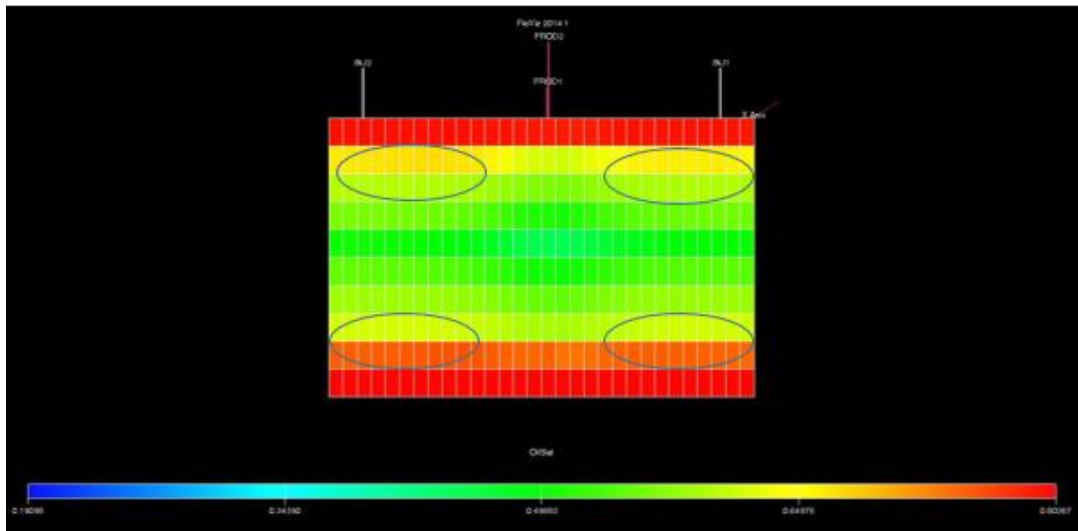

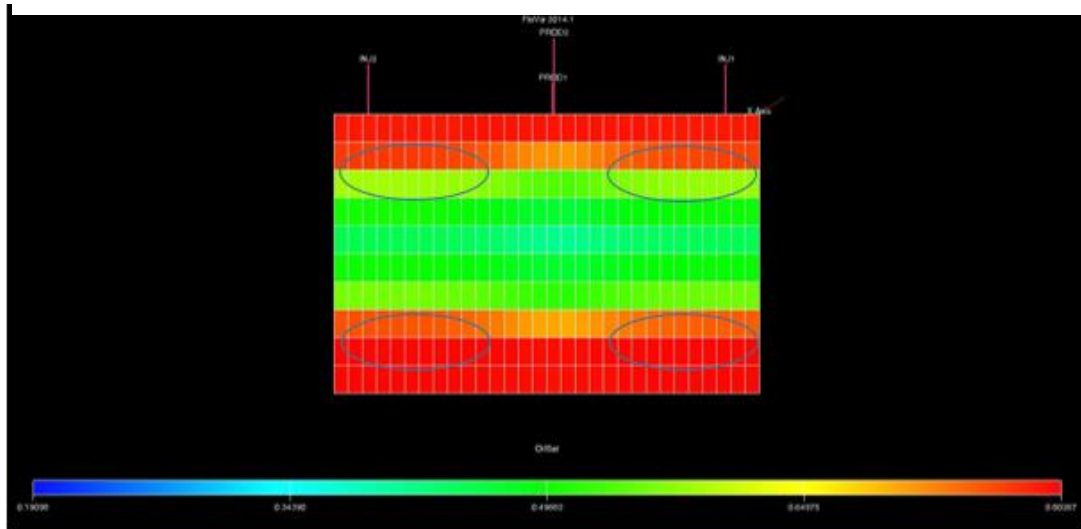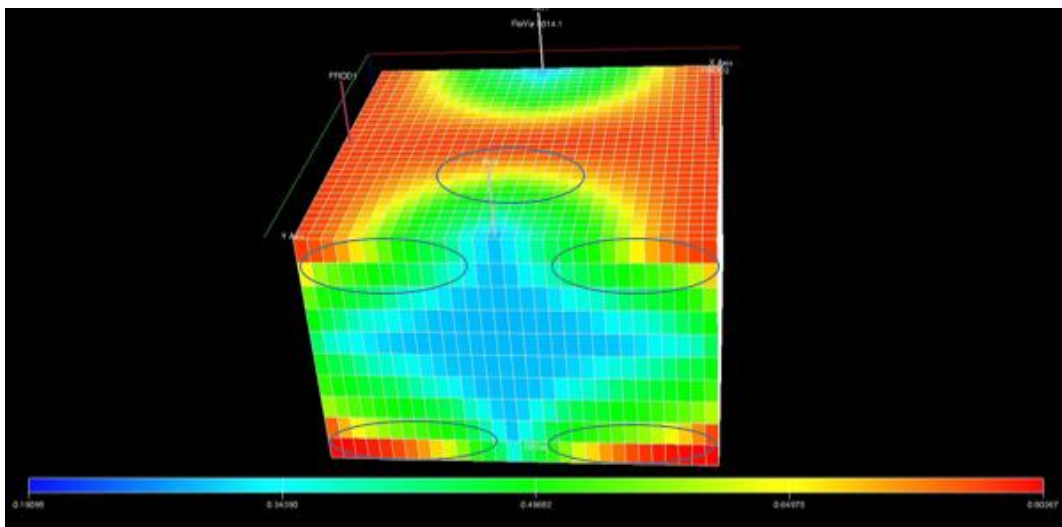*Figure 31: Scenario B oil saturation under the mixed-wet case over 10 years*
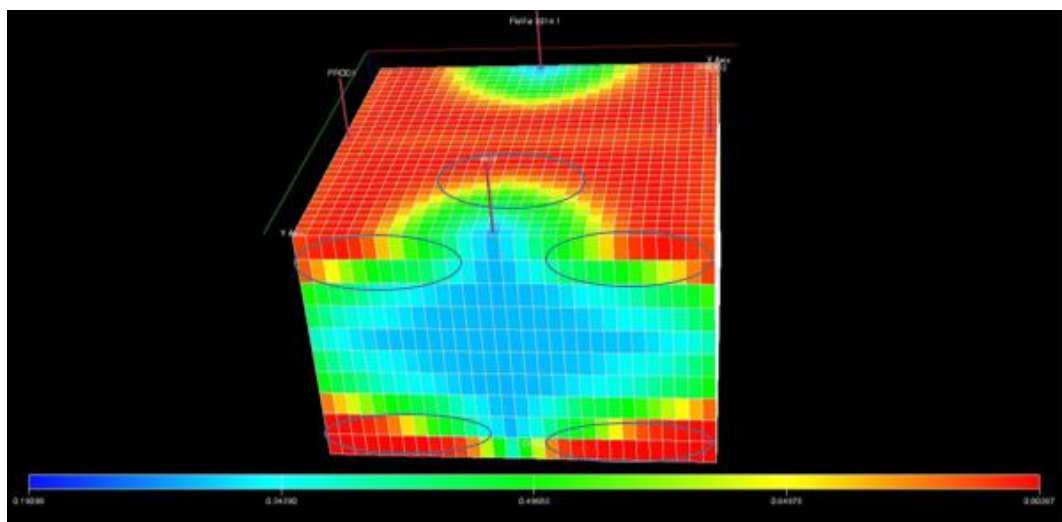
Figure 32: Scenario C oil saturation under the mixed-wet case over 10 years

To summarize the effect of intermittent (wind-powered) and cyclic injection (wind plus a storage solution or gas cogeneration), a higher incremental increase in oil production and less reduction in water production for the oil and mixed-wet reservoirs compared to the water-wet case were seen. It can be concluded that the oil-wet rock is the most suitable for **Scenario B,** while a mixed wet or low oil-wet case will be better for **Scenario A**. The case that produced the highest incremental benefit over **Scenario C** was **Scenario B** combined with the oil-wet rock.

5.3.   Effect of Vertical Transmissibility

Communication between the high and low permeable zones is regarded as a vital parameter for the magnitude of increase in oil production by the cyclic waterflood approach (**Scenario B**), and similarly, is expected to be as significant for the intermittent injection concept (**Scenario A**). Ratio of vertical to horizontal permeability was increased from 0.1 to 0.7 to investigate the effect of increased vertical transmissibility. Obviously, an increase in the vertical permeability was positive for all scenarios with respect to oil recovery and water production, as shown in Figure 33. Improved vertical permeability helps gravitational segregation of the fluids, and allows for an enhanced sweep. For **Scenario A**, Figure 34 shows that the oil recovery incremental benefit over **Scenario C** increases with higher vertical transmissibility till reaching a maximum of 1.3% at a Kv/Kh of 0.5, then it slightly drops. For **Scenario B**, the oil recovery incremental benefit over **Scenario C** is almost stable at 2.4% with higher vertical transmissibility, then it drops to 2.1% at a Kv/Kh of 0.7, as shown in Figure 34. Total water production, on the other hand, diminishes with increased vertical permeability, Table 15. It can also be observed from Table 15, that for **Scenario A** higher vertical permeability reduces water production with a larger incremental benefit compared to **Scenario C** reaching a maximum of 5.9% at a Kv/Kh of 0.7. As for **Scenario B**, total water production is lowered at a higher incremental benefit over **Scenario C** with increasing vertical transmissibility till achieving a peak of 8.2% at Kv/Kh of 0.4, then it slightly drops to 7.9% at a Kv/Kh of 0.7.

Table 15: FWPT and BTT for all main scenarios and different Kv/Kh ratios

VT	Scenario A		Scenario B		Scenario C	
	FWPT (bbl)	BTT (days)	FWPT (bbl)	BTT (days)	FWPT (bbl)	BTT (days)
0.1	30,193	1,500	29,146	1,470	31,412	1,466
0.2	29,305	1,615	28,349	1,589	30,751	1,566
0.3	28,691	1,760	27,843	1,625	30,301	1,630
0.4	28,230	1,803	27,472	1,705	29,921	1,678
0.5	27,844	1,800	27,164	1,720	29,571	1,660
0.7	27,235	1,853	26,664	1,755	28,940	1,760

Higher vertical transmissibility was more beneficial for the increase in incremental benefit achieved by **Scenario A** over **Scenario C**, in comparison to that of **Scenario B**. This can be explained by the fact that **Scenario A**'s shorter off-injection intervals per cycle, and thus shorter formation contact time, was more notably positively affected by better vertical communication between the high and low permeable layers. This enabled **Scenario A** to better sweep low permeability layers off oil, that otherwise would have been left behind at lower Kv/Kh ratios.

As for **Scenario B**, the injection scheme appeared almost unaffected by the rise in Kv/Kh ratios. This can be attributed to the fact that as the on and off-injection intervals' durations per cycle were sufficient to sweep all attainable oil in the low permeability layers even at very low vertical communication. For both **Scenarios A and B**, an increase in vertical transmissibility beyond a given limit affects results in more water being produced from the high permeable layers. This resulted from the gravitational segregation of water from the low permeable layers, and lead to reducing the effect of intermittent and cyclic injection schemes. It can be concluded that once all attainable oil in the low permeability layers has been swept at a given optimum Kv/Kh ratio, going beyond that vertical transmissibility value will be discouraging for the intermittent and cyclic injection effect.
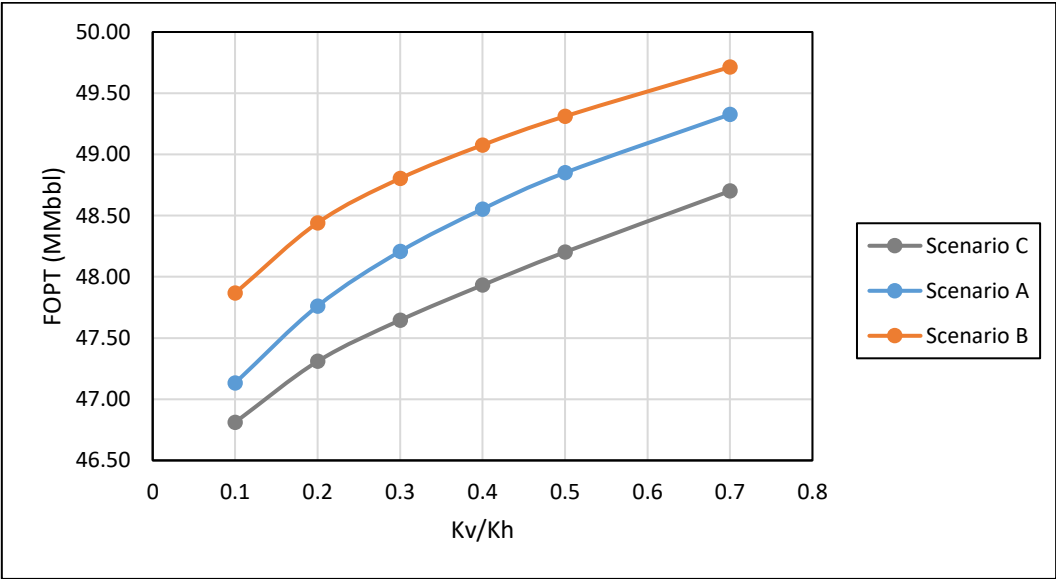
Figure 33: FOPT for different kv/kh-ratios
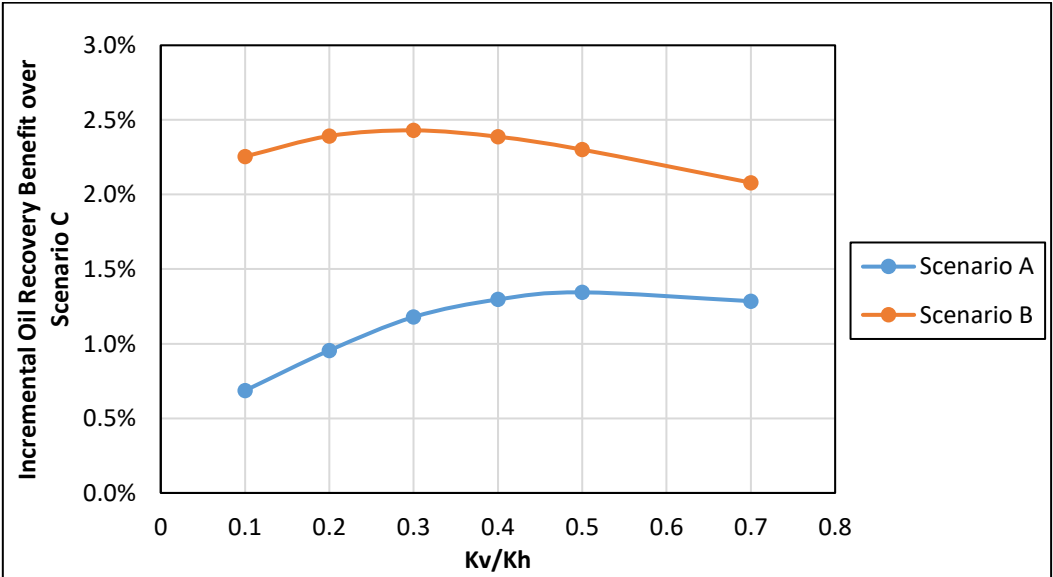
Figure 34: FOPT increase for intermittent injection scenarios over conventional continuous waterflooding

5.4. Effect of Permeability Symmetry

Reservoirs with the presence of layered heterogeneity and permeability differences are the base of obtaining an increase in oil production by cyclic injection. A similar trend is expected for the intermittent injection scheme. The symmetric permeability distribution case (base case) consists of homogenous layers with a high permeable central section surrounded by decreasing permeability layers towards the top and bottom of the reservoir. The thickness of each layer is 10m. The reason behind modelling a layer with considerably higher permeability than the surrounding zones was to increase the total permeability differences within the reservoir, and gain an insight as to whether that will lead to a better sweep efficiency by intermittent and cyclic injection. In this section, an asymmetric permeability distribution and layer thickness with a random permeability distribution is simulated, as shown in Table 16 and Figure 35. No other parameters are changed from the original base case, and the injection/production rates are maintained the same.
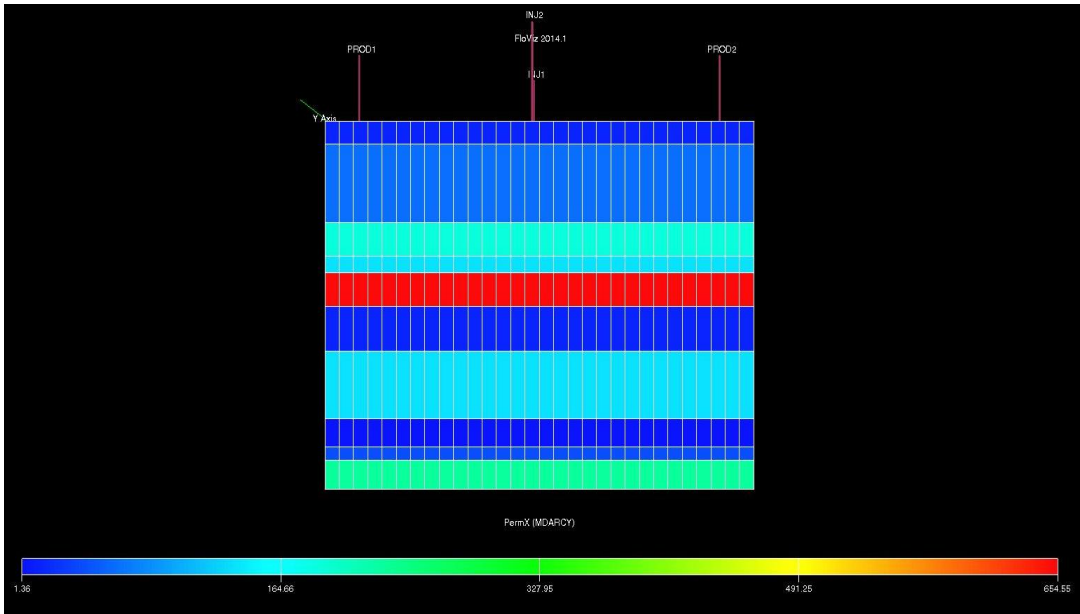
Figure 35: Horizontal permeability distribution for the Asymmetric case

Table 16: Horizontal permeability distribution and layer thickness for the Asymmetric case

Layer	PermX (md)	DZ (ft)
Layer 1	13.64	20
Layer 2	60.64	70
Layer 3	190.91	30
Layer 4	136.36	15
Layer 5	654.55	30
Layer 6	13.64	40
Layer 7	136.4	60
Layer 8	1.36	25
Layer 9	40.91	12
Layer 10	231.82	26

Figure 36 shows the total amount of oil production for all scenarios under the asymmetrical case. For the asymmetrical case, **Scenarios A and B** have shown 21.6% and 20.7% increase in

cumulative oil production relative to the base case. The incremental benefit achieved by intermittent and cyclic flooding injection schemes over **Scenario C** under asymmetrical permeability distribution were 2.5% and 3.4%, respectively. Comparing that to the incremental benefits attained by **Scenarios A and B** under the symmetric base case, it can be concluded that asymmetric permeability distribution is more advantageous for the intermittent and cyclic injection schemes. Higher permeability gradients between consecutive layers lead to more lateral and vertical oil migration during each off-injection intervals, and thus better performance. The net effect of the permeability contrast was increasing the effect of saturations gradient and relative permeability. It can be observed in Figures (34-36) that the larger the volume of low permeability in contact with high permeability channels (as in circled top and bottom layers), the better the effect of intermittent and cyclic flooding. These effects are more evident with longer off-injection intervals per cycle as in **Scenario B** (cyclic flooding).
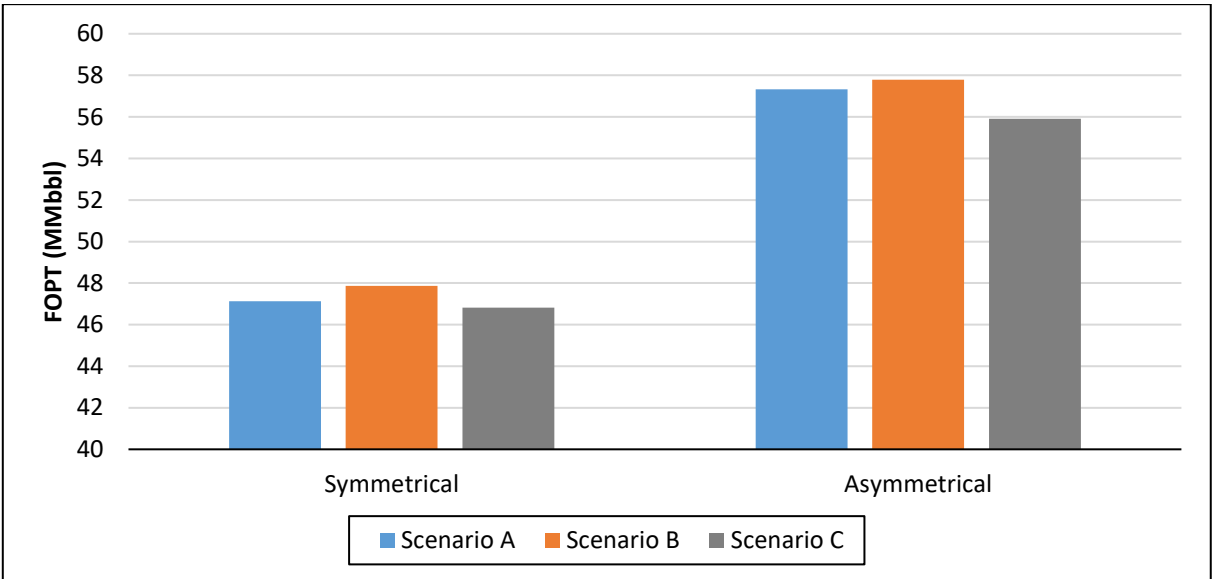
Figure 36: FOPT of all main scenarios under different permeability symmetry cases
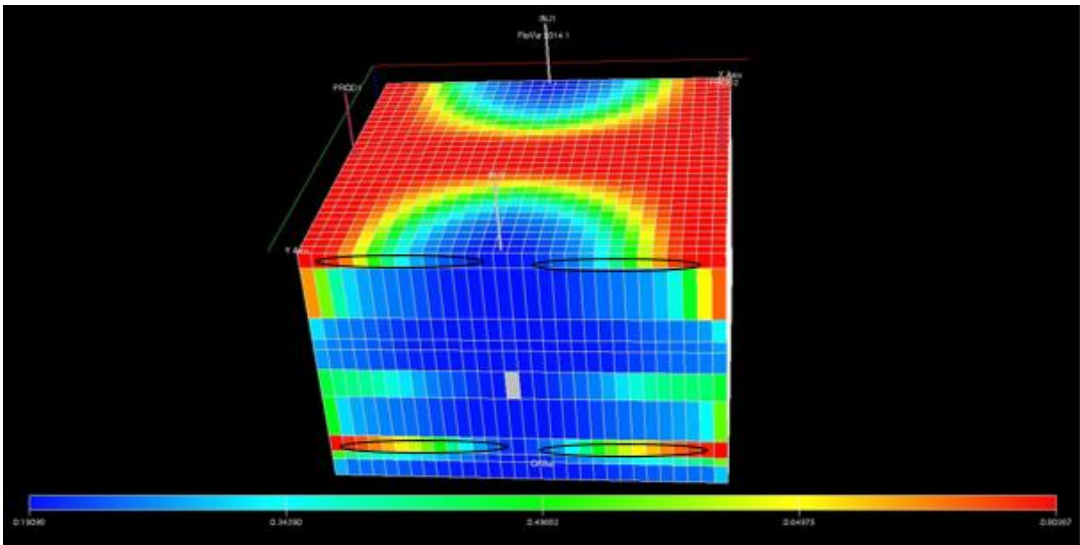
Figure 37: Scenario A oil saturation under the asymmetric permeability case after 10 years

52
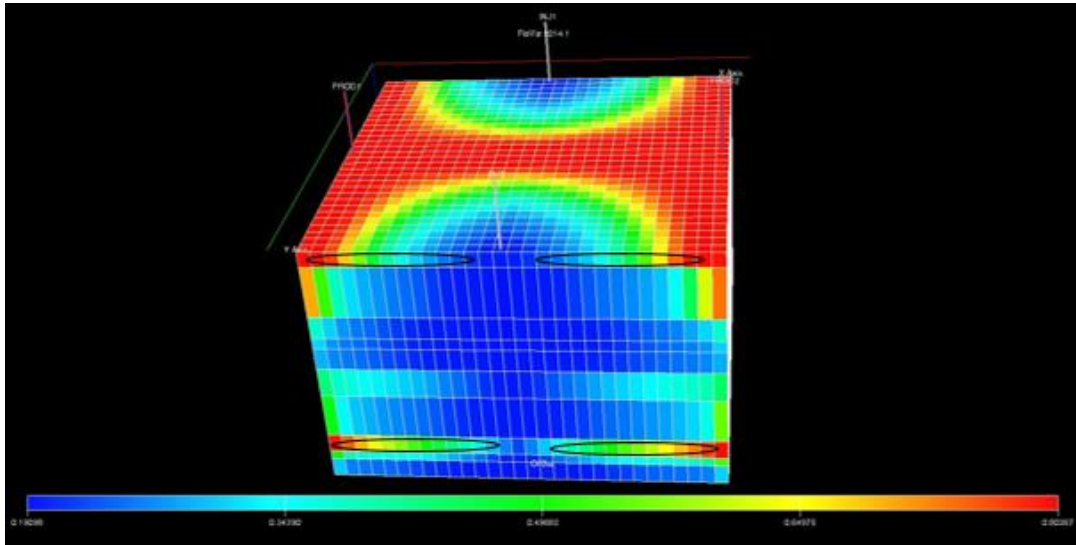
Figure 38: Scenario B oil saturation under the asymmetric permeability case after 10 years
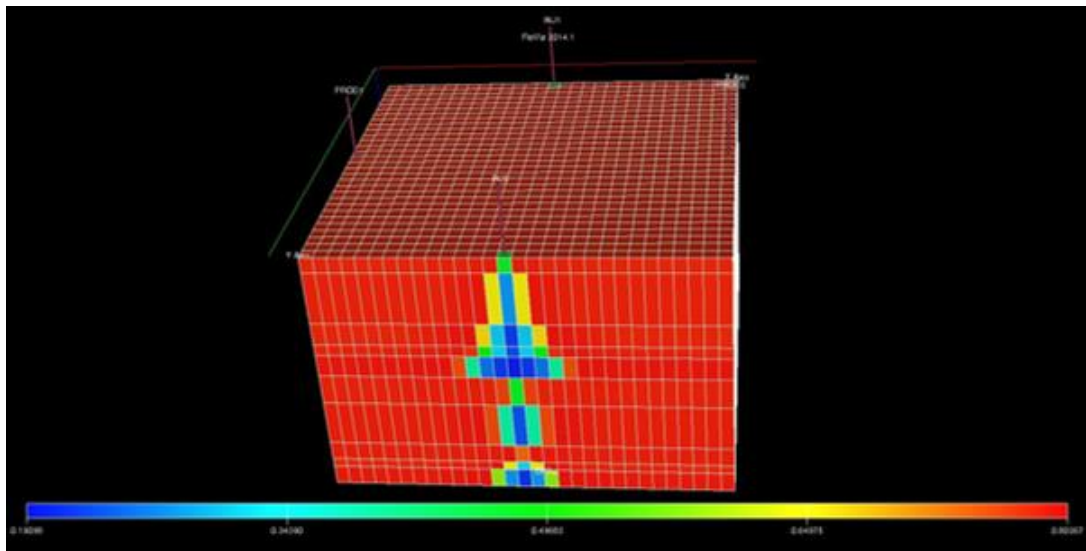
Figure 39: Scenario C oil saturation under the asymmetric permeability case after 10 years

Scenarios A and B have reduced water production under the asymmetrical case by 12% and 15% over **Scenario C**, as shown in Table 17. During the off-injection intervals, the oil saturation increases on the displacement front defining a path of higher saturation, and thus higher relative permeability to oil (and lower for water) compared to the base case, as shown in Figures (37-39). The pressure in the water zones is reduced, and so the oil migration is enhanced based on the higher saturation, pressure gradients and effective permeability under the asymmetric permeability distribution. This oil accumulation, taking place only during the off-injection periods, increments the oil production and lowers the water cut.

Table 17: FOPT, FWPT, and BTT for all main scenarios and different permeability distribution cases

Scenario	Symmetric			Asymmetric		
	FOPT change versus Scenario C	FWPT (Mbbl)	BTT (days)	FOPT Change versus Scenario C	FWPT (Mbbl)	BTT (days)
Scenario A	0.7%	30,193	1,500	2.5%	18,112	1,430
Scenario B	2.3%	29,146	1,470	3.4%	17,495	1,380
Scenario C	-	31,412	1,466	-	20,697	1,325

5.5. Effect of Capillary Pressure/Imbibition

This section aims at quantifying the extent of the role capillary forces play in the oil recovery enhancement by intermittent and cyclic injection schemes versus conventional water flooding. This was done by running zero capillary pressure simulations for **Scenarios A and B**. The results showed an oil recovery drop of 0.2% for the zero capillary pressure case of **Scenarios A and B** compared to the base case. Thus in absence of capillary pressure effects, the incremental benefit in oil recovery achieved by the intermittent and injection **Scenarios A and B** over **Scenario C** will drop down to 0.5% and 2.1%, respectively.

The results prove the impact of capillary forces on enhancing the cross flow intensity, which results in a better sweep for low permeability layers in presence of capillary imbibition effects. However, the capillary imbibition effect has shown to be limited to only 28.6% and 8.7% contribution towards the additional recovery that resulted from applying **Scenarios A and B**, respectively. This can be explained by the fact that the lower the injection rate, the process gets slower and the role played by capillary and gravitational forces in the cross flow become secondary (Shchipanov et al., 2008). For higher injection rates, the viscous forces will increase and take part in forcing water into the tight pores. Pressure gradient among layers will, then, control the compressibility, and be the major contributor to vertical cross flow. The pressure will change more rapidly in water saturated layers than in oil saturated layers (Shchipanov et al., 2008). Therefore, pressure reduces more rapidly in the high permeability layers (mainly water saturated) relative to the low permeable zone that are mostly oil saturated. The result is in an increase in the vertical pressure difference between low and high permeability zones. This explained the higher recovery achieved by **Scenario B** (being the more intensive scheme with higher injection rate, and providing higher pressure amplitudes), and the lower incremental contribution of capillarity effects compared to **Scenario A**.

The remainder of recovery enhancement by the intermittent and cyclic injection schemes can be attributed to the compressibility of the system and gravitational segregation. Reservoir compressibility provides energy for production and faster displacement. During the off-injection intervals the reservoir pressure will be lowered, and the compaction will reduce the reservoir porosity. This decrease in pore volume will expel oil out of the low permeability layers into the high permeability zones.

A simple calculation can be used to illustrate the concept of newly mobilized oil by compression, as in Equations (7-10) (ConocoPhillips, 2013). A drawdown or pressure drop of

1000psi (6.9MPa) will result in a porosity reduction of 1.3%, and the volume of residual oil in the rock will be 0.4% less compared to the initial condition without compaction.

$$C_p = -\frac{1}{V_p} \cdot \frac{dV_p}{dP} \qquad (7)$$

$$Recovery\ Increase = \frac{V_{or\ @initial\ conditions} - V_{or\ @after\ pressure\ depletion}}{V_{p\ @initial\ conditions}} \qquad (8)$$

$$V_{or\ @initial\ conditions} = S_{or} \cdot \varphi_{@initial\ conditions} \cdot V_b \qquad (9)$$

$$V_{or\ @after\ depletion} = S_{or} \cdot (\varphi_{@initial\ conditions} - \varphi_{@after\ pressure\ depletion}) \cdot V_b \qquad (10)$$

Where Cp is the pore compressibility (4×10^{-6} 1/psi), V_p is the pore volume ($3 \times 10^6 m^3$), dP is the pressure drawdown, V_{or} is the residual oil volume (m^3) S_{or} is the residual oil saturation, V_b is the bulk volume ($1 \times 10^7 m^3$). Therefore, zeroing of the injection rate should be expected to mobilize new oil. The more significant the pressure drop is, the higher the amount of newly mobilized oil by compressibility effects. It should be mentioned that the pressure independent properties have not been accounted for in these calculations, which could result in errors. Yet, the concept is clear and promising.

5.6. Effect of Cyclic Initiation

Intermittent initiation time is defined as the time the cyclic or intermittent injection starts. This section investigated the impact of the initiation time on success of **Scenarios A and B**. In all simulations, **Scenario C** was applied from Day 1. The injection scheme shifted to either **Scenario A or B** at certain water cut levels (15%, 25%, 50%, 75%, and 85%). The time when these water cuts are reached is presented in Table18. Table 18 shows a notable decrease in incremental benefit achieved by **Scenarios A and B** over **Scenario C** occurs with later time initiation of the intermittent and cyclic injection schemes. Total amount of water injected in the highest and lowest cases deviated by only 1%.

Table 18: FOPT change for Scenarios A and B versus Scenario C at certain intermittent initiation times

Water cut level at intermittent initiation	Time (days)	FOPT change versus Scenario C	
		Scenario A	Scenario B
0	0	0.69%	2.26%
15%	1080	0.49%	1.35%
25%	1189	0.17%	1.32%
50%	1440	0.11%	1.30%
75%	1892	0.01%	0.09%
85%	2659	-0.10%	0.04%

Results show that the effect of **Scenarios B** is positive for all water cut levels. A similar trend was observed for **Scenario A**, with the exception of initiation at a water cut level of 85%. **Scenarios A and B** achieved the highest incremental benefit in cumulative oil recovery over **Scenario C** at 0.7% and 2.3%, respectively, when applied from Day1. When cyclic injection scheme was initiated after **Scenario C** at a water cut level of 85%, the incremental increase in oil recovery by **Scenarios B** was at its lowest (0.04%). As for the intermittent injection scheme, initiating **Scenario A** at a water cut level of 85% resulted in a slightly negative effect (0.1% decrease in cumulative oil recovery). These results can be attributed to low oil displacement by

water in the low permeable zones with the shorter formation contact times associated with later initiation of intermittent and cyclic injection schemes (over the fixed 10 year simulation period. Longer **Scenarios A and B** application times allow for an increased formation contact time, and thus enhanced gravity and capillary pressure effects. By allowing the fluid exchange to elapse over a longer time period more oil is expected to sweep out of the low permeable zones into the better quality layers. The oil and water production and water cut profiles are given in *Appendix B*.

The results above indicate that it is a better practice to start the application of intermittent and cyclic injection schemes earlier in the field life. Investigation of the suitability of certain water cut levels to the initiation of **Scenarios A and B,** and the consequent impact on cumulative oil recovery should be carried out on case by case basis. As depending on reservoir characteristics, higher water cut levels could still provide a big difference in fluid mobility and phase pressure between the high and low permeable layers that could possibly offset the formation contact time effect referred to above.

5.7. Effect of Reservoir Homogeneity

Stratified heterogeneous reservoirs are claimed to be favorable for cyclic injection, therefore a homogeneous model equal to the base case was modelled to test the theory. The average permeability value for the base case is 142md, which was applied to all ten layers for this homogeneous model. All the ten layers have the same properties, and will act like a single layer. Figure 40 shows that all scenarios resulted in a higher total oil production under the homogenous case relative to the heterogeneous one. For the homogenous case, **Scenario C** resulted in 0.6% and 0.8% higher cumulative oil production over **Scenarios A and B**, respectively. This can be explained by the fact that all oil is in front of the water (as shown in Figures 38-40) and no additional recovery from non-existing poor swept areas is possible. Thus, the positive effect of intermittent and cycling injection schemes is absent.

Table 19: Incremental change in FOPT, FWPT, and BTT of intermittent injection scenarios over Scenario C

Scenario	Heterogeneous			Homogeneous		
	Incremental change in Oil Recovery	Incremental Change in FWPT	BTT (days)	Incremental change in Oil Recovery	Incremental Change in FWPT	BTT (days)
Scenario A	0.7%	-3.9%	1500	-0,6%	-19.6%	3460
Scenario B	2.3%	-7.2%	1470	-0,8%	-15.8%	3460
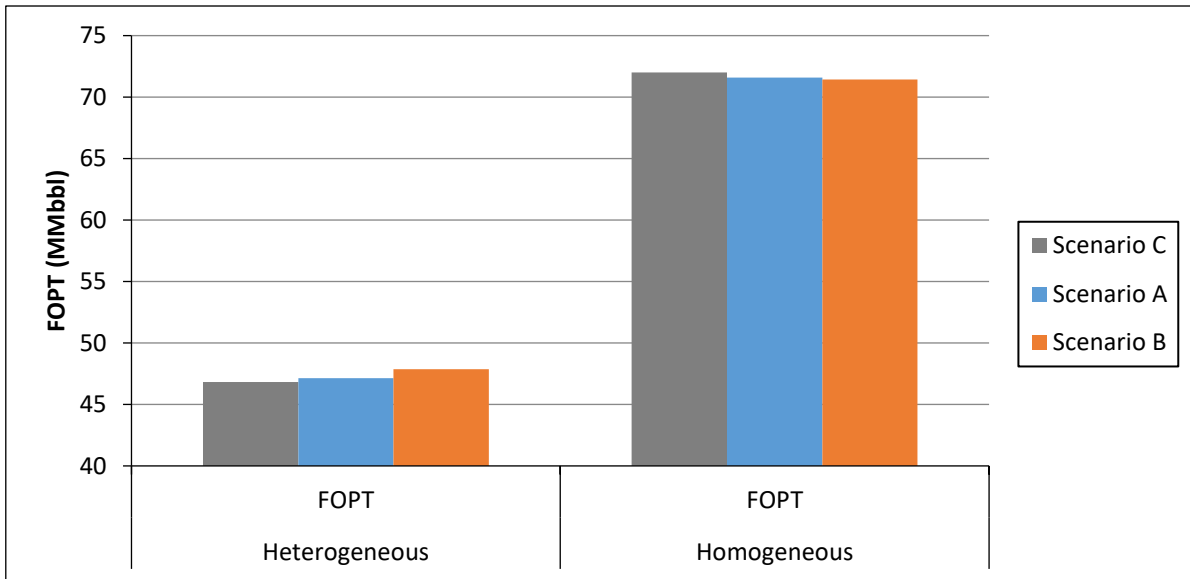
Figure 40: FOPT for all main scenarios under the homogenous and heterogeneous reservoir cases

The small drop in oil production by intermittent and cyclic injection schemes is explained by a small fraction of bypassed oil in top layers, as shown in Figure (41-43). This is attributed to the gravity dominated cross flow that drains more of the injected water towards lower layers of the reservoir during the off-injection intervals. The longer off-injection intervals per cycle of **Scenario B**, thus, resulted in achieving the lowest oil recovery among all investigated scenarios for the homogenous case. As for the continuous flooding of **Scenario C**, the injected water will sweep the oil ahead in a piston-like displacement, and no bypassing of oil occurs. Hence, a late water breakthrough is observed, as shown in Table 19. On the other hand, **Scenarios A and B** resulted in a substantial reduction in water production estimated at 20% and 16%, respectively. By shutting the injector, the amount of water reaching the producer is lower and less water production occur. This section has proved the importance of having significant permeability differences and a relatively high level of reservoir heterogeneity to obtain successful injection schemes as in **Scenarios A and B**.
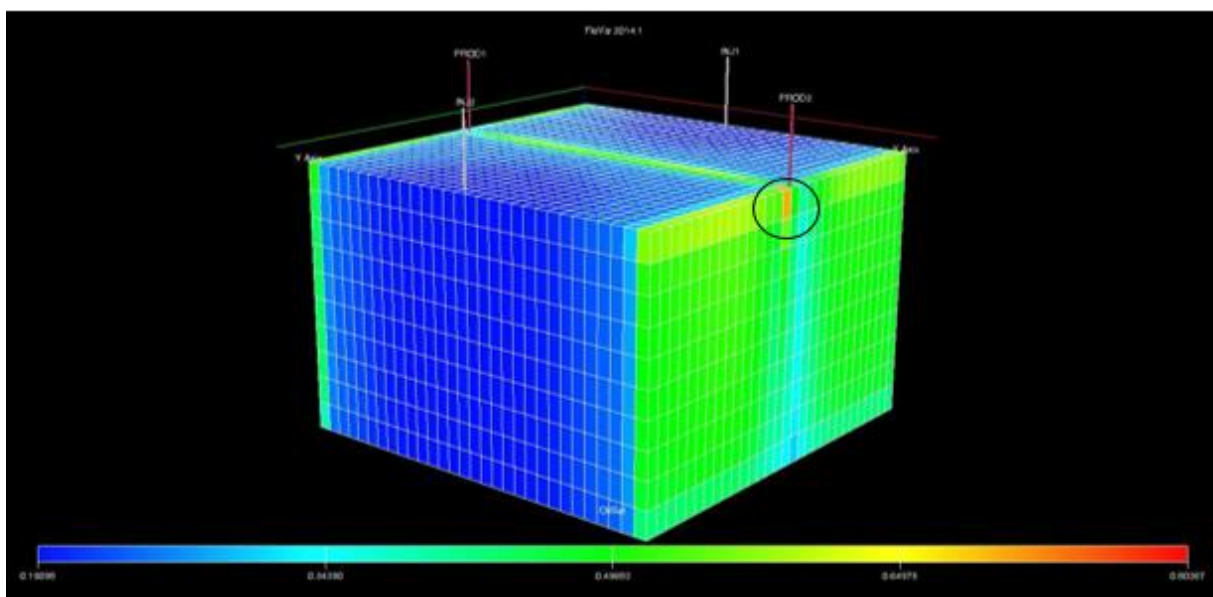
Figure 41: Scenario A oil saturation under the homogenous case after 10 years
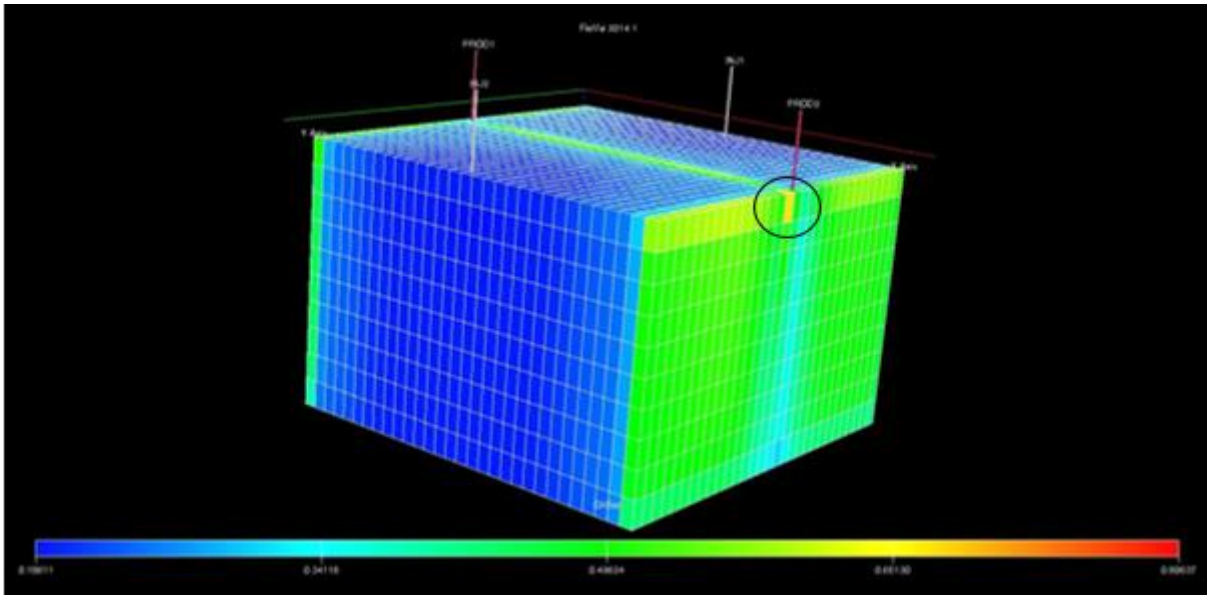
Figure 42: Scenario B oil saturation under the homogenous case after 10 years
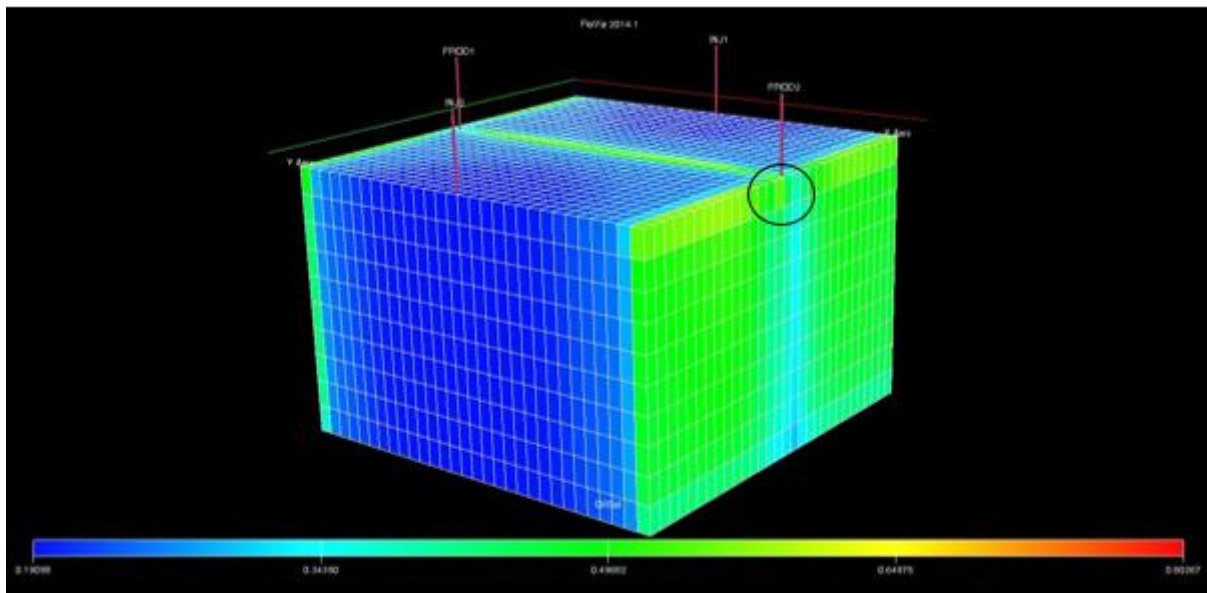
Figure 43: Scenario C oil saturation under the homogenous case after 10 years

5.8. Effect of Wind Speed/Potential

In order to represent daily, monthly, and annual variability, 3-hourly average wind data over the period of 10 years were sourced from Argoss database for Location A, and NDBC database for **Locations B and C**, respectively. MATLAB was used to create an injection schedule that varies every 3 hours based on the wind power output in all Locations throughout the day. This was adapted to the water injection rate. The injection schedule includes injecting at 44,000b/d per injector during time periods when the wind turbine is producing the power required to run the injection pumps of the base case power system at full capacity (4MW), and then zero injection otherwise. This was simulated as on and off injection cycles using the keyword WCYCLE in Eclipse 100. The purpose is to assess whether water injection could tolerate different patterns of wind speed and power generation hourly variations from an oil recovery perspective, through comparison of the results of both locations.

For **Location A**, this case resulted in a total of around 1284 days of water injection, amounting to 87.5MMbbls of water, over the course of 10 years. This corresponds to an overall availability of around 35%, and total on-injection to off-injection ratio of 1:1.9. The longest period of continuous injection per cycle was 7 days, while the longest period of no injection was 23 days and 12 hours. The most occurring on and off injection intervals' duration per cycle was 3 hours. The on-injection to off-injection durations per cycle ratios were placed into bins and probability of occurrence of these bins were calculated for as shown in Table 21. More importantly, the most occurring injection schemes were those of ratio of 1:4(and above) at 27%, followed by 1:1 at 16%, and then 4(and above):1 at 14%, as shown in Table 21 (cycle defined as the injection-on with the subsequent injection-off).

Figures (44-47) shows the resulting FWIR for **Locations B and C** over 3650 days. At **Location B**, the case resulted in a total of around 295 days of water injection (5% availability), amounting to 26MMbbls of water. This corresponds to a total injection to no injection ratio of 1:18. The longest period of continuous injection per cycle was 38 days and 9 hours, while the longest period of no injection per cycle was 74 days and 9 hours. The most occurring on and off injection intervals per cycle were similar at 3 hours. The most occurring injection schemes very dominantly the ratio of 1:4(and above) at 70%, and remotely followed by 1:1 at 9%.
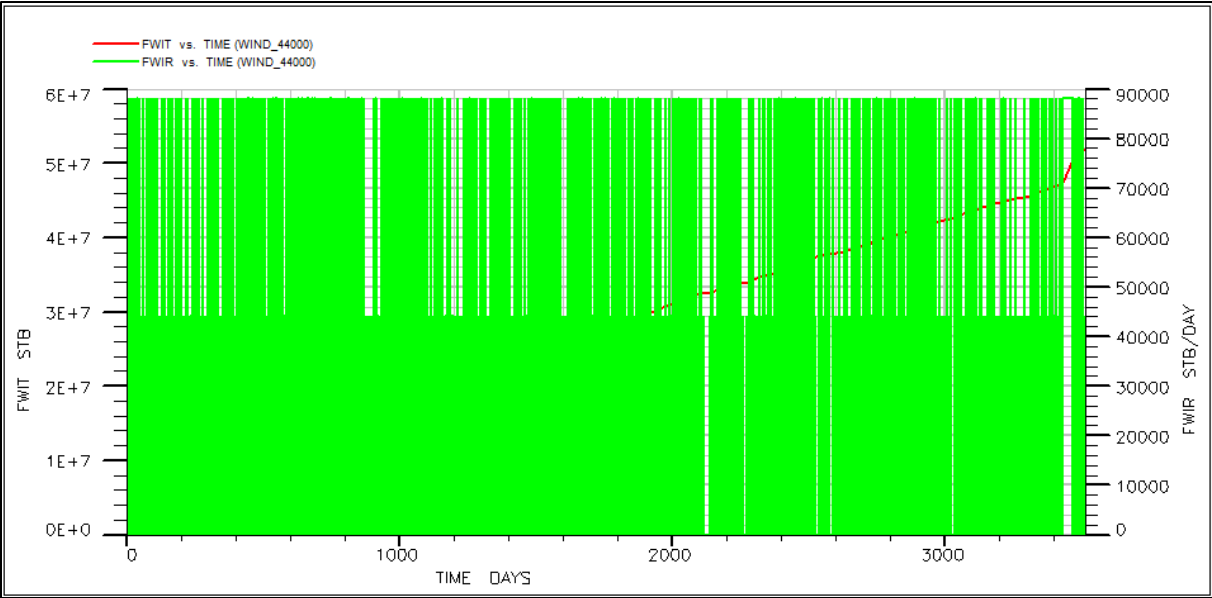
Figure 44: FWIR and FWIT curves for Location B (Case 1) over 10 years
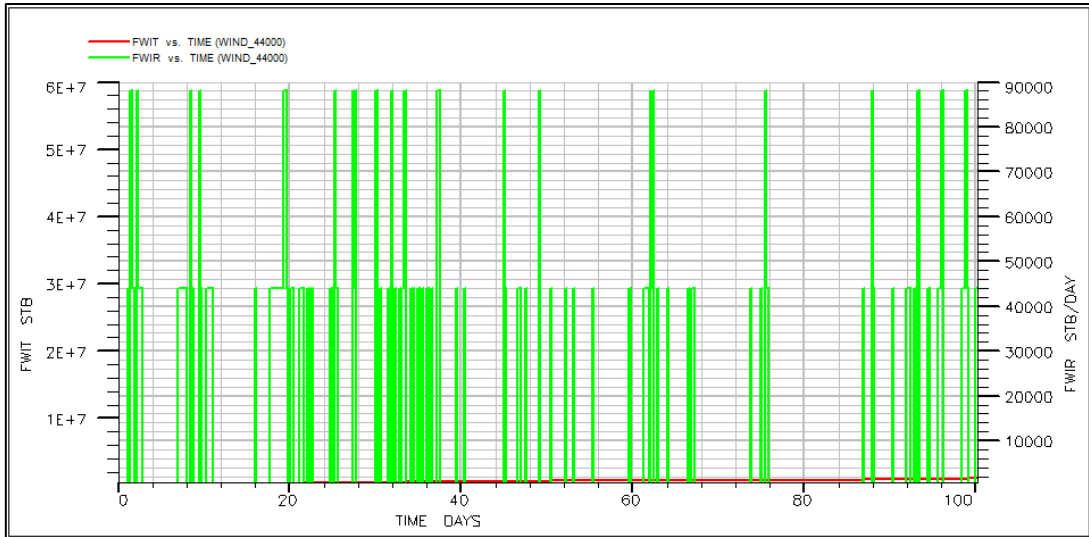
Figure 45: FWIR and FWIT curves for Location B (Case 1) over 100 days

At **Location C**, the case resulted in a total of around 741 days of water injection (20% availability), amounting to 65.2MMbbls of water. This corresponds to a total injection to no injection ratio of 1:3.9. The longest period of continuous injection per cycle was 4 days and 6 hours, while the longest period of no injection per cycle was 44 days and 18 hours. The most occurring on and off injection interval duration per cycle was at 3 hours. The most occurring injection scheme was very dominantly the ratio of 1:4+ at 56%, and remotely followed by 1:1, 1:1.5, and 4+:1 at 6%.
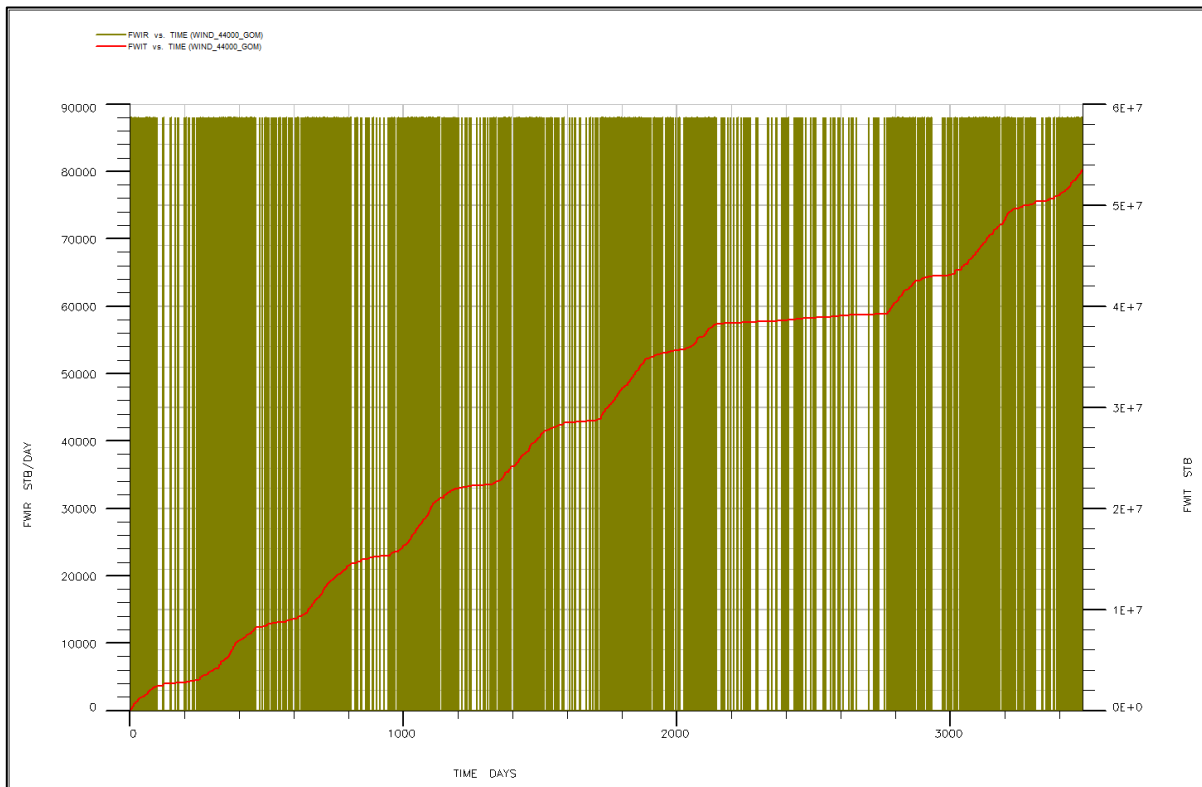
Figure 46: FWIR and FWIT curves for Location C (Case 1) over 10 years
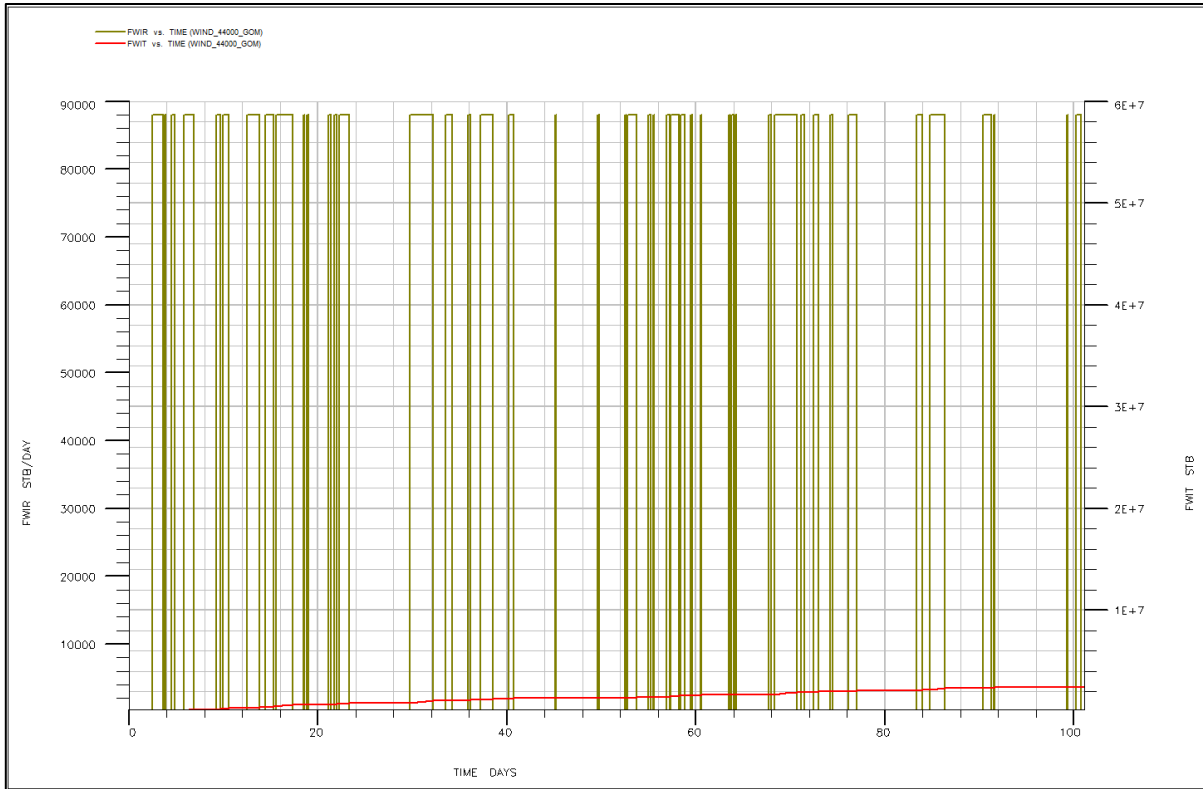
Figure 47: FWIR and FWIT curves for Location C (Case 1) over 100 days

Using the base case 3D reservoir model, all cycles are initiated at the beginning of the production period, at day 1, so that the dominant recovery mechanism is water drive. As expected, the higher wind potential at **Location A** will result in a significantly higher amount of FWIT, followed by **Location C and Location B**, respectively, over the 10 years using the same wind-power system water injection configuration. Consequently, **Location A** achieved 22%, and 17% higher FOPT than **Location B (Case B1) and Location C (Case C1)**, respectively.

5.9. Effect of Wind Variability Pattern

Since **Location A** had significantly higher wind speeds, consequently a higher amount of water was injected relative to **Locations B and C** over the same time period and using the same power configuration. This resulted in a considerably higher cumulative oil recovery for **Location A**. Thus, a higher capacity wind power system configuration was simulated for **Locations B and C**, in order to exclusively study the effect of wind variability pattern in the selected sites on the resulting intermittent water injection scheme and oil recovery. The aim of the newly designed cases was to achieve a similar total water injection volume target similar to that achieved with the base case configuration at **Location A**. The new cases will be referred to as **Case B2 and Case C2**.

For **Location A, and Cases B2 and C2** a power configuration of one G136-4.5MW wind turbine driving two 2MW motors driving two smaller pumps was used. The injection schedule included injecting at 44,000b/d per injector during time periods when the wind turbine is producing the power required to run the injection pumps at full capacity (4MW), and then zero injection otherwise. In **Case B2**, it is assumed that a power system configuration of two G136-

4.5M driving four 2MW motors is applied. The injection schedule includes injecting 74,000b/d (assuming that the reservoir has sufficient injectivity) per injector during time periods when the wind turbines are producing the power required to run all the injection pumps at full capacity (8MW), 37,000 b/d per injector when the wind turbines are capable of running half the pumps at full capacity (4MW), and no injection otherwise. The 'half capacity' injection periods were introduced to increase the injection availability in a relatively low wind speed environment, and arrive at the required total water injection target for the 10-year period via the most practically possible injection rates.

In **Case C2**, it is assumed that a similar power system configuration to that of the base case is applied (one G136-4.5M driving four 2MW motors). However, the injection schedule includes injecting 35,000b/d (assuming that the reservoir has sufficient injectivity) per injector during time periods when the wind turbines are producing the power required to run all the injection pumps at full capacity (8MW), 17,000 b/d per injector when the wind turbines are capable of running half the pumps at full capacity (4MW), and no injection otherwise.

Figures 48 and 49 show the FWIR for **Case B2** over 3650 days. This case resulted in a total of around 822 days of water injection, amounting to 87.5MMbbls of water over the course of 10 years. This corresponds to a water injection availability of around 22%, and injection to no injection ratio of 1:3.5. The longest period of continuous injection (half and full power combined) per cycle was 38 days and 9 hours, while the longest period of no injection per cycle was 24 days. The most occurring on and off injection periods per cycle was 3 hours. More importantly, the most occurring injection schemes were those of ratio of 1:4+ at 36%, followed by 1:1 at 14%, and then 1:2 at 9%, as shown in Table 21.

Table 20: Detailed injection schemes for Scenario B and different Scenario A locations

Injection Scheme	Scenario B	Scenario A				
		Location A	Location B		Location C	
			Case B1	Case B2	Case C1	Case C2
on/off	1 to 3	1 to 1.9	1 to 18	1 to 3.5	1 to 3.9	1 to 1.3
on/total	25%	35%	5%	22%	20%	44%
total on (days)	900	1284	295	822	741	1618
total off (days)	2750	2366	3355	2828	2909	2032
total ½ (days)	NA	NA	NA	527	NA	755

Table 21: Probability of occurrence for various on/off injection scheme ratios of all Scenario A location cases

Injection Scheme	Location A	Location B		Location C	
		Case B1	Case B2	Case C1	Case C2
1 to 4+	27%	70%	36%	56%	27%
1 to 4	2%	2%	4%	3%	4%
1 to 3.5	2%	1%	2%	2%	2%
1 to 3	5%	3%	6%	2%	5%
1 to 2.5	2%	2%	3%	4%	3%
1 to 2	7%	2%	9%	4%	7%
1 to 1.5	5%	3%	7%	6%	5%
1 to 1	16%	9%	14%	6%	17%
1.5 to 1	5%	1%	3%	4%	6%
2 to 1	6%	2%	6%	2%	7%
2.5 to 1	2%	0%	1%	2%	3%
3 to 1	4%	1%	3%	2%	3%
3.5 to 1	1%	0%	0%	1%	1%
4 to 1	2%	1%	1%	1%	2%
4+ to 1	14%	2%	4%	6%	9%

Table 22: Variability of injection schemes for all Scenario A location cases

Injection Scheme	Location A	Location B		Location C	
		Case B1	Case B2	Case C1	Case C2
on>off	34%	8%	19%	18%	31%
on=off	16%	9%	14%	6%	17%
on<off	50%	83%	67%	76%	53%
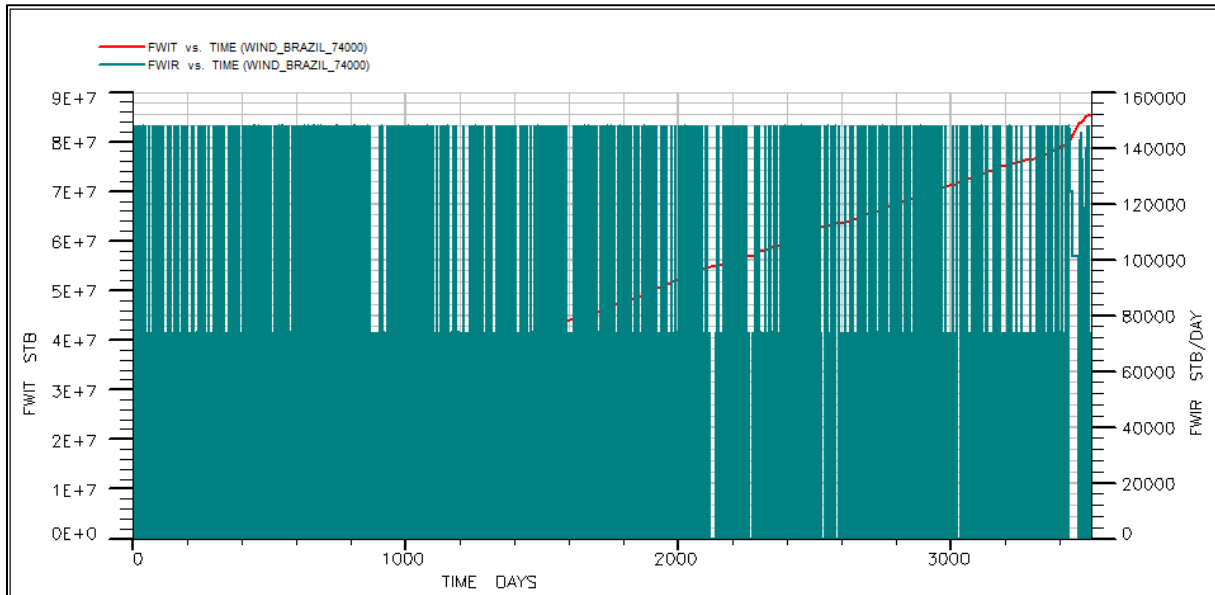
Figure 48: FWIR and FWIT curves for Location B (Case 2) over 10 years
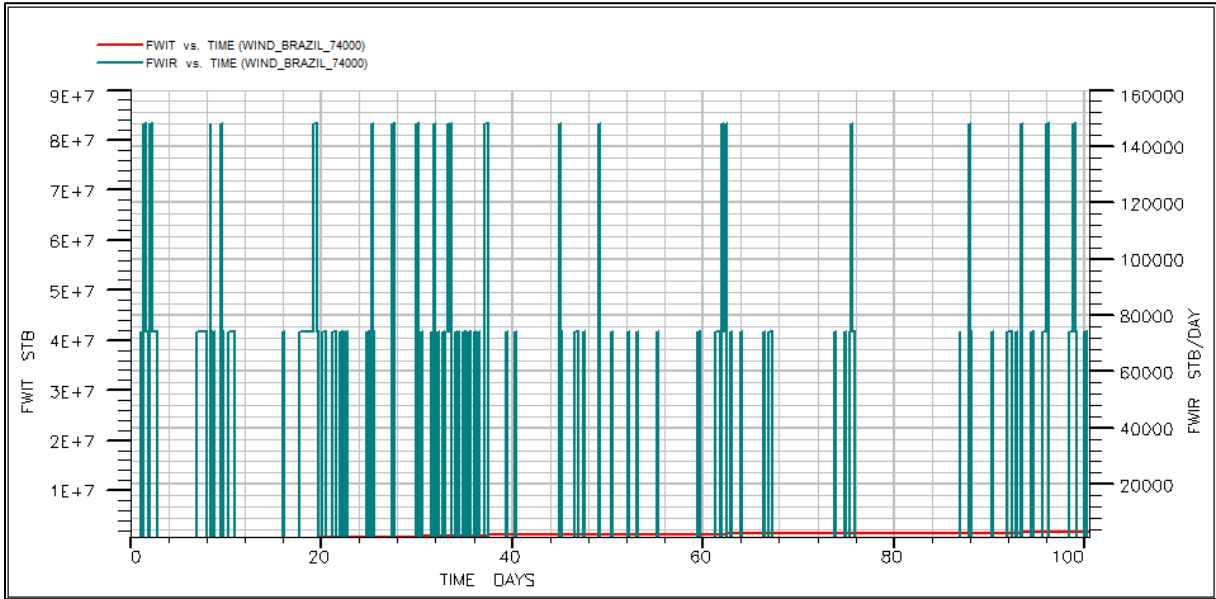
Figure 49: FWIR and FWIT curves for Location B (Case 2) over 100 days

Figures 50 and 51 show the FWIR for **Case C2** over 3650 days. This case resulted in a total of around 1618 days of water injection, amounting to 86.7MMbbls of water over the course of 10 years. This corresponds to a water injection availability of around 44%, and injection to no injection ratio of 1:1.3. The longest period of continuous injection (half and full power combined) per cycle was 6 days and 21 hours, while the longest period of no injection per cycle was 12 days and 3 hours. The most occurring on and off injection periods per cycle was 3 hours. More importantly, the most occurring injection schemes were those of ratio of 1:4+ at 27%, followed by 1:1 at 17%, and then 4+:1 at 9%, as shown in Table 21.
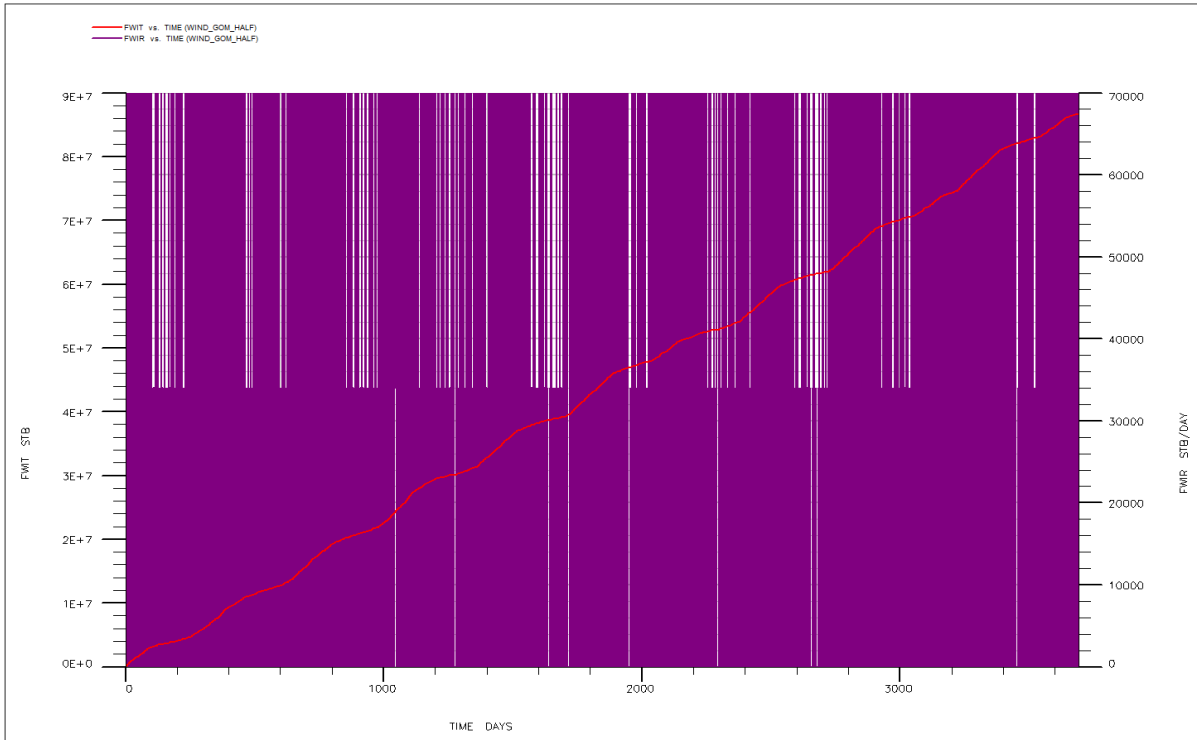
Figure 50: FWIR and FWIT curves for Location C (Case 2) over 10 years

Figure 51: FWIR and FWIT curves for Location C (Case 2) over 100 days

Case B2 was the more intensive injection scheme that provided the higher injection rate during the 'full capacity' periods (and longer injectors shut-in period (very close to the literature optimum scheme of 1:3) compared to that of **Location A and Case C2**, respectively. The additional oil produced during **Case B2** can be directly related to the greater pressure amplitude observed during the pressurizing (injection-on) and de-pressurizing periods (injection-off), Figure 49. The pressure was changing above and below the pressure observed under **Location A and Case C2**, Figure 52. It should be noted that for a real field the injection pressure is limited with respect to capacity and formation damage, and could not be increased above any unreasonable value. Comparing **Case B2** to **Location A**, this effect was, however, offset by lower injection rate during the 'half capacity' periods (527 days in total, which is around 64% of the on-injection intervals). The result was still a slight incremental cumulative oil production increase of 0.3% and 3% in favour of **Case B2** over **Location A and Case C2**, respectively. Therefore, a more intensive injection scheme should be applied for a water-wet reservoir from an oil recovery potential perspective.
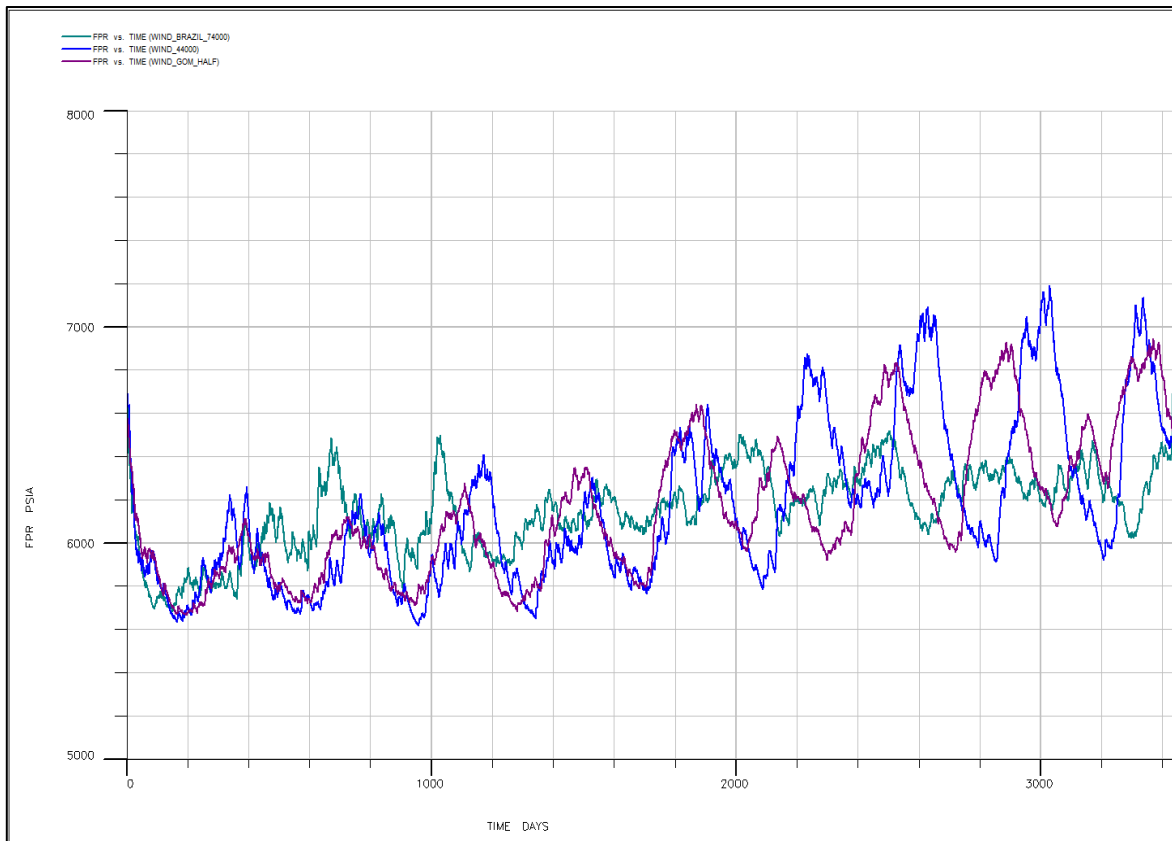
Figure 52: FPR curves for Location A (blue), Case B2 (turquoise) and Case C2 (purple) over 10 years

In **Case B2**, the off-injection period per cycle was larger than the on-injection period (regardless of the injection rate) for around 67% of the number of cycles compared to 50% and 53% for **Location A and Case C2**, respectively. This led to a slightly enhanced contact time between the injected water and formation between on-injection cycles for **Case B2**, especially with the low permeable zones, and thus improved water imbibition took place. The major factor for increased production by intermittent and cyclic scenarios is attributed to the increasing the oil saturation in the high permeable layers by gravitational and capillary forces. Imbibition of injected water will take place into the low permeability layers during the off-injection cycles, and force countercurrent flow of oil into the high permeability zones. The intermittent injection scheme of **Case B2** better sweeps low permeability layers, and leave slightly less oil behind. High permeable layers have experienced approximately the same sweep.

The oil and water production profiles over time for the **Location A**, **Case B2 and Case C2** are given in Figure 53, respectively. The daily, monthly and annual variations in the wind-generated water injection is reflected as similar oscillations in oil and water rates, as shown in Figure 50. In conclusion, the simulation results indicate that during the simulated period of 10 years, there is little difference in oil production between daily-intermittent scheme of **Location A** and that of **Case B2**, despite the notable difference in wind variability pattern and resultant intermittent injection scheme. This proves that the wind variability pattern effect, in other words variations of water injection with hourly increments, is negligible as long as the cumulative amounts of water injected into the reservoir (during the same time-span) are the same. The preference in locations selection for the offshore wind powered water injection candidate sites from a wind

resource perspective should be based mainly on average wind speed. Upon almost doubling the power system capacity for **Case B2** compared to **Location A** to make use of the seemingly better intermittent injection scheme, only a marginal increase in oil recovery was realized. Thus, locations with high enough annual/quarterly mean wind speeds to provide a given injection target volume at a practical rate, which the reservoir injectivity allows, and relatively lower capacity power system configuration than others should have the priority. It should be mentioned that the designed liquid production and injection rates for all scenarios have not been optimized, and could have been modified for better performance. (Appendix B). Moreover, it should be mentioned that this conclusion needs to be confirmed by the economic analysis of the respective cases.
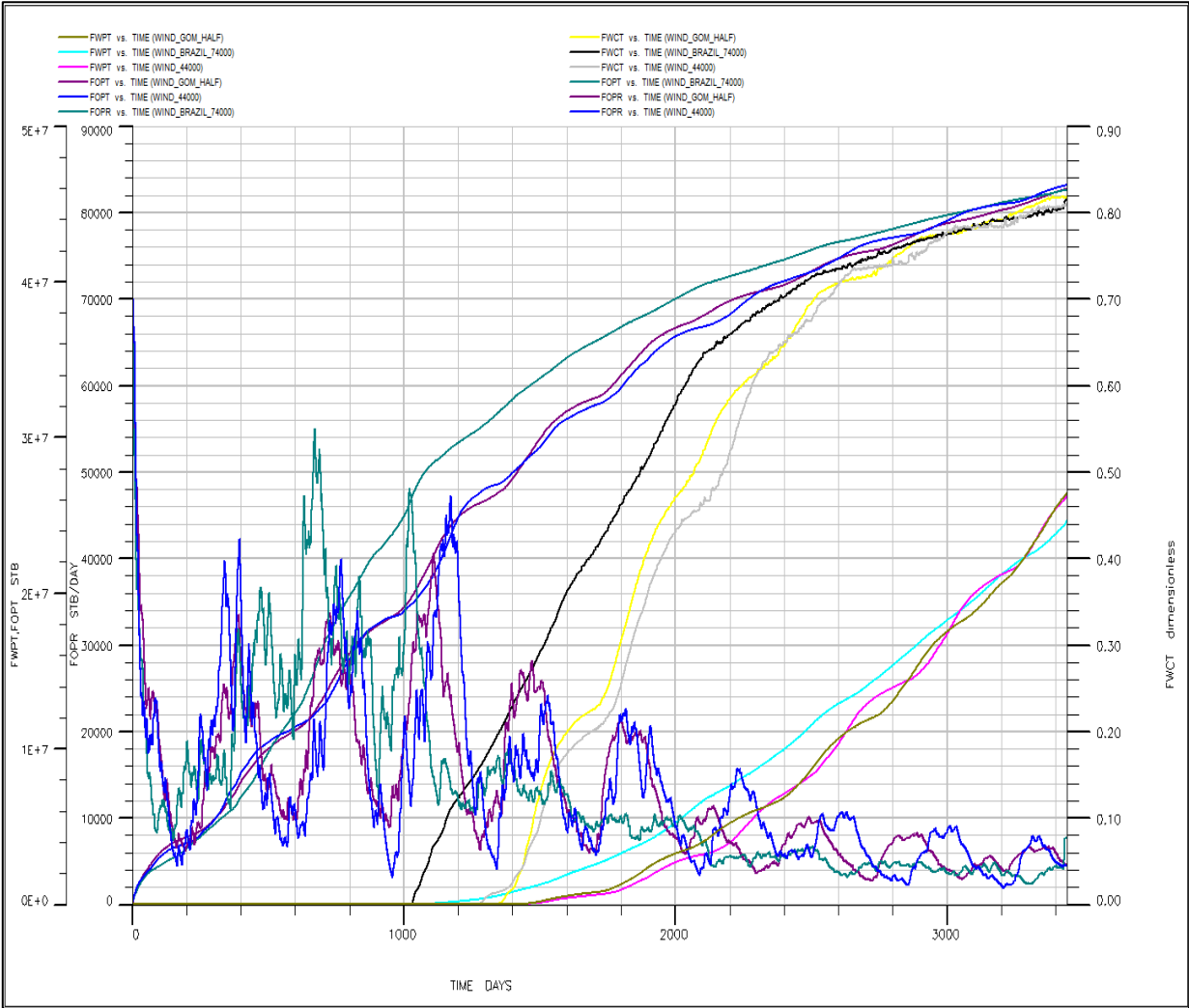
Figure 53: FOPR, FOPT, FWCT, and FWPT curves for Location A, Case B2 (BRAZIL), and Case C2 (GOM) over 10 years

6. Economic Analysis

This chapter aims at studying the economic feasibility of the project. This was done by building a discounted cash flow financial model for the integrated system design to estimate the Capex, Opex, internal rate of return (IRR), and NPV over the simulated 10 year period, for all scenarios. The model incorporated historical 5 year average oil and gas prices, simulated injection/production volumes, and other economic assumptions shown below, Table 23. Furthermore, a sensitivity analysis investigated the effect of oil and gas prices, discount factor, step-out distance to platform, and applied carbon tax. It is important to note, that Capex and Opex, as calculated here, does not include the costs power umbilical and other balance of system components which are relevant to actual projects, but are equivalent for all simulated scenarios. The purpose of this analysis remains to showcase the potential economic feasibility of **Scenarios A and B** under specific set of conditions rather than in absolute terms. Given that the above assumptions are realistic, they are deemed acceptable for this investigation. The results provided are valid under the assumption that the offshore field development costs the water injection is applied from day 1 and thus estimates of offshore oil field development and operation costs for the respective scenarios were incorporated in the model. Should the water injection project be considered exclusively as an acceleration secondary recovery process that starts later in the field life as a result of poor natural drive, only costs of facilities upgrade should be accounted for the investment decision making. The results presented for each case are better utilized for comparison rather than appraisal purposes.

Table 23: Base case economics conditions and assumption used in the built financial model

Base Case Economic Conditions	
Distance to host platform	20km
Discount Factor (DF)	7.25%
Oil Price	54.6€/bbl
Gas Price	325€/ton
Carbon Tax	50€/ton
Corporate Tax	25%

6.1. Economic Feasibility

The parameters to account for in an economic feasibility study of wind-powered water injection systems are highly case dependent. Thus, the current high-level study therefore only focuses on a few key parameters when comparing the simulated scenarios. For **Scenarios A and B**, total Capex for the offshore oil facilities and development, wind structure, marine operations and logistics are the two main Capex drivers. The pump system costs are also significant in the overall investment, and are expected to have higher costs for the intermittent and cyclic injection scenarios (due to higher requirements of injection rates and power capacity). The O&M cost and performance varies significantly depending on offshore oil field and its designed production facilities, wind turbine failure rates, repair times and wind and wave data. The resulting annual average operation and maintenance included parts, and vessel costs. The development and production assumptions are hypothetical, but realistic. Some parts of the models have been simplified for conceptual ease and to more directly highlight the effects of the key performance factors.

6.3.1. Capital Expenditure

No water injection flowline was considered for all scenarios, as subsea injection system of raw seawater was assumed. The solution has been successfully implemented both on the Norwegian Continental Shelf (NCS) and internationally (DNV GL, 2014).

Offshore oilfield development costs were estimated based on the type of production facility required at **Location A**, respective plateau production rates of each scenario and the consequent required production handling capacities, as well as costs of drilling 4 wells (same for all scenarios). The result was calculated to be around €176m, €200m, €127m for **Scenarios A, B, and C**, respectively (UK OGA, 2017).

The cost of the 4.5MW wind system designed to run the main injection pumps was contributed to Capex with around €18m. This was based on IRENA (2017) report that took into account up to date market and modelled data of wind generation cost trends and drivers. According to (IRENA, 2017), total investment costs of offshore wind systems, having subtracted the grid connection costs, were estimated to be around 4000€/kW. Capital costs include turbine capital cost (development, engineering management, substructure and foundation, site access, electrical infrastructure, installation, and plant commissioning) and balance of system (insurance, and contingency). The initial costs consist of the cost to purchase, transport and install the wind turbine, as well as costs associated with permits and supporting infrastructure. As is to be expected, foundations account for a considerable percentage of total costs, due to the expense of design and operations of severe offshore environment. On average, these account for around 18% of installed costs (IRENA, 2017). This share is mainly affected by water depth, conditions on the seabed, turbine loading, rotor and nacelle weight and the speed of the rotor. Then, comes the main 4MW water injection pumpset, capable of providing a flow rate that can vary up to 88,000 barrels per day, estimated at €1.7m (Slatte, 2014). For **Scenario A**, total Capex was calculated to be around €195.7m.

Despite having similar wind system, and water injection system as **Scenario A**, **Scenario B** Capex was significantly higher due to reliance on conventional power cogeneration from the host platform. The additional costs were mainly due to cabling costs (600€/m) from the host platform to the subsea injection system (20km apart) totalling at €12m (DNV GL, 2014). Also a 4MW gas turbine and associated systems (boiler, feed pump, generators, thrust motor, installation piping etc.) was required for this case to be able to sustain the 47,000 b/d injection rate when wind power falls short, which was estimated to cost around (€2m). For **Scenario B** total Capex was calculated to be €235.5m.

For Scenario C, the second major Capex contributor was the cabling costs estimated at €12m. This was followed distantly by the 1MW gas turbine case and associated systems costs estimated at €0.71m. The 1MW water pumpset cost was €0.21m. For **Scenarios C**, total Capex was calculated to be €139.6m. Since **Scenarios A and B** have significantly higher oil production rates (40Mbbl/day and 50Mbbl/day, respectively), they are expected to have higher Capex compared to the conventional **Scenario C** (20Mbbl/day). This was mainly driven higher

capacity offshore production facilities required. The difference in plateau oil production rates was significantly higher than that of the ultimate oil recovery resulting from each scenario.

6.3.2. Operational Expenditure

The offshore O&M costs included labour, vessels, spare parts, equipment, maintenance, land-based support, and project administration. The O&M cost and performance for the wind system is highly dependent on wind and wave data. However, the O&M estimate used above was merely based on the general reference, and did not take into account the specific wind and wave data any of the selected locations in this study. Enhanced system reliability will favourably affect the maintenance frequency, particularly for unscheduled maintenance, and Opex reduction. Manufacturers are making an effort to lower these costs considerably by developing novel designs requiring less regular service visits and experience less downtime. Furthermore, as wind turbines exhibit economies of scale as in reduction of investment costs with higher turbine capacities, similar economies of scale could potentially take place for O&M lifetime costs. As for the offshore oil field Opex were mainly driven by required facilities type and size for each scenario, logistics and administration, and wells.

For **Scenario A**, constant annual O&M costs were mainly driven by the annual offshore oil field Opex (13€/bbl) and wind turbine O&M annual costs (110€/kW/year) estimated at around €61.2m and €0.5m on average, respectively (UK OGA, 2017; IRENA, 2017). Another contributor to Opex was the O&M and spare parts for the 4MW pumpset (€0.27m). This resulted in a total 62m of operation expenditure on average annually for **Scenario A**.

For **Scenario B**, annual Opex costs were driven by slightly higher the average annual offshore oil field Opex (€62.2m), and the same wind turbine and 4MW pumpset O&M compared to **Scenario A**. This was in addition to the cost of fuel for the backup gas turbine needed for the cyclic injection scheme which adds €0.66m to the Opex annually, which was estimated based on assumed fuel consumption of 0.255 kg/kWh, gas price of 325€/ton, and 30% gas turbine efficiency (Slatte, 2014). Using the 1:3 cyclic injection scheme with 30 days base period, that leads to 3 months of on-injection required per year (totalling at 30 months over the 10 year simulation period). Since the goal is to have as high as possible wind energy share in power cogeneration for water injection, mean monthly wind speeds over the course of the simulation period were analysed to choose the optimal months for on-injection periods at **Location A**. The optimal months are the combination of months that will provide the highest wind power production over 10 years among (January, May, September), (February, June, October), and (March, July, November). The analysis showed that it's best to have the on-injection periods in the group of (February, June, November). Based on the power production for the selected months, an estimated power requirement of 55.36MWh needed to be provided by the gas turbine on the host platform over 10 years (55.5 tons of fuel). Annual emission cost was estimated at €0.28m annually, based on carbon emissions of 2.75 kg/kgfuel, and a carbon tax of 50€/ton. For **Scenario B**, total annual Opex costs were calculated at €63.6m.

For **Scenario C**, the offshore oil field Opex and pumpset O&M costs (€0.07m) associated system spare parts costs for this case were lower than that of **Scenarios A and B**, as a result of the lower power requirement (4MW vs 1MW) and lower plateau production rates. This was slightly offset by the fuel and emission costs estimated at 1m, and 0.44m on annual basis,

respectively. The fuel and emission costs estimate was based on a power requirement of 87.6MWh over 10 years. For **Scenario C**, Opex was calculated at €61.9m annually on average. Thus, **Scenario B** had the highest average annual Opex by a small margin, while **Scenario A and C** had approximately the same Opex.

6.3.3. Net Present Value and Internal Rate of Return

NPV was calculated using Equation 11 below. As for IRR, it was calculated via excel, by setting NPV equal to zero and solve for the discount factor. The only form of revenue associated with for all scenarios is from sale of oil based on simulated production amounts. In general, all scenarios were proved economically feasible for the simulated reservoir. All scenarios generated positive NPVs and higher IRRs than discount factors (DFs). Furthermore, the generated income (before and after tax) in each year exceeded the annual costs. For the oilfield characteristics, economic assumptions and the simulated reservoir model, **Scenario C** generated an NPV higher than **Scenarios A and B** by 6.4% and 8.7%, respectively. Furthermore, **Scenario C** had the highest IRR, followed by **Scenarios A and B**, respectively. This is mainly attributed to the higher capex associated with **Scenario A and B**, due to the larger size of facilities require to handle their associated plateau production rates. The incremental benefit in cumulative oil recovery achieved by **Scenarios A and B** over **Scenario C** was not significant enough to overshadow the previous. Possible optimization of **Scenarios A and B** recovery processes (production and injection rates, wells layout, etc) can potentially generate higher incremental recovery benefits to narrow down or overturn the economic edge of **Scenario C**. In summary, the obtained results prove that at similar reservoir, oilfield, wind resource and economic conditions **Scenarios A and B** provide a commercially feasible alternative to the conventional continuous gas powered water injection. Yet, Scenario C remained the favourable option exclusively from an NPV and IRR economic decision perspective in light of the modelled conditions.

$$NPV = \sum_{t=0}^{n} \frac{CF_t}{(1 + DF)^t} \qquad Equation\ 11$$

Where CF is the undiscounted net after-tax cash flow during the simulation period, DF is the discount factor, and t is the simulation period over which the cash flow was received

6.4. Net Present Value Sensitivity analysis

This section demonstrates the effect of varying different project parameters on the NPV. All parameters were varied in range of -30% to +30% relevant to the design base case, one factor at a time while keeping all other parameters constant.

6.4.1. Oil and Gas price sensitivity:

The base case for oil and gas prices was set by averaging annual mean prices over the past 5 years. Crude oil and natural gas prices have historically moved in tandem as a result of the linkage between the two commodities on the supply and demand sides. Thus for the high and low cases, the prices of both commodities were changed simultaneously with the same percentage up and down. The revenues for all scenarios were affected by the oil price only, having assumed zero gas production in the simulations. The NPV for all scenarios dropped by around 200%, as prices dropped from the high case to the low case, Figure 54. **Scenario A** had

no sensitivity towards the gas price movement, as only **Scenarios B and C** relied on gas turbines for power generation. For all the simulated oil and gas price cases, **Scenario C** remained the highest generating NPV injection scheme. For the high prices case, the incremental NPV increase of **Scenario C** over **Scenarios A and B** dropped to 5.2% and 6.6% compared to 6.4% and 8.7% in the base case, respectively. As for the low prices case, **Scenario C** was 16.2% and 27.5% higher than **Scenarios A and B**, respectively. The sensitivity results proved that wind-powered intermittent and cyclic injection schemes were commercially viable under all simulated oil and gas price cases for the modelled reservoir and economic conditions. The high sensitivity the NPV has shown towards oil and gas prices confirmed their critical importance for sanctioning of offshore oil recovery enhancement projects. Furthermore, it was proved that a high oil price environment is more favourable for **Scenario A and B**, due to the increased economic value of the incremental oil recovery benefit achieved over **Scenario C**.
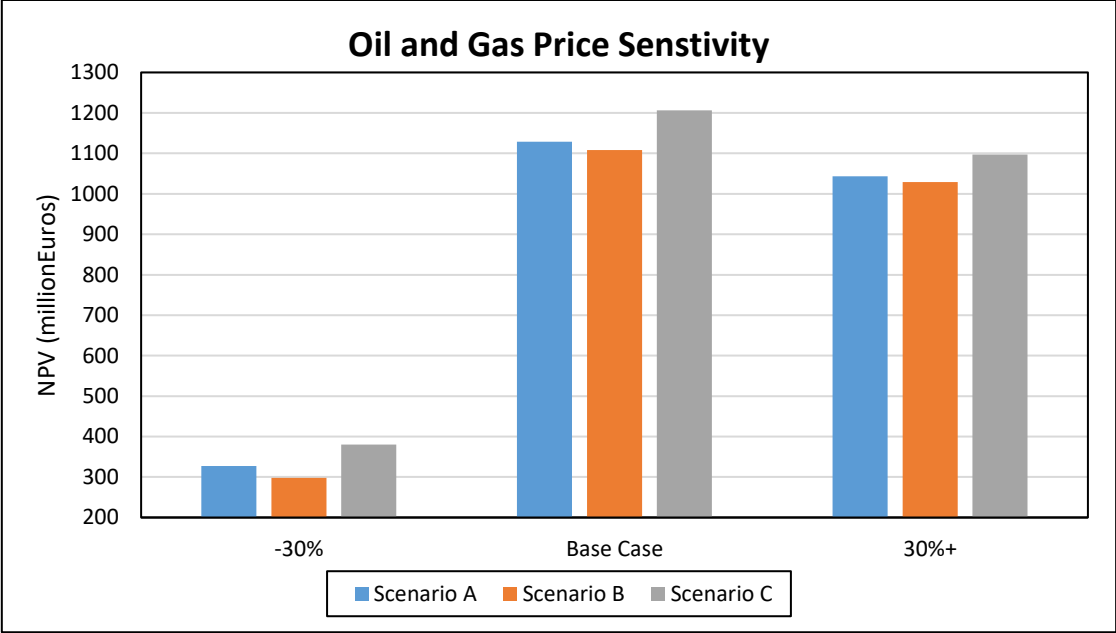
Figure 54: Oil and gas price sensitivity

6.4.2. Discount Factor Sensitivity

The base case for the discount factor was set based on the sector's weight of debt (average gearing of 16.53), marginal corporate tax rate (25%), cost of debt (2.4%), annual inflation rate (2.5%), country risk premium (0.5%), risk free rate (0.9%), market premium (7.1%), and assuming a large company profile (CME Group, 2018). The DF was shown to be the second highest sensitivity affecting the NPV of all scenarios. The NPV for all scenarios increased by around 24%, as the DF dropped from the high case to the low case, Figure 55. For all the simulated DF cases, **Scenario B** remained the highest generating NPV injection scheme. For the high DF case, the NPV of **Scenario C** was 7.5% and 9.9% higher than **Scenarios A and B**, respectively. As for the low DF case, **Scenario B** was 5.6% and 7.7% higher than **Scenarios A and B**, respectively. The sensitivity results proved that wind-powered intermittent and cyclic injection schemes were commercially viable under all simulated DF cases for the modelled reservoir and economic conditions. Also, a lower DF environment is considered more favourable for **Scenarios A and B**.
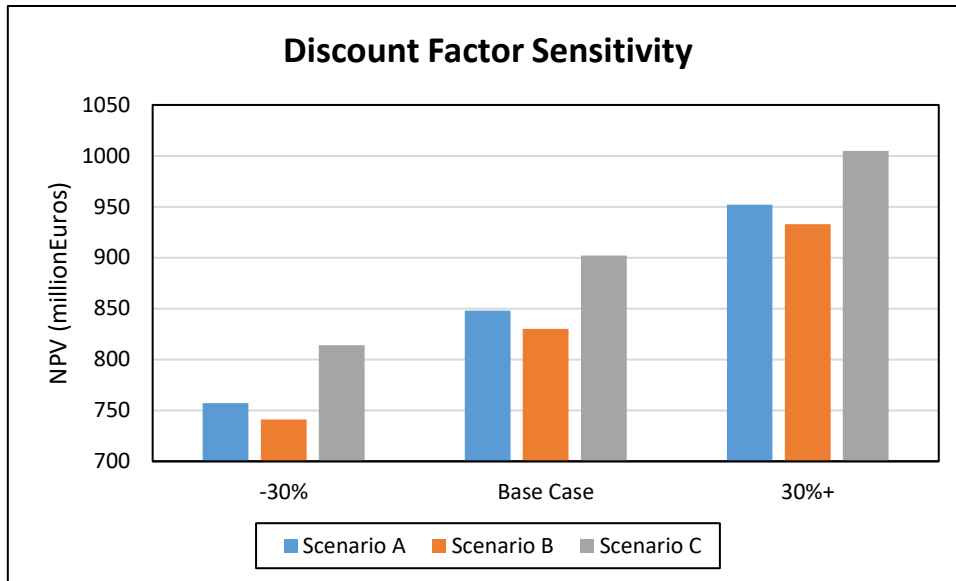
Figure 55: Discount factor sensitivity

6.4.3. Distance to Platform Sensitivity

The distance between the satellite injection well (subsea) and the host platform is to a large extent decisive for the costs of the offshore water injection operations. At some locations the distances can be in the order of several kilometers long. Thus, long power cables procurement and installation are major cost drivers in the traditional solutions and can be associated with operational risks. The operational risks stems from the costly systems being susceptible to damage that can cause production loss, and consequently require expensive repair. Furthermore, the longer the distances, the higher the power required.

The base case for this sensitivity was set at 20km. The NPV for **Scenarios B and C** increased by 0.8%, as the distance to platform dropped from the high case to the low case, Figure 56. **Scenario A** showed no sensitivity towards the distance to platform, as no cabling or water injection flowline from the host platform to the subsea injection system is required in that case (umbilicals that connect the wind power and injection system to wellhead was not accounted for in all cases). For all the simulated distances to platform cases, **Scenario C** remained the highest generating NPV injection scheme. For the high distance to platform case, the NPV of **Scenario C** was 6.3% and 8.7% higher than **Scenarios A and B**, respectively. As for the low prices case, **Scenario B** was 6.5% and 8.7% higher than **Scenarios A and B**, respectively. The sensitivity results proved that wind-powered intermittent and cyclic injection schemes were commercially viable under all simulated distance to platform cases for the modelled reservoir and economic conditions. The sensitivity the NPV has shown towards the distance to platform confirmed its importance for favouring **Scenarios A and B** over **Scenario C**, however longer distances to platform ranges are expected to further highlight this effect. Wind powered intermittent and cyclic injection schemes are expected to be economically competitive alternatives to conventional gas powered continuous flooding especially when host platform capacity is limited or injection wells are located far away.
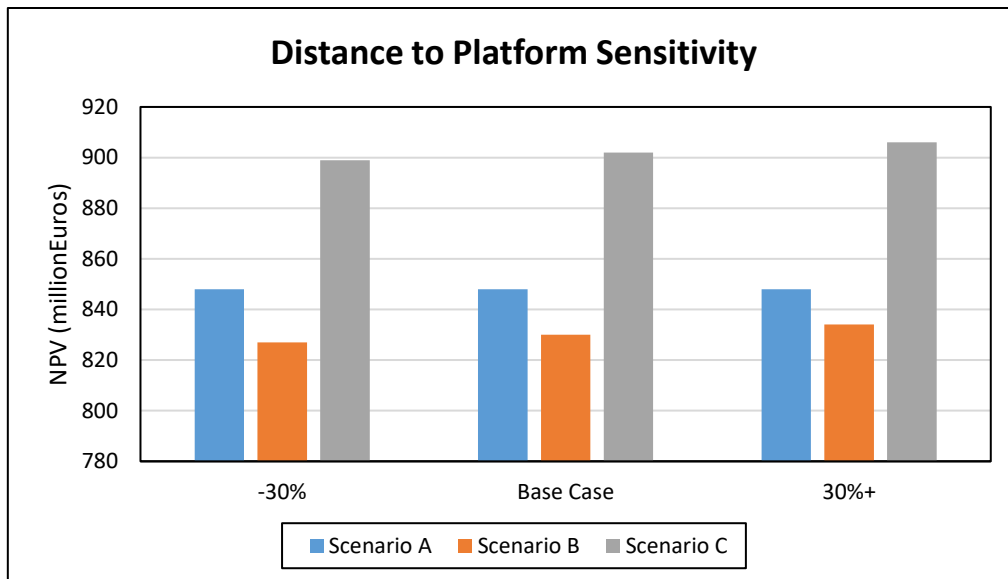
Figure 56: Distance to platform sensitivity

6.4.4. Wind Resource and Wind System Design Sensitivity

For **Location B (Case B2),** the wind power system for water injection was 1.7 times bigger than that of **Scenario A**. The aim of the larger power configuration for **Case B2** was to achieve a certain injection volume target for **Location B** similar to that attained at **Location A** (despite the higher wind power potential at **Location A**). **Location B (Case B2)** had almost double the Capex and 35% higher Opex estimate than **Scenario A**. Eventually **Location B** (**Case B2)** recovered 0.3% more oil than **Scenario A**. The increase in oil recovery by **Location B (Case B2)** seemed marginal compared to the expenses incurred as a result of the larger power system configuration. Although **Location A** showed a slightly higher IRR, the economic analysis proved that **Location B (Case B2)** had a higher NPV compared to **Scenario A** by around 1.3%. This is attributed to the fact that the significantly higher injection rates at **Location B (Case B2)** resulted in recovering 36% more oil than **Scenario A** by the end of year 3. Even though over 10 years the differences in cumulative oil recovery between both cases came down to 0.3%, the large amount of oil recovered by **Location B (Case B2)** early in the project lifetime had a significant effect on the NPV (using a 7.25% discount factor). This showed that offshore locations with relatively lower wind resource than **Location A** can still be suitable candidates for wind powered intermittent water injection projects under similar reservoir and economic conditions, despite the need for larger and more costly wind power systems. Offshore sites with superb wind power have shown to provide the highest IRR for **Scenario A**. Locations with relatively lower wind resource (good level of wind power potential) could still achieve a higher NPVs. This remains case dependent, as the reservoir need to have similar characteristics, sufficient injectivity to withstand the higher injection rates. Also, the wind variability pattern will still need to provide a favourable intermittent injection scheme.

6.4.5. Carbon Tax Sensitivity

The base case for carbon tax was set at 50€/ton, similar to the current tax for emissions on the Norwegian Continental Shelf (Slatte, 2014). The NPV for Scenarios B and C only slightly increased by around 0.7% and 0.13%, as the carbon tax dropped from the high case to the low case, Figure 60. **Scenario A** showed no sensitivity towards the carbon tax, as the fully wind powered water injection case was assumed to have zero emissions (full lifecycle and process

chain emissions were out of scope for this study). Since they were assumed equal for all scenarios, the emissions associated with powering utility pumps, feed pumps, and seawater lift pumps were ignored. This can be deemed acceptable as the results presented for each case are meant for comparison rather than appraisal purposes. For all the simulated carbon tax cases, **Scenario C** remained the highest generating NPV injection scheme. For the high carbon tax case, the NPV of **Scenario C** was 6.3% and 8.7% higher than **Scenarios A and B**, respectively. As for the low prices case, **Scenario C** was 6.5% and 8.7% higher than **Scenarios A and B**, respectively. The sensitivity results proved that wind-powered intermittent and cyclic injection schemes were commercially viable under all simulated carbon tax cases for the modelled reservoir and economic conditions. Despite the NCS being known to have the most stringent environmental regulations worldwide, the low sensitivity the NPV has shown towards the carbon tax confirmed the need for significantly higher carbon tax to incentivise more environmentally friendly practices in offshore oilfields. **Scenario A and B**, respectively, are expected to win further economic advantage over **Scenario C** with higher carbon taxes and more stringent offshore environmental regulations.
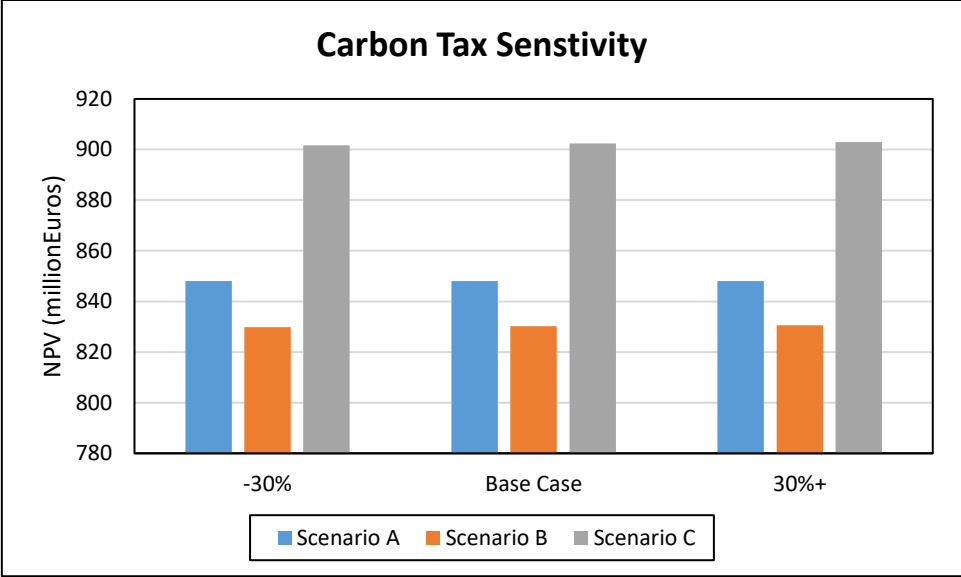
Figure 57: Carbon tax sensitivity

Concluding the NPV analysis, the results (Figures 58-60) show that the NPV of the project is most sensitive to oil and gas price, and discount factor respectively. The highest NPV case was achieved by **Scenario C** at an oil and gas prices of 62.45€/bbl and 422.5€/ton, while the lowest NPV case was for **Scenario B** at an oil and gas prices 33.63€/bbl and 227.5€/ton. **Scenario A** had no sensitivity to carbon tax, distance to platform, nor natural gas price, as expected.
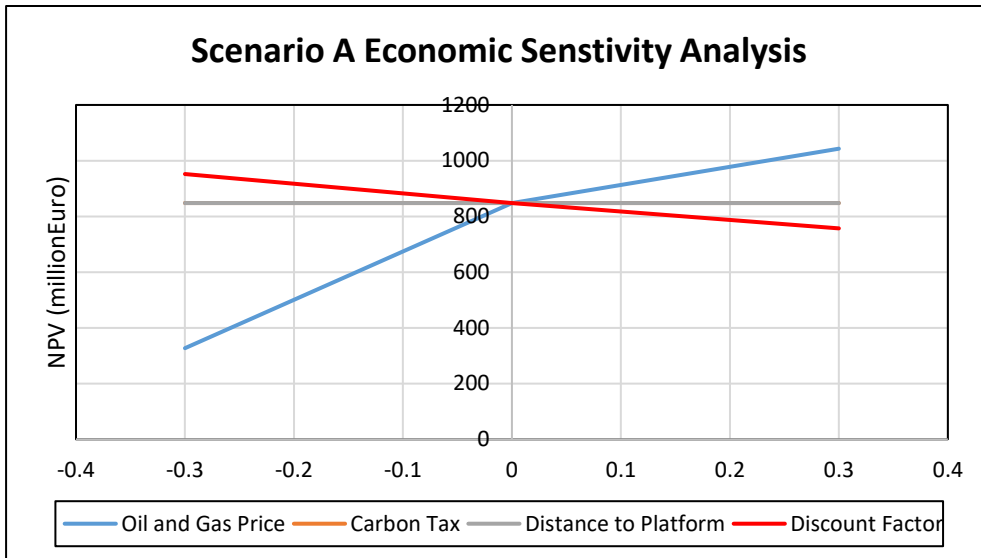
Figure 58: Economic sensitivity analysis for Scenario A
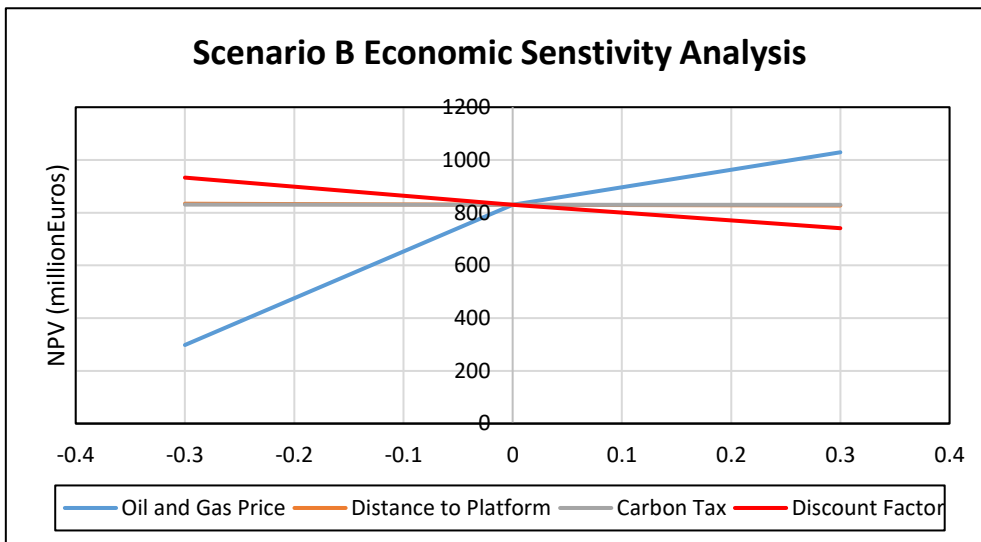
Figure 59: Economic sensitivity analysis for Scenario B
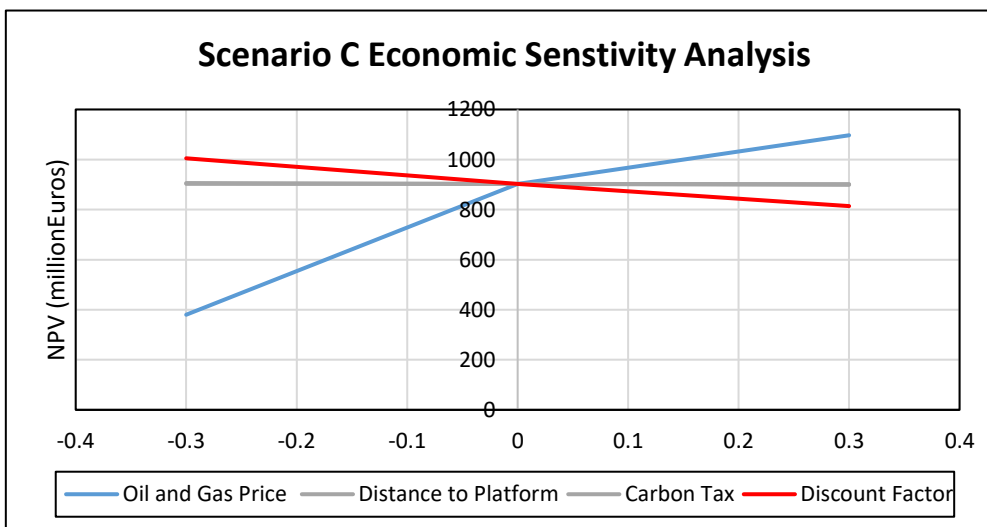
Figure 60: Economic sensitivity analysis for Scenario C

7. Environmental Analysis

This chapter briefly discusses the main environmental considerations with respect to the wind system at **Location A** that should be taken into account for the EIA studies of **Scenarios A and B** (mostly similar to offshore oil facilities considerations) and quantifies their energy efficiency, as well as the respective fuel and emission savings relative to **Scenario C**. Since **Scenario A** is based on **Location A** specifications (25m water depth), a fixed monopole foundation is assumed. In different offshore settings, other environmental considerations could apply.

Scenario B had a the highest energy efficiency in terms of the number of crude oil barrels recovered per MWh at 554bbls/MWh, compared to 383bbls/MWh and 534bbls/MWh for **Scenarios A and C**, respectively. For **Scenarios B and C**, CO_2 emissions are estimated to be 55.5kt and 87.8kt, respectively, over the project lifetime. It was estimated that **Scenarios A and B** give fuel savings 20.2kt and 11.7kt, respectively, over **Scenario C**. With a carbon tax of 50€/ton and a gas price estimate of 325€/ton, the operational cost savings for **Scenarios A** was estimated at €9.4m and €14.4m, respectively, for fuel and carbon tax costs. Both wind powered intermittent and cyclic injection schemes presented a considerable environmental advantage relative to conventional continuous gas powered waterflooding. However, the actual environmental improvement offered by **Scenario A** is more significant in comparison to cogeneration **Scenario B**. As discussed in section 6.2.5, the results proved the need for significantly higher carbon tax to incentivise more environmentally friendly practices in offshore oilfields. **Scenario A and B**, respectively, are expected to win further economic advantage over **Scenario C** with higher carbon taxes and more stringent offshore environmental regulations.

During the construction and operational phases of the wind turbine's life a direct interaction with the environment occurs. This environmental contact takes place in the form of disturbance, noise and the introduction of foreign objects in an already established ecosystem. This construction noise could negatively affect animals, as in purpoises for example, that depend mainly on ultrasound to hunt. Hammering in such sites should be avoided by a 20km radius (Gordon et al., 2007). Figure 61 shows the signal of a monopile hammer blow (pile driving). On the other hand, some animals can be positively influenced by the wind structure following the end of the construction phase. As certain marine species favour being in proximity to these new structures. The study of wind turbine's impact on the ecosystem is difficult to assess due to the diversity of the marine species present, and at times the impossibility fully understanding possible alternate drives for them to remain or depart the offshore wind site. Generally, tagging provides a way further investigation of the behaviour of specific species of interest that are known to exist in the site under study. However, the issue of the scatter caused by the individuality of every sample can still arise, deeming the obtained data quite unreliable (Wisner et al., 2015).
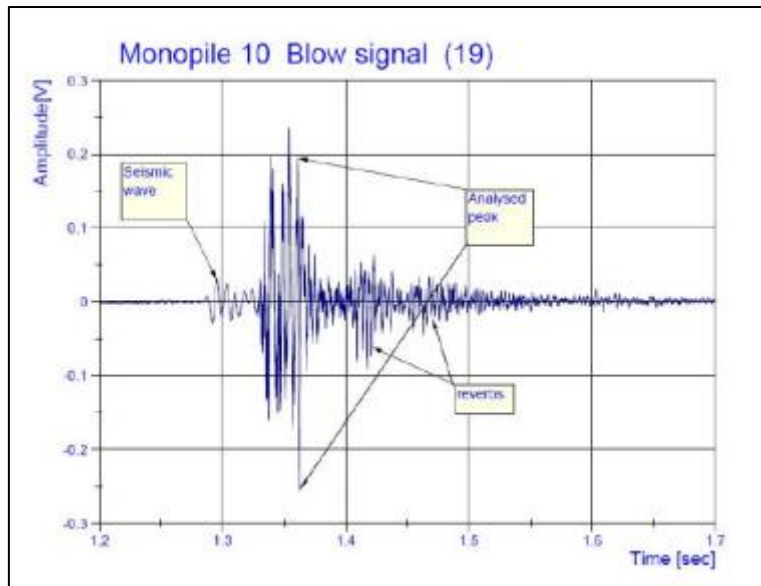
Figure 61: Monopile blow signal, (Wisner et al., 2015)

Furthermore, other animals will be at risk based on the extent of the physical presence of the tower and the rotor in the sky. Birds being hit and killed by the blades is known to be a serious threat. However, it has been noted that bird strikes have higher probability of occurrence on land than offshore. This has been mainly attributed to landscape distractions being considerably less offshore. Some statistics as well as the general sensitivity of sea-birds to offshore wind turbines are shown in Figure 62. **Location A** appeared to be situated in region of medium concern with respect to sea-birds. It should be mentioned that the natural habitat was not fully taken into account for the project design nor the environmental impact assessment (Lindeboom, 2018). It is possible that such consideration could compromise the environmental performance of the project. Thus, a detailed case by case studies are advised for actual projects sanctioning and feasibility studies.
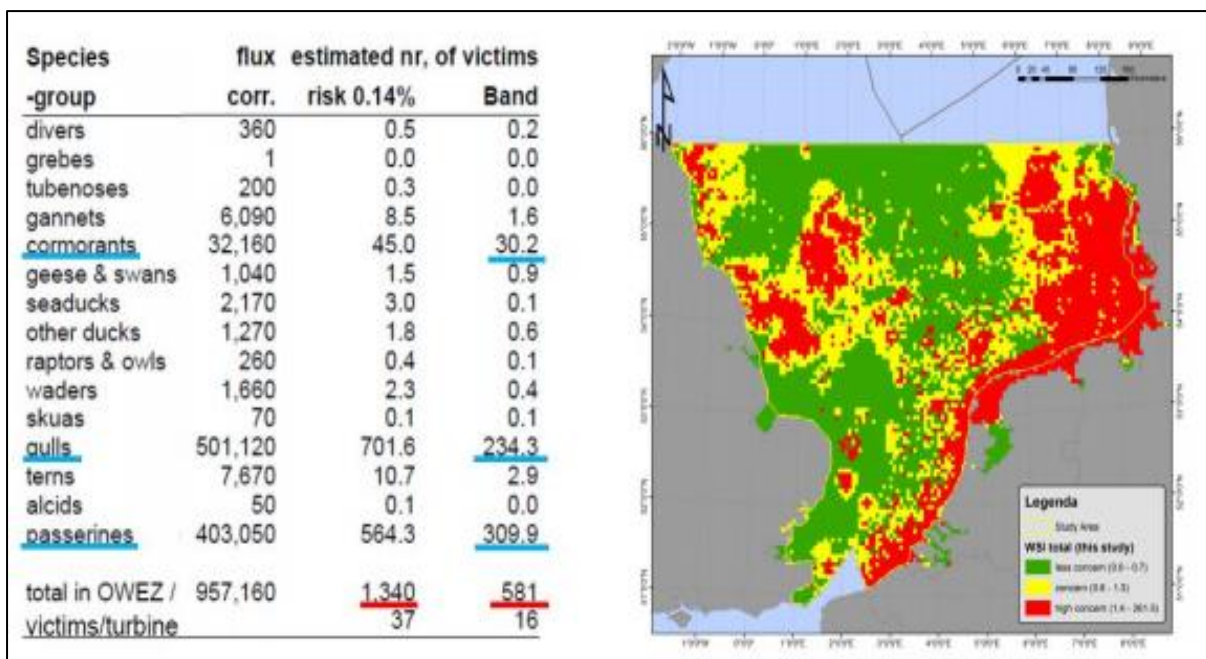
Figure 62: Bird strike and sea-bird sensitivity, (Lindeboom, 2018)

8. Conclusions

This thesis shows interesting and promising results regarding wind-powered water injection in offshore oilfields. To sum up the findings of this simulation study the following conclusions can be made in form of answer to the research main and sub-main questions:

- **Can the reservoir performance (from an oil recovery perspective) tolerate the intermittency of offshore wind power and hence, water injection?**

Disregarding reservoir injectivity limitations, the variable scheme intermittent injection (varying 3-hour cycles) and cyclic injection scheme (fixed monthly cycles) scenarios that incorporated a wind power system exceed the ultimate oil production achieved by conventional continuous waterflood, and are therefore potentially attractive from a reservoir performance perspective. Wind-powered intermittent and cyclic injection schemes, however, will require higher injection rates and larger power capacities to arrive at a given target injection volume compared to traditional gas-powered continuous water flooding.

- **If yes, under which reservoir conditions can the offshore wind-powered water injection process be technically and economically feasible?**
- *For the modelled base case reservoir conditions (heterogeneous and layered structure), what is the best injection scheme among the simulated scenarios? What is the effect of increasing the injection rate for various schemes?*
- *What are the key reservoir performance indicators? What is the extent of the role of each indicator?*
- *How does different ranges of reservoir properties affect the total oil recovery achieved different water injection schemes, and the incremental recovery benefits achieved by wind-powered injection scheme over continuous flooding? And why?*
- *What is the optimum initiation time for wind-powered intermittent and cyclic injection schemes?*

Wind-powered cyclic water injection scheme, being the more intensive injection scheme that provided the highest injection rate and longest injectors shut-in period per cycle as well as overall, achieves the highest cumulative oil production estimated at around 2.3% higher than gas-powered continuous water injection. Increasing injection rate for both schemes is beneficial up to a certain limit, beyond which the incremental oil recovery increase diminishes.

The effect of a specific intermittent or cyclic injection ratio (of injection to no-injection) is strongly controlled by the injection rate. Reservoir performance favors the more intensive schemes (higher ratio of off-injection period per cycle to the on-injection period per cycle and longer overall off-injection duration) with higher injection rates. This was attributed to key performance factors addressed in the project including enhancing contact time between formation and injected water, enhanced gravitational and capillary effects, improved water imbibition towards low permeability layers, vertical cross flow enhancement, fluid redistribution during off injection periods which limited water channelling, greater pressure amplitudes, and benefiting from the high saturation and pressure gradients. Capillary imbibition was responsible for almost third of the incremental recovery benefit achieved by the fully wind-

powered water injection scheme, and compressibility effects were responsible for another third. As for the cyclic water injection scheme, only less than 10% of the incremental recovery benefit was attributed to capillary effects, while the compressibility effects contributed with less than 20%.

Wind-powered intermittent and cyclic injection schemes are technically feasible under all wettability conditions in layered heterogeneous reservoirs. However, cyclic injection schemes achieved the highest incremental oil recovery benefit over conventional continuous flooding in case of an oil-wet rock. The variable fully wind-powered intermittent injection scheme was a more favourable option for mixed wet reservoirs.

Wind-powered intermittent and cyclic injection schemes are technically feasible under all vertical transmissibility conditions in heterogeneous reservoirs. Both schemes were proved beneficial for higher vertical transmissibility ratios in heterogeneous reservoirs up to a given limit, beyond which the incremental recovery benefit achieved diminishes. Both wind-powered schemes achieve higher oil recovery than conventional continuous injection for both symmetric and asymmetric permeability distributions. However, the incremental benefit diminished in symmetric distribution conditions.

Wind-powered intermittent and cyclic injection schemes achieve higher oil recovery than conventional continuous injection only in reservoirs with high heterogeneity levels. In homogeneous reservoirs, continuous water injection recovered slightly more oil (around 1%). Both wind-powered schemes are beneficial from an oil recovery perspective at various initiation times and water cut levels in the heterogeneous layered reservoirs. However, the earlier in field life either of both schemes are applied, the higher the incremental recovery benefit.

- **Under which offshore wind resource conditions can the wind-powered water injection process be technically and economically feasible?**
- *What are the levels of wind potential, wind climate types, and wind variability patterns under which the project is technically and economically attractive?*
- *What are the suggested/common ways to characterize the wind resource and select potential candidate offshore locations for this thesis concept?*

Offshore oil field sites with higher wind potential (outstanding level) achieve relatively higher oil recovery in heterogeneous layered reservoirs for a given fixed wind system design, due to a significantly higher amount of water injected over a given period. Wind variability did affect the seasonal produced oil and water rates, which should be taken into account in actual oil fields development planning. Offshore locations with lower levels of wind potential (down to good level) can also potentially achieve slightly higher oil recovery than continuous water injection, using higher power capacity wind systems and assuming a favourable wind variability pattern.

- **Under which economic conditions can the offshore wind-powered water injection process be feasible?**
- *What are the key economic drivers of wind powered intermittent and cyclic water injection schemes?*
- *For the modelled base case, how does various scenarios rank in terms of Capex, Opex, NPV and IRR? And why?*

- *How are the feasibilities of all scenarios affected under different economic conditions in terms of NPV and IRR?*
- *How do different levels of wind power potential affect the economics of the project?*

Wind-powered intermittent and cyclic injection schemes are economically feasible mainly in heterogeneous layered reservoirs. This was supported by generating positive net present values for all simulated cases under a given range of economic conditions. Fully wind-powered intermittent injection scheme generated higher net present value and internal rate of return compared to the cyclic injection scheme which combines wind power with gas cogeneration, mainly due to the significantly lower capex required for the former. Both wind-powered schemes are considered more economically favourable under higher oil price environment, lower weighted average cost of capital, longer distances separating host platform and injection wells, higher carbon tax and more stringent environmental conditions. Conventional gas-powered continuous water injection generated higher net present value and internal rate of return than the wind-powered injection schemes, mainly as a result of a significantly lower capex for the former that overshadowed the incremental recovery benefit and higher revenues achieved by the former. Establishing the wind-powered water injection concept in offshore oil sites with wind potential down to good level will require significantly larger wind system to reach slightly higher cumulative oil recoveries over 10 years compared to sites with outstanding wind potential for a given target injection volume. However, the amount of oil recovered earlier in the field life (within the first 3 years of production) was considerably higher in the former case, as a result of the increased injection rates associated with the higher power system and injection capacity added. These incremental revenues generated in the short term will have a magnified effect on the net present value for the modelled discount factor.

- **What are the environmental benefits resulting from applying fully and partially offshore wind-powered water injection in terms of energy efficiency and emissions reduction, approximately? What are the resultant fuel and carbon tax cost savings?**

Wind-powered intermittent and cyclic injection schemes have a considerable environmental advantage relative to conventional gas-powered continuous water flooding. The wind and gas cogeneration cyclic injection scheme had a the highest energy efficiency in terms of the number of crude oil barrels recovered per MWh followed by the fully wind-powered intermittent water injection scheme and gas powered continuous flooding, respectively. Both fully and partially wind-powered scenarios gave fuel savings of around 20.2kt and 11.7kt, respectively. The combined operational cost savings for fuel and carbon costs were estimated at €9.4m and €14.4m, respectively.

In conclusion, this thesis painted the potential of wind powered intermittent and cyclic water injection schemes in offshore oilfields in a favorable light. The concept is clearly in need of further detailed studies, and case by case analysis for project sanctioning. However, strong oil recovery performance, economic, and environmental feasibility, under similar reservoir and economic conditions to those modelled and recommended in this thesis, is evident.

9. Limitations and Recommendations for Future Work

This paper has evaluated the reservoir engineering, economic, and environmental feasibility of wind powered water injection in offshore oilfields. While many factors have been considered, a number of assumptions and simplifications were made.

The wind system availability is a major challenge for the project that should be addressed in more detail. The system is in islanding operation at a remote site. If outages or failures occur in the system it may take comparatively long for the system to be repaired. Increasing the availability of the system can be achieved by increasing the level of redundancy. By paralleling subsystems with the same functionality, an outage in one of them will not lead to an overall system outage. Hence, the areas where redundancy is applied need to be considered carefully for optimum cost efficiency. Moreover, an off the shelf pump system that allows for the variable power provided by a wind turbine generator should be selected.

Further detailed studies for selected studies should be carried out. It is crucial to identify all local, regional, and national permits required for a proposed site with respect to technical and environmental issues. Additionally, studying other projects that have operated in the same region is recommended for identification of similar potential issues. The technical and economic effects associated with wave data (among other environmental conditions) in the selected sites weren't considered the locations considered in this study fell within a similar range of water depths and distances from shore. Investigating the feasibility of the proposed concept in a wider ranges of location characteristics is recommended.

The simulated cases for wind powered intermittent water injection experienced varying on and off injection durations per cycle. However, during on-injection cycles the injection rate was fixed, as injection was only allowed when the wind system was producing its rated power. Running cases that allows water injection at varying injection rates across the wind turbine power curve spectrum is recommended for further investigation. The thesis simulations considered a simplified case of a 3D box model, 2 producers, 2 injectors, and one wind turbine. It will be quite interesting to widen the scope of the study to include a real reservoir 3D model with a more realistic number of producers and injectors for field development, and potentially several wind turbines. The offshore wind farm layout and control strategy could then be optimized for a favourable field injection scheme. In that case, studying alternating injection patterns between different injectors (and wind turbines) will also be a meaningful study focus. A storage system design for application of **Scenario B** and other possible cyclic injection schemes will also be a valuable addition.

Severe risk analysis is necessary before an intermittent or cyclic waterflood is applied in any field. As the high complexity and simultaneous events in a field makes the effect of intermittent and cyclic injection difficult to analyze. The electrical system configuration and suitability for 3-hourly on and off switching of pumps weren't considered in this study. It should be mentioned that only powering of the main injection pumps were considered in this thesis, including the balance of the system power requirements will require a scaled up wind system design, and could affect the economics of the concept. However, since the effect is expected to be equal for all simulated scenarios, the results obtained are valid for comparison purposes. Furthermore, it

was assumed that the cycling of injection rate does not lead to significant pore pressure variation in the reservoir that might lead to compaction or fracturing. It should be mentioned that no reservoir geomechanics were included in the study. This assumption needs to be examined more carefully in light of the observation of greater injection pressure to reach annual water injection targets as well as for application of variable scheme injection to lower permeability reservoirs.

Relative permeability was set equal for the imbibition and drainage process. This could result in an unrealistic view of the intermittent or cyclic water injection processes. As, the capillary hysteresis and relative permeability curves at the micro level yields that fluids in the reservoir will switch between imbibition and drainage with alternating pressure could potentially lead to a higher recovery. Furthermore, oil-water and oil-gas capillary pressures were set equal for all three wettability cases due to shortage of data, and should have been estimated to better illustrate the difference in wettability.

For further analysis on capillary pressure effects and flow type, more cases of the capillary curve could be simulated with different injection schemes and base periods. Also, the impact of layer thickness and permeability differences could be further analysed by running more cases with different ratios. Plugging of zones producing higher volumes of water could potentially demonstrate interesting results under intermittent or cyclic injection, and consequently aid in further understanding the topic. The effect of critical gas saturation during the off-injection intervals at pressures below bubblepoint pressure will be an interesting investigation. Another feature for further investigation is the well control and boundary condition, as this was not managed up to the utmost level.

Several simplifications were applied for the economic analysis. Constant Opex was assumed for various project components including the wind system. As wind power generation matures further, some decline in costs as a result of economies of scale could be realized. Additionally, all economic calculations were on a before inflation, and depreciation among the various scenarios. The scope of sensitivity analysis could go beyond the 30% up and down range in the cases considered, taking into account the volatility of oil and gas prices, discount factors, and carbon tax pricing for example. In short, there appear to be considerable alternate economic scenarios to consider.

Variation in reservoir and wind characteristics makes it complicated to create a standard optimum practice workflow, thus further detailed studies for wider range of wind, reservoir and economic conditions is recommended to further define screening criteria for candidate offshore oilfields. Also, a case by case analysis is essential for project sanctioning.

References

Ackerman S., (1995): "Sea and Land Breezes", University of Wisconsin.

Anderson W., (1987): "Experimental Study of Carbonated Water Injection".

Babadagli T., (1994): "Injection Rate Controlled Capillary Imbibition Transfer in Fractured Systems".

Behrembruch P., and Gode H., (2006): "Two-Phase Relative Permeability Prediction: A Comparison of the Modified Brooks-Corey Methodology with a New Carman-Kozeny Based Flow Formulation".

CME Group, (2018):"Weighted Average Cost of Capital".

ConocoPhillips, (2013): "Cyclic Injection Procedure".

Elkins L. and Skov A., (1986): "Cyclic Water Flooding the Spraberry Utilizes End Effects to Increase Oil Production Rate", Journal of Petroleum Technology.

Ezekwe N., (2011): "Petroleum Reservoir Engineering Practice", Pearson Education Inc.

Feller. F, (2017): "WIN WIN - Wind-Powered Water Injection", DNV GL.

Fjaer E., (2004): "Petroleum Related Rock Mechanics", Elsevier.

Gordon J., Thompson D., Gillespie D., Lonergan M., Calderan S., Jaffey B., and Todd V., (2007): "Assessment of the potential for acoustic deterrents to mitigate the impact on marine mammals of underwater noise arising from the construction of offshore windfarms", University of St Andrews.

Groenenboom J., Wong S., Meling T., Zschuppe R., and Davidson B., (2003): "Pulsed Water Injection During Waterflooding".

International Renewable Energy Agency (IRENA), (2017): "Renewable Energy Generation Costs 2017".

Langdalen H., (2014): "Cyclic Water Injection: A Simulation Study", NTNU.

Leonid S., Nils H., Lars K., and Anton S.: "Cyclic Water Injection Improves Oil Production in Carbonate Reservoir", Statoil Hydro.

Li X., and Yortsos Y., (1993): "Critical Gas Saturation: Modeling and Sensitivity Studies".

Lindeboom H., (2018): "Wind energy from the North Sea: environmental impacts and future developments", Wageningen University & Research.

Miao W., Jia H., and Wang D., (2012): "Active power regulation of wind power systems through demand response".

Milan P., (2008): "The stochastic power curve analysis of wind turbines", University of Oldenburg, Germany.

Mone C., (2016): "Offshore geared wind turbine swt-4.0-130 and 4.0-120. Siemens AG-WIND".

National Renewable Energy Laboratory (NREL), (2005): "Wind Energy Resource Atlas".

Nord L., Andresen T., Walnum H., and Nekså P., (2016): "Modelling and Simulation of CO_2 (Carbon Dioxide) Bottoming Cycles for Offshore Oil and Gas Installations at Design and Off-design Conditions".

Owens W., and Archer D., (1966): "Waterflood Pressure Pulsing for Fractured Reservoirs".

Peng O. and Yanosik J., (1988): "Pressure Pulsing Waterflooding in Dual Porosity Naturally Fractured Reservoirs", SPE.

Perez D., Federico S., and Sezai U.: "Cyclic Water Injection in San Jorge Gulf Basin, Argentina", YPF.

Pooladi-Darvish M., and Firoozabadi A., (2000): "Solution-gas Drive in Heavy Oil Reservoirs", University of Calgary.

Prabhakar A., (2013): "Is Cyclic Water Injection Likely to Work?: A Numerical Investigation", Imperial College of London.

Putra E., Fidra Y., and Schechter D., (1999): "Use of Experimental and Simulation Results for Estimating Critical and Optimum Water Injection Rates in Naturally Fractured Reservoirs", SPE.

Qingfeng Y., Bingyu J., and Jiping Y., (1995): "Mechanism of Cyclic in Waterflooding in Vertically Heterogeneous Reservoirs".

Rao D., Girard M., and Sayegh S., (1992): "The Influence of Reservoir Wettability on Waterflood and Miscible Flood Performance".

Ritter M., (2008): "The Physical Environment: Global scale circulation", University of Wisconsin–Stevens Point.

Rublev A., Ishimov A., and Fedoroc K., (2012): "Predictions of cyclic water injection on Urenskoe oil field", SPE.

Shchipanov A., Surguchev L., Jakobsen S., (2008): "Improved Oil Recovery by Cyclic Injection and Production".

Sheng J., (2013): "Evaluation of the EOR potential of gas and water injection in shale oil reservoirs", Texas Tech University.

Slätte J., Sandberg J., Flach T., Dekker G., and Sixtensson C., (2014): "Wind-powered Subsea Water Injection Pumping: Technical and Economic Feasibility", DNV GL.

Stirpe T., and Guzman J., (2004): "Cyclic Water Injection Simulations for Evaluations of its Potential in Lagocinco Field".

Surguchev L., Korbøl R., Haugen S. and Krakstad O., (1992): "Screening of WAG injection Strategies for Heterogeneous Reservoirs", SPE European Petroleum Conference, France.

Surguchev L., Koundin, A., Melberg, O., Rolfsvåg, T. and Menard W., (2002): "Cyclic Water Injection: Improved Oil Recovery at Zero Cost".

Surguchev L., Giske N., Kollbotn L., and Shchipanov A., (2008): "Cyclic Water Injection Improves Oil Production in Carbonate Reservoirs", SPE.

Torsaeter O., and Abtahi M., (2003): "Experimental Reservoir Engineering Laboratory Workbook", NTNU.

U.K. Oil and Gas Authority, (2018): "Analysis of UKCS Operating Costs in 2017".

U.S. Energy Information Administration (EIA), (2018): "U.S. Crude Oil and Natural Gas Proved Reserves".

Wais P., (2017): "A review of Weibull functions in wind sector", Cracow University of Technology.

Wei L., (2013): "Sequential Coupling of Geochemical Reactions with Reservoir Simulations for Waterflood and EOR Studies", SPE.

Weinstein H., Chappelear J., and Nolen J., (1986): "Second Comparative Solution Project: A Three-Phase Coning Study".

WindEurope, (2017): "Wind in Power 2017: Annual Combined Onshore and Offshore Wind Energy Statistics".

Wisner G., Stammen E., Dilger K., Sychla H., Stein P., Kornemann C., and Gattermann J., (2015): "Adhesive bonding of measurement equipment on impact-driven offshore monopile foundations".

Yang Y., and James J.: "Experimental Investigation of Light Oil Recovery from Fractured Shale Reservoirs by Cyclic Water Injection", Texas Tech University.

Yaozhong Y., Tao D., and Chenfeng W., (2006): "The Reservoir Simulation Research and Extending Application About Cyclic Water Injection", SPE.

Zhongrong L., Xianzhi S., Yongsong Q. and Xuezhong C., (1995): "Methods and Effects of Cyclic Waterflooding in the Southern Oilfields of Daqing Placanticline". SPE Advanced Technology Series.

Zheng C., Xiao Z., Peng Y., Li C., and Du Z., (2017): "Rezoning Global Offshore Wind Energy Resources", Ludong University, China.

Appendix A: Basic Petroleum Engineering Definitions

Porosity

Porosity is defined as the pore volume of the rock divided by the bulk volume. It is a measure of its storage capacity of fluids. Porosity can be classified into 2 main types being primary porosity and secondary porosity. The primary porosity is formed during the deposition of the rock. The secondary porosity is developed after deposition, and is caused by geological processes or ground stresses (Torsæter and Abtahi, 2003). It can also be classified based on pores connectivity into total and effective porosity; total porosity includes all open pore space in a rock, while the effective porosity only considers the interconnected spaces in the rock. Porosity is mainly affected by grain structure, size, sorting and packing (Ezekwe, 2011).

Permeability

Permeability is a measure of the ability of the reservoir rock, to transmit fluids (Ezekwe, 2011). Absolute permeability is the measurement of the permeability with only one fluid present in the reservoir rock (Schlumberger, 2014). In case more the system contains more than one fluid, the ability a certain fluid to flow is referred to as the effective permeability of that fluid. The permeability depends mainly on reservoir porosity and pressure (Ezekwe, 2011).

Relative permeability

The relative permeability is the ratio of effective permeability to absolute permeability (Ezekwe, 2011). The relative permeability curves of a certain fluid, both drainage and imbibition, are mainly based on the endpoint fluid saturations, and their corresponding endpoint permeabilities. The drainage curve refers to a route with decreasing saturation of the wetting phase, while the imbibition curve designates the a process with increasing saturation of the wetting phase (Torsæter and Abtahi, 2003).

Phase mobility

Mobility of a given fluid is defined as the ratio of relative permeability to the viscosity of that fluid. As for the mobility ratio (M), it refers to the ratio of the displacing fluid mobility to that of the displaced fluid (Schlumberger, 2018).

Fluid saturation

Fluid Saturation refers to the ratio of a given fluid volume to the pore volume in the reservoir (Torsæter and Abtahi, 2003). Since, the relative permeability of a certain fluid depends mainly on the saturation, therefore the fluid distribution in the reservoir controls the areal sweep. It should be mentioned that quick flow of water through high permeability zones reflects a higher water saturation.

Wettability

Wettability refers to the preference of the reservoir rock to adhere a certain fluid on its surface rather than the other. Rock wettability varies between strongly water-wet and strongly oil-wet. The wettability of a fluid can be expressed by the contact angle of the liquid-solid surface. The wetting characteristics of the fluid increases with decreasing contact angle (Rao et al., 1992).

The fluid distribution and multi-phase flow in the reservoir is governed by rock wettability. The wetting phase mainly occupies the tight spreading over as a layer on the rock surface, while the non-wetting phase will be largely present in the bigger pore spaces. Thus, the behavior and success of waterflooding is dependent on the type of wettability in the reservoir (Anderson, 1987).

Capillary forces

As any two immiscible fluids get in contact with one another, a pressure difference develops between those fluids, which is referred to as the capillary pressure. In other words, the capillary pressure is defined as the difference in pressure between the non-wetting and wetting phases in a given reservoir. The capillary forces acting in a reservoir originates from the surface and interfacial tensions between the rock and fluids, pore size and structure, as well as the wetting phase of the fluids present (Ahmed, 2006).

Critical gas saturation

Critical gas saturation refers to the value at which free gas starts to flow in the reservoir (Li and Yortsos, 1993).

Primary recovery

Primary recovery is defined as the hydrocarbons amount that can be produced by means of the natural energy drive in the reservoir. The basic form of a primary drive is related to the fluid and rock compressibility (Schlumberger, 2018).

Secondary recovery methods

Secondary recovery processes are applied to increase hydrocarbon production, following the primary recovery phase. This is done by either providing the reservoir with an external pressure support in order to maintain the reservoir pressure or sweeping the hydrocarbons in place towards the producers. The most common secondary recovery techniques include water and gas injection either by converting existing production wells or drilling new infill injection wells in proximity to the producers (Schlumberger, 2018).

Appendix B: Simulations and Results

Table 24: Year 1 average monthly wind speeds for all locations

Year 1			
Month	A	B	C
Jan	9,4	5,5	9.5
Feb	9,2	4,9	8.1
Mar	10,7	4,1	8.1
Apr	8,4	5,8	5.6
May	7,6	4,8	5.5
Jun	6,9	6,0	5.2
Jul	7,0	6,3	5.4
Aug	9,8	5,3	5.8
Sep	9,2	5,4	7.2
Oct	10,4	5,8	7.3
Nov	13,0	5,3	9.8
Dec	9,9	5,2	8.3

Table 25: Year 2 average monthly wind speeds for all locations

Year 2			
Month	A	B	C
Jan	13,5	6,5	10.5
Feb	8,4	5,4	7.4
Mar	8,6	7,3	8.2
Apr	7,7	7,0	5.8
May	9,0	6,9	6.6
Jun	7,0	6,8	5.5
Jul	8,6	6,4	6.0
Aug	8,1	6,6	5.6
Sep	7,9	8,1	7.5
Oct	10,1	8,7	8.6
Nov	9,3	8,0	9.3
Dec	13,2	6,1	10.2

Table 26: Year 3 average monthly wind speeds for all locations

Year 3			
Month	A	B	C
Jan	13,0	7,3	8.7
Feb	8,9	6,4	8.0
Mar	12,4	6,1	7.7
Apr	9,6	7,1	7.0
May	7,3	7,4	5.9
Jun	8,1	5,4	5.5
Jul	5,9	6,6	5.6
Aug	8,0	6,9	6.4
Sep	10,2	7,4	8.2
Oct	9,6	8,3	9.5
Nov	9,0	5,9	9.7
Dec	12,7	4,7	10.5

Table 27: Year 4 average monthly wind speeds for all locations

Year 4			
Month	**A**	**B**	**C**
Jan	14,0	4,9	10.2
Feb	13,1	6,4	7.6
Mar	12,7	5,7	7.3
Apr	9,0	5,3	6.2
May	6,8	5,7	5.1
Jun	8,7	6,1	5.3
Jul	7,1	5,8	5.5
Aug	8,5	5,7	6.6
Sep	9,5	5,4	6.5
Oct	8,8	5,4	9.4
Nov	10,2	4,9	8.7
Dec	8,6	5,6	9.0

Table 28: Year 5 average monthly wind speeds for all locations

Year 5			
Month	**A**	**B**	**C**
Jan	10,4	5,6	9.6
Feb	10,7	5,4	8.7
Mar	8,4	6,4	6.6
Apr	6,8	6,1	6.4
May	9,1	5,8	6.0
Jun	7,1	5,5	5.6
Jul	7,9	5,1	4.8
Aug	7,8	4,3	5.3
Sep	9,3	5,2	8.6
Oct	10,2	5,3	9.7
Nov	12,4	5,4	10.0
Dec	10,1	5,2	9.1

Table 29: Year 6 average monthly wind speeds for all locations

Year 6			
Month	**A**	**B**	**C**
Jan	7,8	5,0	9.7
Feb	13,6	5,7	9.4
Mar	8,7	6,2	6.3
Apr	8,3	6,1	6.1
May	7,6	6,8	5.5
Jun	8,5	6,3	6.1
Jul	6,9	5,8	9.4
Aug	6,6	5,9	7.6
Sep	8,3	4,2	8.6
Oct	10,1	3,4	9.2
Nov	10,6	4,0	6.2
Dec	12,1	5,0	4.6

Table 30: Year 7 average monthly wind speeds for all locations

Year 7			
Month	A	B	C
Jan	13,0	5,2	9.5
Feb	10,6	5,4	8.1
Mar	10,3	5,6	8.1
Apr	8,5	5,9	5.6
May	7,9	6,0	5.5
Jun	9,5	5,1	5.2
Jul	9,5	5,0	5.4
Aug	8,7	5,9	5.8
Sep	9,9	5,0	7.2
Oct	13,8	5,4	7.3
Nov	9,9	5,3	9.8
Dec	11,7	4,9	8.3

Table 31: Year 8 average monthly wind speeds for all locations

Year 8			
Month	A	B	C
Jan	12,4	4,2	8.7
Feb	11,4	5,3	8.0
Mar	7,6	5,4	7.7
Apr	8,2	5,8	7.0
May	8,1	5,9	5.9
Jun	7,5	4,6	5.5
Jul	7,9	6,3	5.6
Aug	6,8	5,2	6.4
Sep	8,6	4,9	8.2
Oct	10,5	5,7	9.5
Nov	11,2	5,3	9.7
Dec	14,0	4,6	10.5

Table 32: Year 9 average monthly wind speeds for all locations

Year 9			
Month	A	B	C
Jan	11,0	4,9	9.6
Feb	12,1	6,0	8.7
Mar	9,7	5,3	6.6
Apr	7,5	6,0	6.4
May	8,0	5,9	6.0
Jun	7,6	5,5	5.6
Jul	7,3	5,5	4.8
Aug	6,1	5,8	5.3
Sep	8,7	4,3	8.6
Oct	12,0	4,8	9.7
Nov	12,8	4,2	10.0
Dec	11,9	4,8	9.1

Table 33: Year 10 average monthly wind speeds for all locations

Year 10			
Month	**A**	**B**	**C**
Jan	10.2	5.4	10.2
Feb	9.1	6.4	7.6
Mar	8.6	5.8	7.3
Apr	9.3	6.1	6.2
May	8.2	7.7	5.1
Jun	7.5	11.5	5.3
Jul	7.1	7.6	5.5
Aug	7.6	6.0	6.6
Sep	10.1	6.9	6.5
Oct	11.2	6.4	9.4
Nov	10.1	6.7	8.7
Dec	10.6	6.5	9.0

Table 34: Cumulative oil recovery for all scenarios at simulated wettability cases

Scenario	WW FOPT (bbl)	OW FOPT (bbl)	MW FOPT (bbl)
Scenario A	46,811,720	30,316,590	36,418,320
Scenario B	47,132,910	30,667,230	36,952,780
Scenario C	47,867,350	31,404,580	37,625,270

Table 35: Simulation results for all scenarios at simulated reservoir heterogeneity cases

Scenario	Heterogeneous			Homogeneous		
	FOPT (bbl)	FWIT (Mbbl)	BTT (days)	FOPT (bbl)	FWPT (Mbbl)	BTT (days)
Scenario C	46,811,720	31,412	1,466	71,995,420	1,462	3440
Scenario A	47,132,910	30,193	1,500	71,591,420	1,176	3460
Scenario B	47,867,350	29,146	1,470	71,429,070	1,231	3460

Table 36: Cumulative oil recovery of Scenarios A and B at various initiation time cases

Water Cut Level	Time (days)	Scenario B FOPT (bb)	Scenario A FOPT (bbl)
0	0	47,867,350	47,132,910
15%	1080	47,444,230	47,042,400
25%	1189	47,427,650	46,864,810
50%	1440	47,419,960	46,890,850
75%	1892	47,219,900	46,854,090
85%	2659	46,829,410	46,787,480

Table 37: Scenario B injection scheme and base period sensitivities

Injection Scheme	#1:3		#1:2	
Base Period (DAYS)	15	30	15	30
FOPT (bbl)	47,937,436	47,867,348	47,797,788	47,864,956
FWPT (Mbbl)	28,473.70	29,145.50	29,078.93	29,400.52
BTT (days)	1493	1470	1488	1473

Table 38: Injection rate sensitivity for all scenarios

Scenario A		Scenario B		Scenario C	
Injection rate (bbl/d)	FOPT (bbl)	Injection rate (bbl/d)	FOPT (bbl)	Injection Rate (bbl/d)	FOPT (bbl)
36,700	44,443,636	39,250	44,816,204	10,000	44,363,468
44,000	47,132,912	47,000	47,867,348	12,000	46,811,724
56,000	50,784,916	60,000	51,931,624	15,000	49,665,984
62,000	52,232,564	80,000	53,897,880	17,000	51,259,356
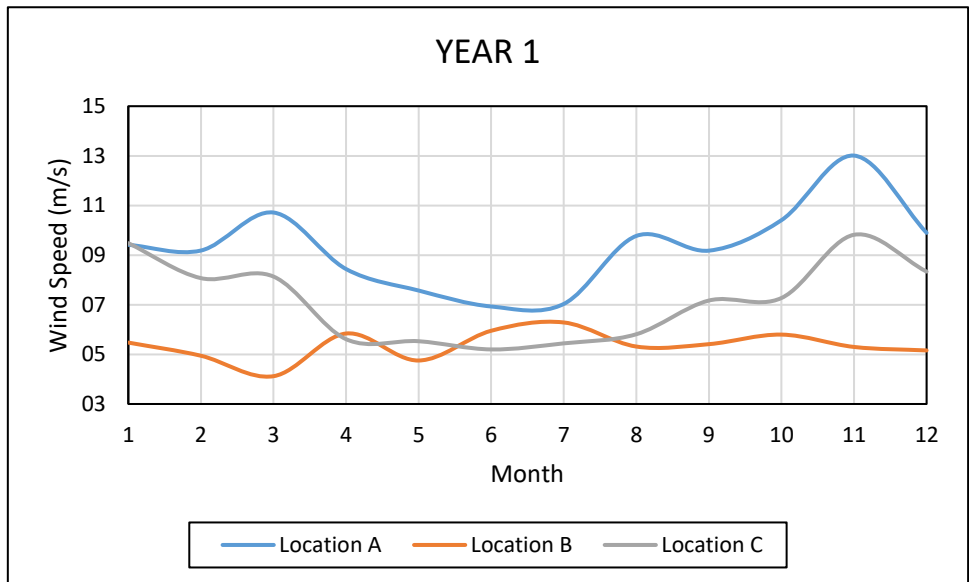
Figure 63: Year 1 average monthly wind speeds for all locations
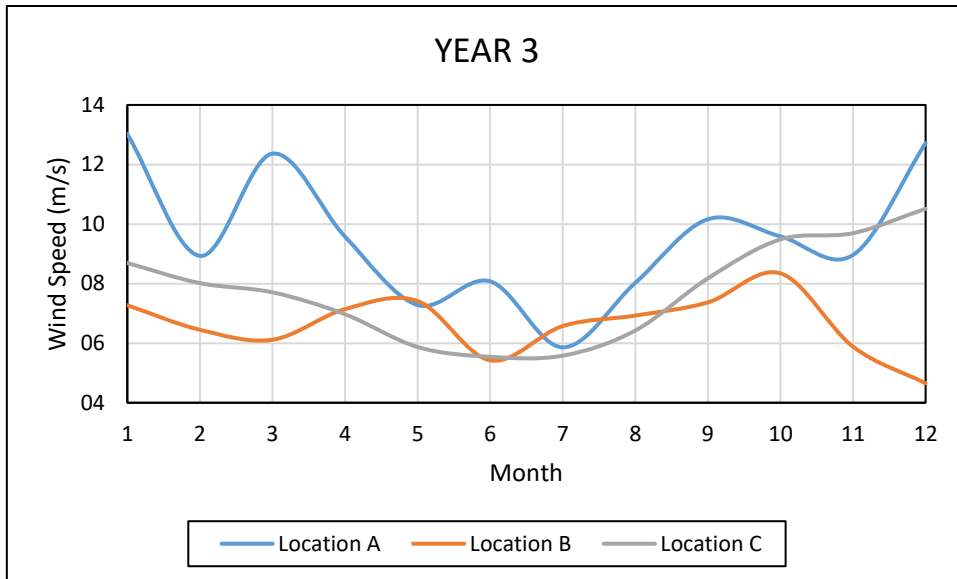
Figure 64: Year 3 average monthly wind speeds for all locations
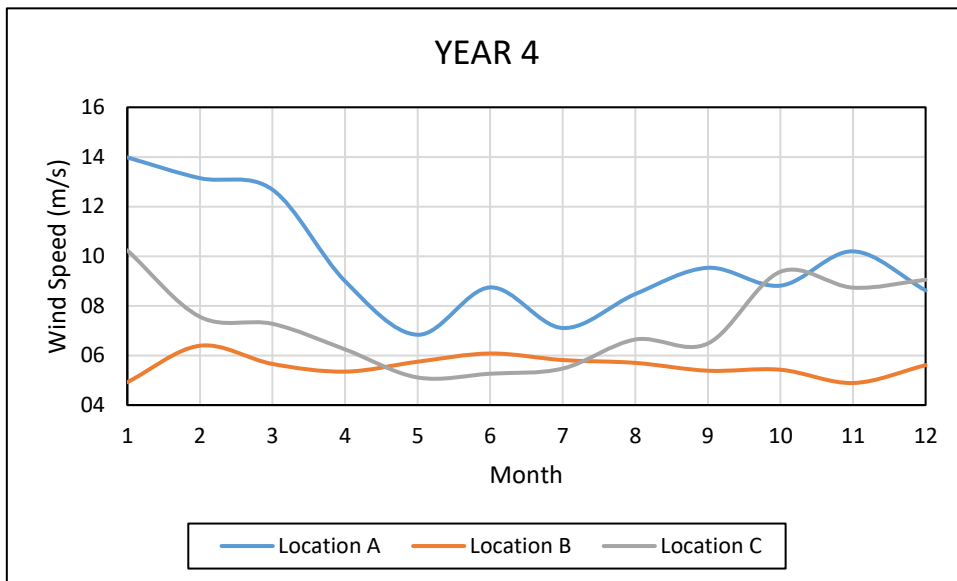
Figure 65: Year 4 average monthly wind speeds for all locations
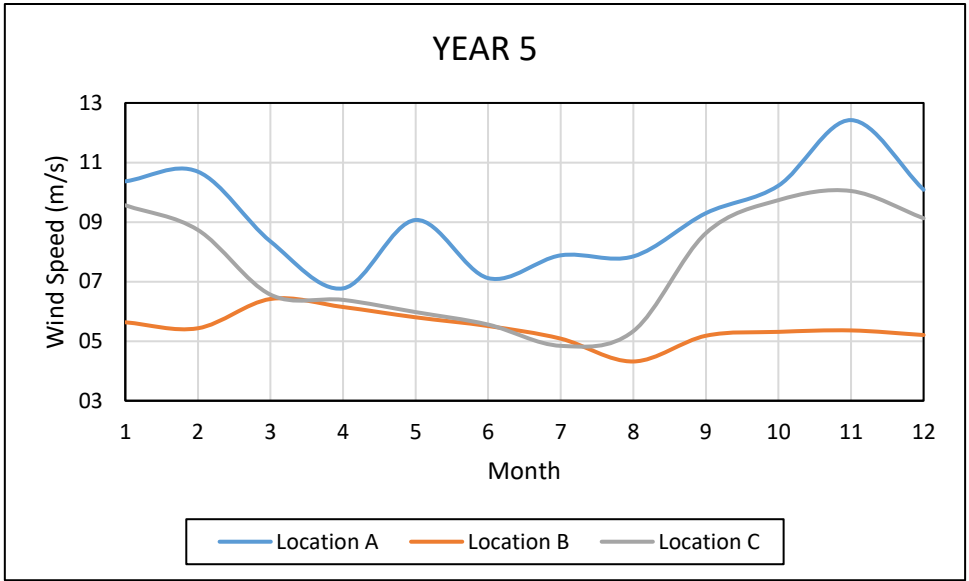
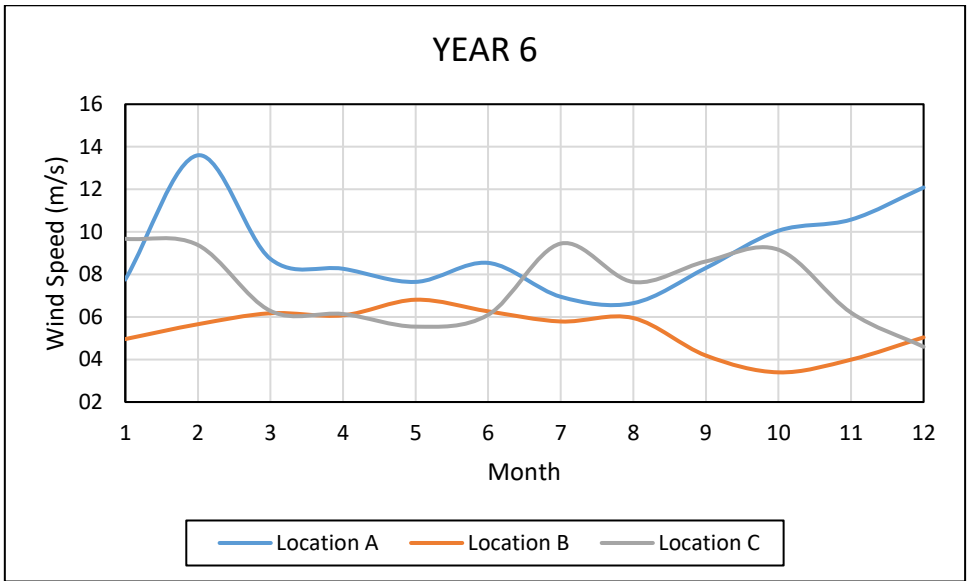*Figure 66: Year 5 average monthly wind speeds for all locations*

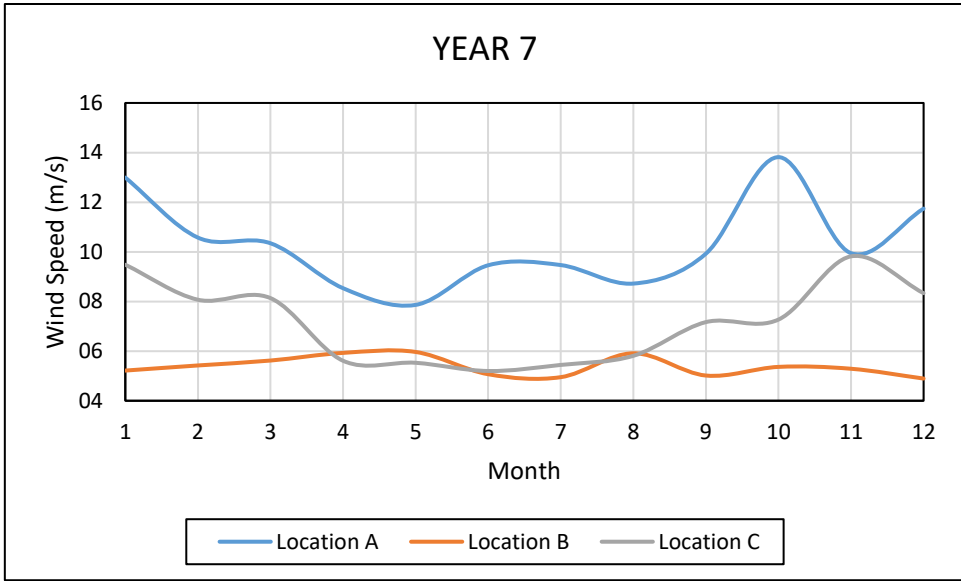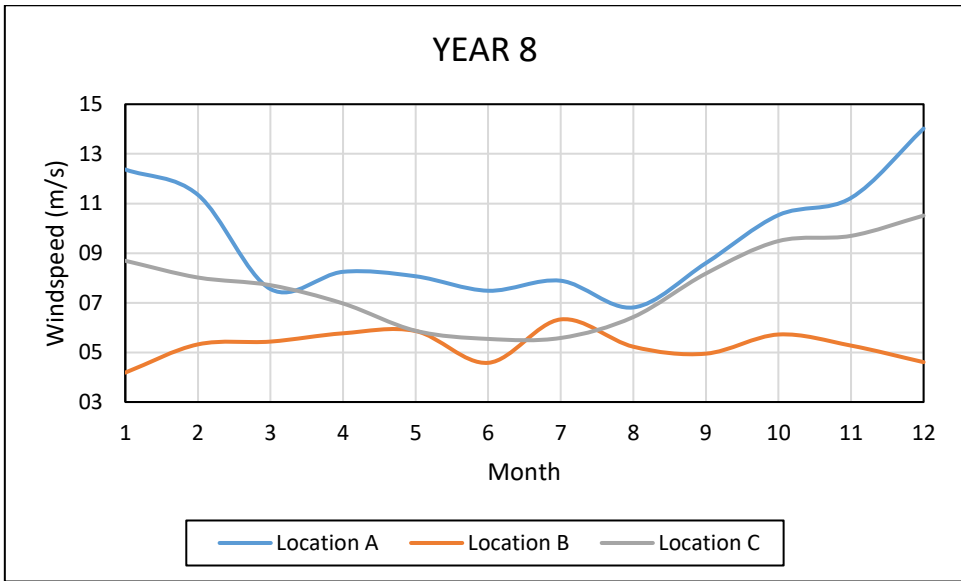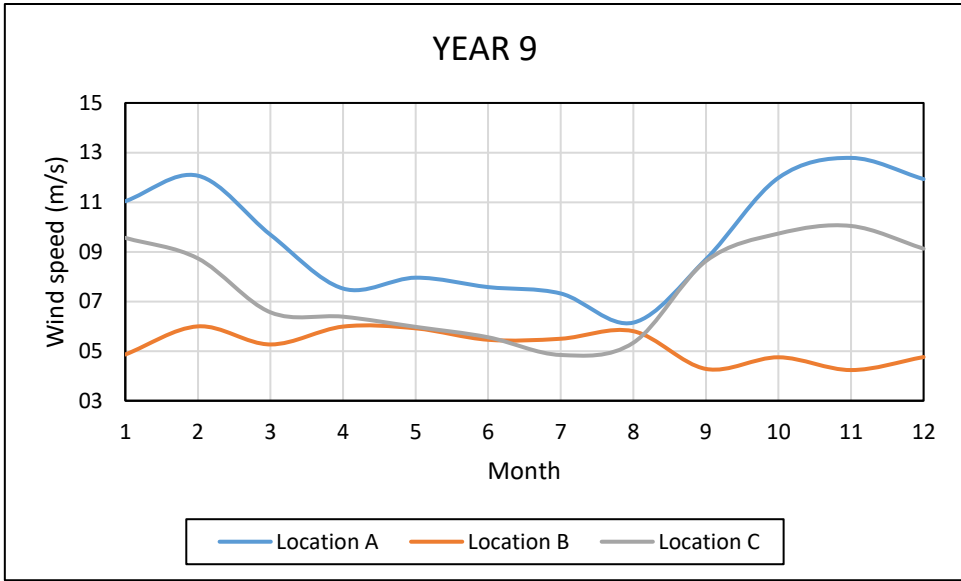*Figure 67: Year 6 average monthly wind speeds for all locations*

Figure 68: Year 7 average monthly wind speeds for all locations

Figure 69: Year 8 average monthly wind speeds for all locations

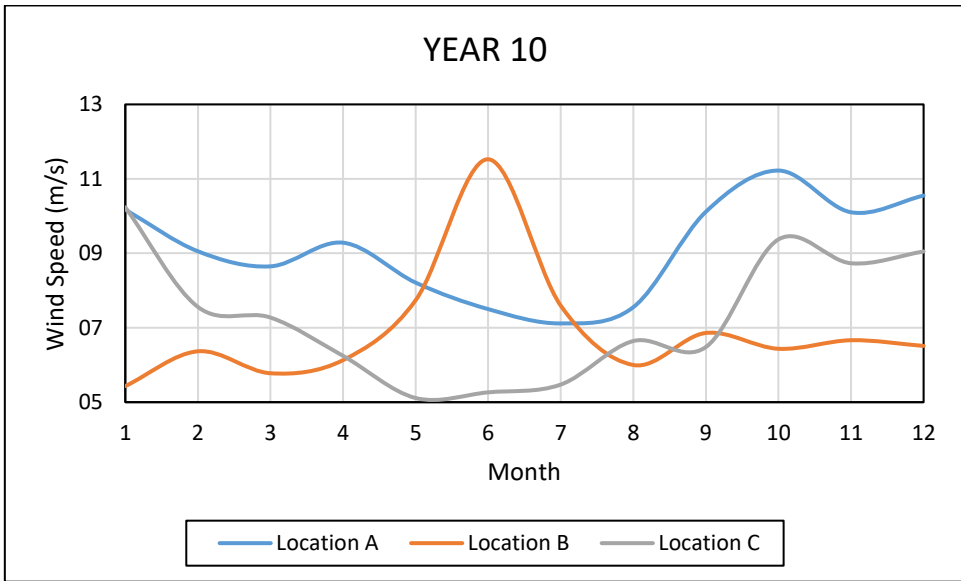*Figure 70: Year 9 average monthly wind speeds for all locations*
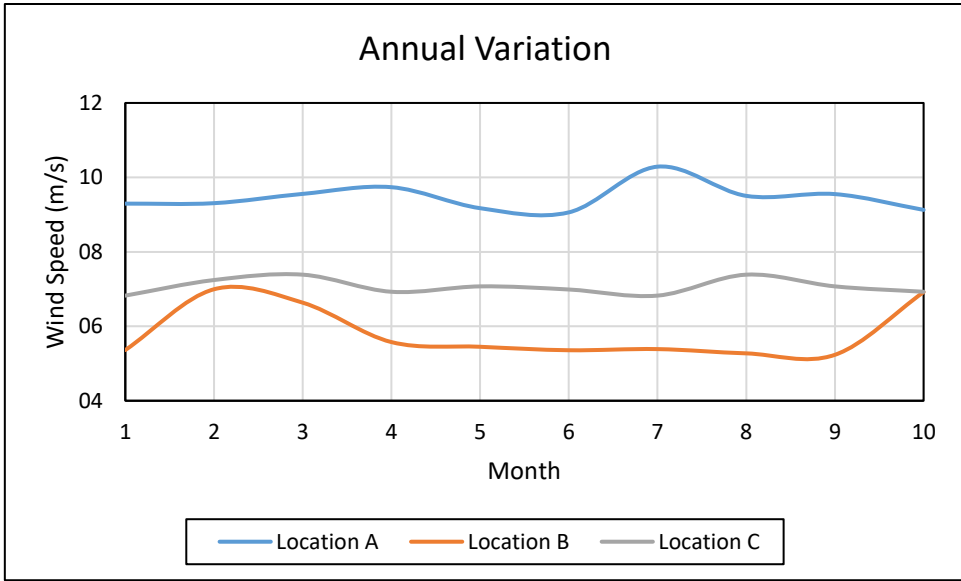

Figure 71: Year 10 average monthly wind speeds for all locations

Figure 72: Year 10 average monthly wind speeds for all locations